Synthesis of Optically Active Half-Sandwich Complexes with Bidentate and Tridentate Ligands

Synthese von optisch aktiven Halbsandwich-Komplexen mit zwei- und dreizähnigen Liganden

Dissertation

Zur Erlangung des Doktorgrades

Doktor der Naturwissenschaften (Dr. rer. nat.)

der Naturwissenschaftlichen Fakultät IV
– Chemie und Pharmazie
der Universität Regensburg

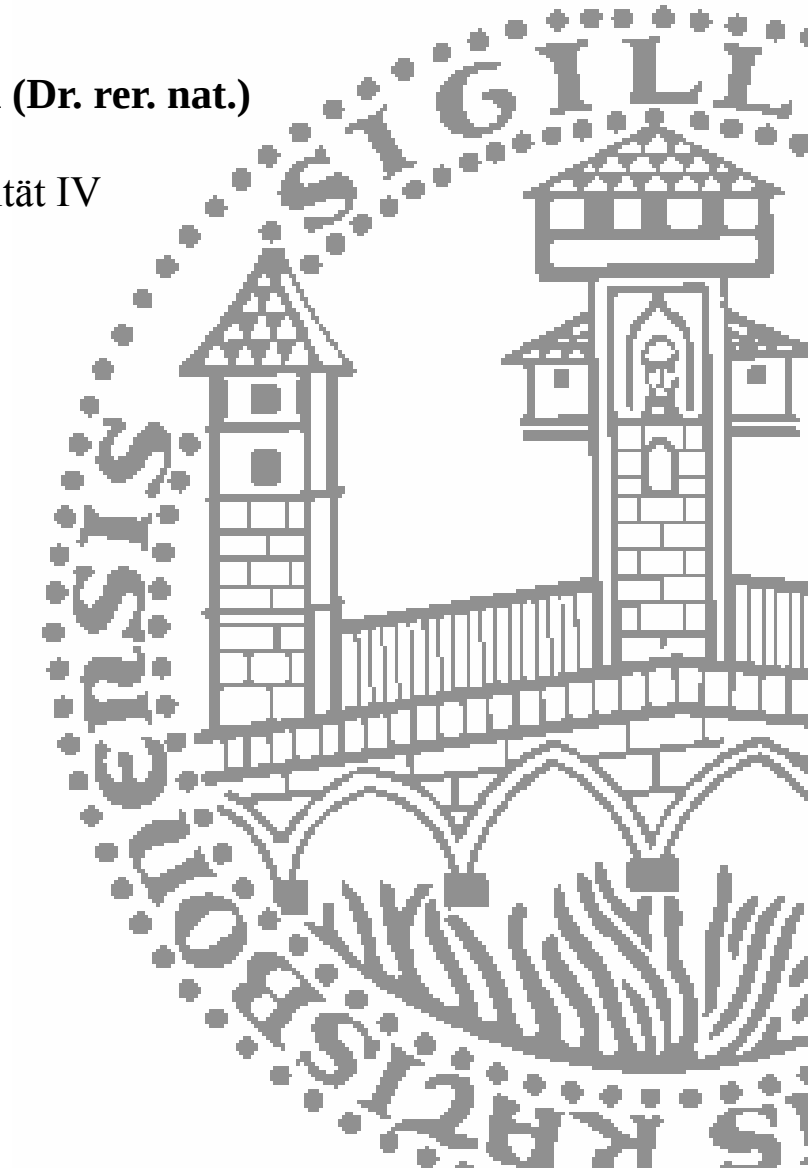

vorgelegt von

Takashi Tsuno

aus Chiba, Japan

November 2007

Synthesis of Optically Active Half-Sandwich Complexes with Bidentate and Tridentate Ligands

Synthese von optisch aktiven Halbsandwich-Komplexen mit zwei- und dreizähnigen Liganden

Dissertation

Zur Erlangung des Doktorgrades

Doktor der Naturwissenschaften (Dr. rer. nat.)

der Naturwissenschaftlichen Fakultät IV ─ Chemie und Pharmazie
der Universität Regensburg

vorgelegt von

Takashi Tsuno

aus Chiba, Japan

November 2007

Prüfungsausschuss: Diese Arbeit wurde angeleitet von Prof. Dr. H. Brunner
Promotionsgesuch eingereicht im September 2007

Vorsitzender:	Prof. Dr. R. Winter
Prufungsausschuss:	Prof. Dr. H. Brunner
	Prof. Dr. Th. Troll
	Prof. Dr. M. Scheer

Die vorliegende Arbeit entstand in der Zeit von April 2003 bis April 2004 am Lehrstuhl Prof. Dr. H. Brunner, Institut für Anorganische Chemie der Universität Regensburg und von Mai 2004 bis Juni 2007 im Department of Applied Molecular Chemistry der Nihon Unuversity, Japan.

Meinen hochgeschätzen Lehrer,

Herrn Prof. Dr. Henri Brunner

danke ich an dieser Stelle sehr herzlich für die ausgezeichneten Arbeitsbedingungen, die ich in Regensburg hatte, und für die vielen Anregungen und Diskussionen in der Zeit seit ich wieder in Japan bin.

Für Rieko,

meinen Sohn Sakuya und meine Tochter Erika

子曰，不患無位，患所以立，不患莫己知，求爲可知也，
論語　里仁第四　十四

Der Meister sagte: "Mach' Dir keine Sorgen um einen guten Posten, sondern Sorge dafür, dass Du etwas hast, mit dem Du ihn verdienst.
Mach' Dir keine Sorgen darüber, dass Dich niemand kennt, sondern trage Sorge, Dich so zu verhalten, dass man Dich kennen wird."
Die Analekten des Konfuzius Lunyu 4.14.

Contents

1 Introduction

1.1 Enantioselective Catalysis with Organometallics

Organometallics, with their metal-carbon bonds, lie at the interface between classical organic and inorganic chemistry in dealing with the interaction between inorganic species and organic molecules. The organometallic field has provided a series of important conceptual insights, surprising structures, and useful catalysts both for industrial processes and for organic synthesis. Optically pure substances are increasingly in demand for pharmaceuticals, agrochemicals, human food additives, and animal food supplements. An optically active organometallic is capable of very high levels of asymmetric induction in preferentially forming one enantiomer of a chiral product. Because an organometallic catalyst reenters each catalytic cycle with its chiral information, large amounts of optically active compounds can be prepared by using small amounts of an optically active organometallic. Public concern for the environment has led to the rise of green chemistry with the object of minimizing both energy use and chemical waste in industry and commerce. A strategy is atom economy in which reactions are chosen that minimize the formation of by-products or unreacted starting materials. Climate change will become severe enough to force government action to mandate the use of renewable resources. Enantioselective catalysis with organometallics will be a promising approach to meet this demand.[1,2)]

1.2 Chiral Three-Legged Piano Stool Complexes

It is generally accepted that the η^5-C_5H_5 ligand occupies three coordination positions at a metal atom. Therefore, all the compounds $[C_5H_5ML^1L^2L^3]$, neutral or cationic, in which M is a transition-metal and L^1, L^2, and L^3 are either two-electron or one-electron ligands, have to be considered as derivatives of the octahedron (Chart 1-1, top) with the C_5H_5 ring occupying three coordination positions *cis* to each other.

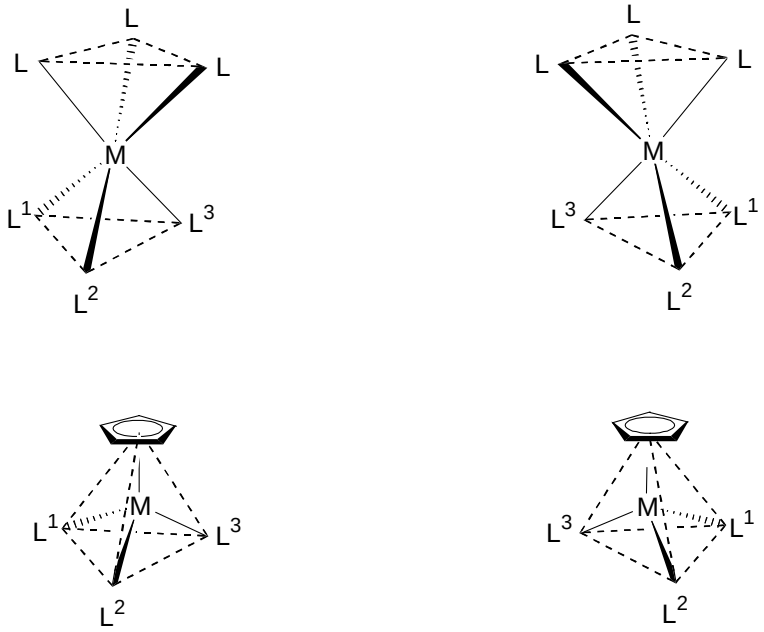

Chart 1-1.

In complexes of the type $[C_5H_5ML^1L^2L^3]$ the transition-metal atom M is surrounded by four different ligands, being an asymmetric center like an asymmetric carbon atom. Thus, for a compound of formula $[C_5H_5ML^1L^2L^3]$ there are two optical isomers, typical for a tetrahedron (Chart 1-1, bottom).[3-5] Such organometallics have *pseudo*-tetrahedral structures and are called three-legged piano-stool complexes or half-sandwich complexes as an idiomatic usage. Brunner and his group initiated a systematic study of *pseudo*-tetrahedral chiral three-legged piano-stool complexes and reported the preparation of optically active manganese complexes (*R*)- and (*S*)-$[C_5H_5Mn(CO)(NO)PPh_3]PF_6$ in 1969.[6,7] These complexes could be isolated via diastereoisomer separations (Scheme 1-1).

Organometallic compounds with a d^6 electron count act as precursors of Lewis acid catalysts in various organic reactions. The perspective of using optically active three-legged piano-stool complexes as chiral catalysts seems appealing in this respect. However, it is imperative to ensure configurational stability of the catalysts, as racemization of the optically active organometallics would result in a loss of the enantiomeric excess of the products.

Design of optically active ligands is a challenging problem. In pioneering studies the monodentate Horner phosphines PPhPrMe, containing chiral P atoms, were introduced as ligands into the rhodium-catalyzed enantioselective hydrogenation of C=C bonds.[8,9] Soon,

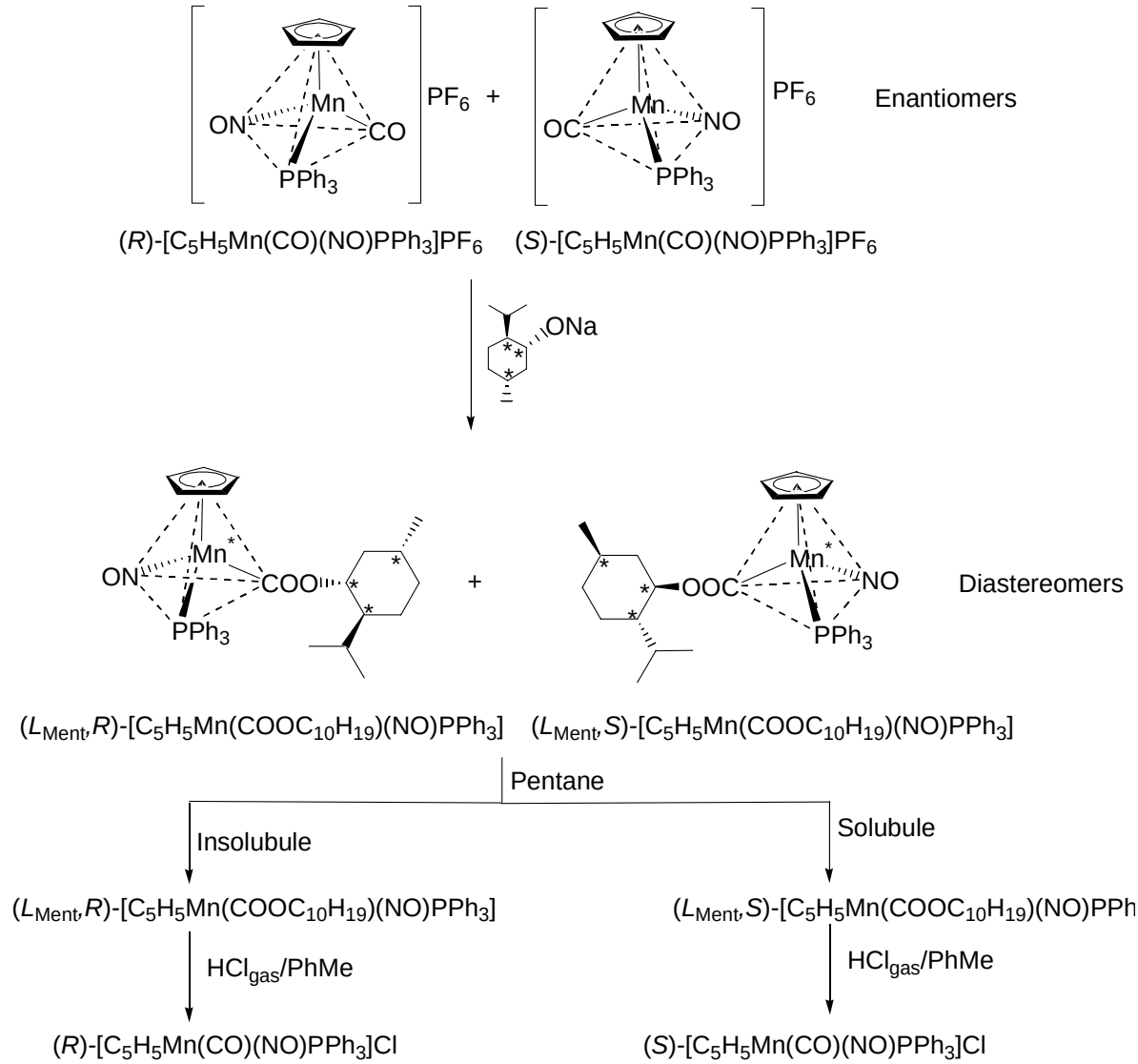

Scheme 1-1.

however, bidentate phosphine ligands took over. Owing to the bidentate binding, a chelated ligand can adopt only a limited number of conformations compared with two univalent ligands, this reduction being advantageous for the optical induction in product formation.[10] The well-known frequently used bisphosphines are shown in Chart 1-2.[11] These ligands are commercially available. In recent years many optically active bidentate ligands including P-N, P-O, N-N, and N-O types have been prepared and used in enantioselective catalysis. In chiral half-sandwich complexes of the type $[C_5H_5ML^1L^2L^3]$ two of the monodentate ligands can be replaced by unsymmetrical chelate ligands such as Prophos or Norphos (Part 4 of this Thesis).

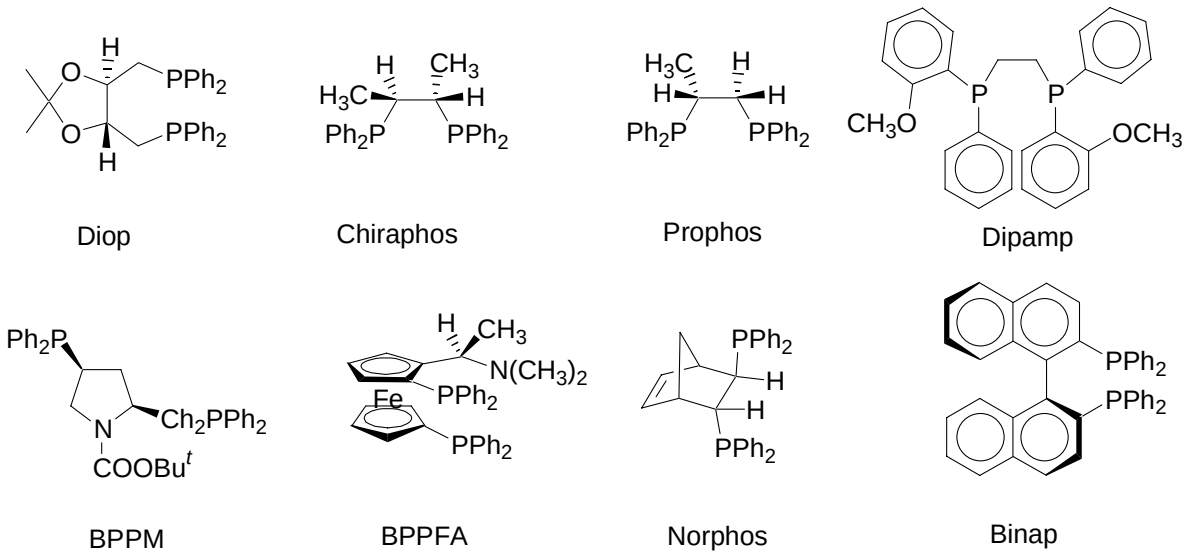

Chart 1-2.

Planar chirality is generated by coordination of unsymmetrically substituted π-ligands to metal atoms.[12,13] Using trisubstituted cyclopentadienes with an anchor diphenylphosphanyl ligand, Takahashi and his group synthesized planar chiral piano-stool complexes which were also chiral at the metal atom (Chart 1-3).[14,15] These complexes were successfully used as asymmetric catalysts for allylic alkylation reactions.[16] Interestingly, in some of the systems described the diastereomer ratio is under thermodynamic control, in others it is under kinetic control. Takahashi's complexes can change the metal configuration by dissociation of one of the unidentate ligands followed by inversion of the resulting pyramidal intermediate. A change of the planar chirality requires a cleavage of the Cp-M bond and a recoordination of the Cp ligand with its other side.

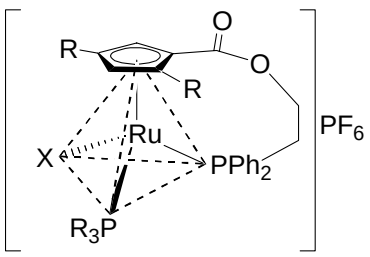

Chart 1-3.

Ward and coworkers designed a novel arene ligand (P-Ar-N) with two different meta-substituents and reported the preparation of planar chiral piano-stool complexes (Scheme 1-

2).[17-19] Diastereomers (R,S_P)- and (R,R_P)-[(PArN)$RuCl_2$] were isolated by flash chromatography. Treatment of the respective diastereomer with TlOTf in THF/H_2O displaced both chlorides to afford (R,S_P,R_{Ru})- and (R,R_P,S_{Ru})-[(PArN)$RuOH_2$]$(OTf)_2$. These complexes may change their planar chirality (and concomitantly their metal configuration) only by dissociation of the metal-arene bond and recoordination of the arene with the other side.

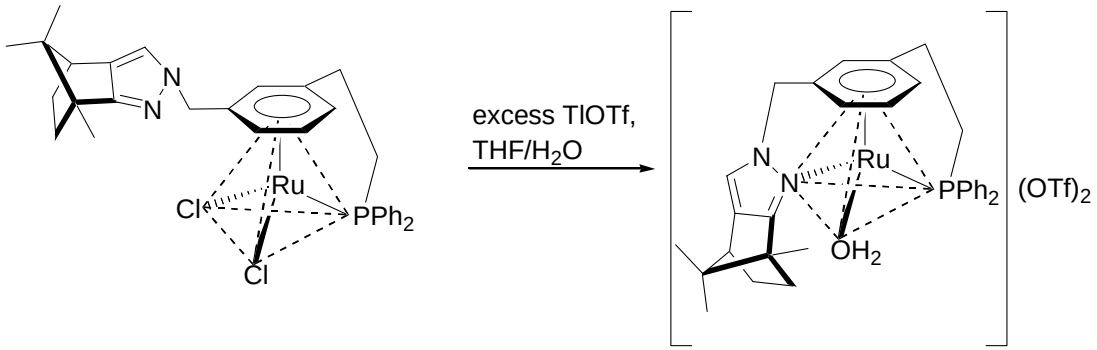

(R,S_P)-[(PArN*)$RuCl_2$] (R,S_P,R_{Ru})-[(PArN*)Ru]$(OTf)_2$

Scheme 1-2.

Dissociation of a monodentate ligand in a three-legged piano-stool complex [η^5-$C_5H_5ML_3$] leaves a two-legged fragment which may be a stable compound or an intermediate ready for subsequent addition reactions. Does a two-legged piano-stool complex [η^5-$C_5H_5ML_2$] maintain its structure with a vacant site in place of the dissociated ligand or does it rearrange simultaneously to its formation or subsequently to give a planar species? The perspective of using three-legged piano-stool complexes as catalyts has already been emphasized. It also has been mentioned that it is important to ensure configurational stability of the catalyst. With respect to chiral-at-metal compounds of the type [η^5-$C_5H_5MLL'X$] that means an intermediate [η^5-C_5H_5MLL'] would retain chirality as long as it is pyramidal, whereas it would lose chirality when it becomes planar. Of course, a good performance of chiral catalysts requires a high pyramidal stability of the intermediates [η^5-C_5H_5MLL']. These issues were studied for the chiral-at-metal half-sandwich compounds [CpMn(NO)(PPh_3)COOR] (R = CH_3 or L-$C_{10}H_{19}$)[4,5] and [CpMn(NO)(PPh_3)C(O)R] (R = CH_3, Ph, p-C_6H_4R')[20], discussed extensively in the introduction to Part 4 of this Thesis. MO calculations showed that fragments [η^n-$C_nH_nM(CO)_2$] are pyramidal, the planar species being transition states, whereas fragments [η^n-$C_nH_nM(PH_3)_2$] adopt planar configurations.[21,22]

It is well known that organometallic derivatives of rhodium and ruthenium are catalysts in many organic reactions and stereochemical implications have been addressed. In particular, for the design of three-legged piano-stool ruthenium complexes as catalysts knowledge of the configurational stability of pyramidal two-legged piano-stool intermediates is essential. Planar two-legged piano-stool complexes [CpRu(PR_3)Hal] were reported[23] and planarity was assigned to species such as $[CpRu(P\text{-}P)]^+$ on the basis of spectroscopy.[24] Furthermore, the planarity was supported by MO calculations.[21] On the other hand, the stereochemistry of halide substitution was investigated by treating [(MentC_5H_4)Ru(PPh_3)(CO)Cl] with NaI and with $AgBF_4$/MeCN followed by NaI, respectively (Scheme 1-3).[25] The substitution reactions were stereospecific taking place with retention of configuration at the metal atom. This result suggests that two-legged piano-stool ruthenium intermediates $[(MentC_5H_4)Ru(PPh_3)(CO)]^+$ are pyramidal.

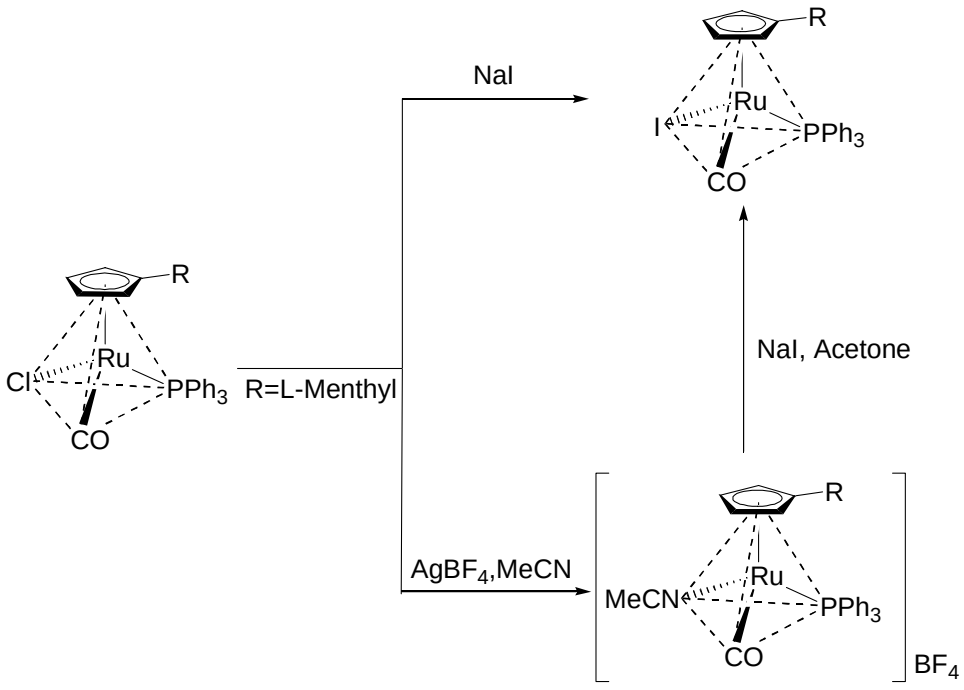

Scheme 1-3.

Consiglio et al. investigated the stereochemical course of reactions of the chiral-at-metal half-sandwich ruthenium complexes (R_C,R_{Ru})-/(R_C,S_{Ru})-[CpRu(Prophos)Cl] in which Prophos is (*R*)-1,2-bis(diphenylphosphanyl)propane. The stereochemical outcome of these reactions implied retention of configuration at the metal atom.[4] Scheme 1-4 shows the displacement of the chloride ligand with acetonitrile which was described to be stereospecific (see below) occurring with retention of configuration at the ruthenium atom.[26,27]

Irrespective of these examples – the last example (R_C,R_{Ru})-/(R_C,S_{Ru})-[CpRu(Prophos)Cl] will have to be modified in Part 4 of this Thesis – the metal configuration in three-legged piano-stool complexes of the type [$C_5H_5ML^1L^2L^3$] tends to change, initiated by dissociation

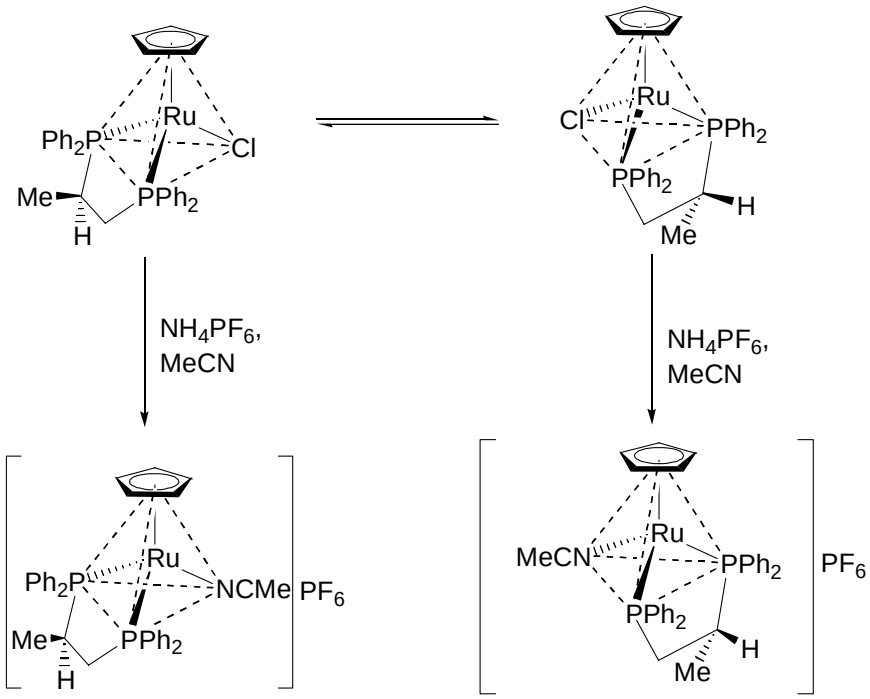

Scheme 1-4.

of one of the monodentate ligands. Therefore, the successful application of chiral-at-metal complexes as effective asymmetric catalysts is still limited due to the inherent lability of the configuration at the metal center. It would be desirable to control the metal configuration such that only a catalyst with a single metal configuration is present during catalysis. New ideas and results concerning the stability of the metal configuration in three-legged piano-stool complexes will be presented in Parts 2, 3, and 4 of this Thesis.

1.3 Purpose and Organization of This Thesis

In Part 2 of this Thesis, chiral three-legged piano-stool rhodium complexes with the bidentate ligand (L_{Ment})-PN_{Ment} and the tripodal ligand (L_{Ment},S_C)-$CpHPN_{Ment}$ are described. Whereas the complexes (L_{Ment},S_C,R_{Rh})- and (L_{Ment},S_C,S_{Rh})-[$CpRh(PN_{Ment})Cl$]X with the bidentate ligand epimerized by a change of the labile metal configuration, the complex (L_{Ment},S_C,R_{Rh})-[($CpPN_{Ment}$)RhCl]X with the tripodal $CpPN_{Ment}$ ligand was obtained with a

fixed metal configuration, unable of any configurational change. Hal substitution reactions in the complex (L_{Ment},S_C,R_{Rh})-[(CpPN$_{Ment}$)RhCl]X with fixed metal configuration occurred with retention of configuration at the metal atom.

As the compounds [(CpPN$_{Ment}$)RhCl]X in Part 2 were salts, in Part 3 neutral Ru complexes with the tripodal ligand (L_{Ment},S_C)-CpHPN$_{Ment}$ are presented. Surprisingly, in these complexes the tripodal ligand bound to the metal atom only via Cp and P, the N$_{Ment}$ arm staying dangling.

In Part 4, the results of Hal exchange and epimerization of the compounds (R_{Ru},S_C)- and (S_{Ru},S_C)-[CpRu(Prophos)Cl] are described. A detailed stereochemical discussion concerning the pyramidal stability of the intermediates (R_{Ru},S_C)- and (S_{Ru},S_C)-[CpRu(Prophos)]$^+$ is presented which corrects and extends ideas and results given in the literature.

Part 2 has been published as a communication (*Organometallics* **2004**, *23*, 4006-4008) and as a full paper (*J. Organomet. Chem.* **2004**, *689* 4244-4262). Part 3 has been published as a full paper (*J. Organomet. Chem.* **2006**, *691*, 2739-2747). Part 4 will be submitted to *Organometallics* as a full paper. Therefore, deviating from the general format of a PhD Thesis, Parts 2, 3, and 4 are presented in their published form with their titles, abstracts, specific introductions, results and discussion sections, experimental parts, and references sections. Consequently, Part 1, the Introduction of this Thesis, will be followed by its own References. The Thesis will end with Part 5, an Appendix containing the details of the X-ray structure determinations.

1.4 Summaries of This Thesis

1.4.1 Summary of Part 2

PN ligands **1** and **2**, derived from 2-diphenylphosphanylmethylpyridine, were synthesized, to which in the backbone a tether to a cyclopentadiene system and for comparison an ^{i}Pr substituent were attached. The chiral compounds were resolved by introduction of a menthoxy substituent into the 2-position of the pyridine system. The tripod ligand **1** contains three different binding sites (Cp, P, and N) connected by a resolved chiral carbon atom. (S_C)-Configuration of this tripod ligand enforces (R_{Rh})-configuration at the metal atom in the half-sandwich rhodium complex (L_{Ment},S_C,R_{Rh})-**4**. The opposite metal configuration is inaccessible.

Substitution of the chloro ligand in (L_{Ment},S_C,R_{Rh})-**4** by halide (Br, I) or pseudohalide (N_3, CN, SCN) ligands occurs with retention of configuration. However, in the reaction of (L_{Ment},S_C,R_{Rh})-**4** with PPh_3 the pyridine arm of the tripod ligand becomes detached from the metal atom. In the Cp*Rh and CpRh compounds of the bidentate PN ligands **2** and **3** both metal configurations are accessible and they equilibrate fast. The stereochemical assignments are corroborated by 4 X-ray analyses.

1.4.2 Summary of Part 3

Treatment of the chiral tripod ligand (L_{Ment},S_C)-CpH(PN_{Ment}) **1** with $(Ph_3P)_3RuCl_2$ in ethanol afforded the two chiral-at-metal diastereomers (L_{Ment},S_C,R_{Ru})- and (L_{Ment},S_C,S_{Ru})-[Cp(PN_{Ment})Ru(PPh_3)Cl] (70% de) in which the cyclopentadienyl group and the P atom of the ligand coordinated at the metal center. The (L_{Ment},S_C,R_{Ru})-diastereomer was isolated by crystallization from ethanol-pentane and its structure was established by X-ray crystallography. The (L_{Ment},S_C,R_{Ru})-diastereomer epimerized in $CDCl_3$ solution at 60 ^oC in a first-order reaction with a half-life of 56.6 h. In alcoholic solution epimerization occurred at room temperature. Substitution of the chloride ligand in (L_{Ment},S_C,R_{Ru})- and (L_{Ment},S_C,S_{Ru})-[Cp(PN_{Ment})Ru(PPh_3)Cl] by nitriles NCR (R = Me, Ph, CH_2Ph) in the presence of NH_4PF_6 gave mixtures of the diastereomers (L_{Ment},S_C,R_{Ru})- and (L_{Ment},S_C,S_{Ru})-[Cp(PN_{Ment})Ru(PPh_3)NCR]PF_6. Treatment of (L_{Ment},S_C,R_{Ru})- and (L_{Ment},S_C,S_{Ru})-[Cp(PN_{Ment})Ru(PPh_3)Cl] with piperidine or morpholine in the presence of NH_4PF_6 led to the chiral-at-metal diastereomers (L_{Ment},S_C,R_{Ru})- and (L_{Ment},S_C,S_{Ru})-[Cp(PN_{Ment})Ru(PPh_3)NH_3]PF_6 (6% de).

1.4.3 Summary of Part 4

The chiral-at-metal diastereomers ($R_{Ru,}R_C$)- and ($S_{Ru,}R_C$)-[CpRu(P-P')Hal], P-P' = (*R*)-Prophos and (*R*,*R*)-Norphos, Hal = Cl, Br, and I, were synthesized, separated, and characterized by X-ray crystallography. In particular, the compounds ($R_{Ru,}R_C$)- and ($S_{Ru,}R_C$)-[CpRu(Prophos)Cl] were investigated which had been the starting material in the preparation of many new compounds with retention of the Ru-configuration. Erroneously, in the 1980's

these compounds had been considered to be configurationally stable at the metal atom. Halide exchange reactions and epimerization studies were carried out in methanol/chloroform mixtures. The rate determining step in these reactions was the dissociation of the Ru-Hal bond in ($R_{Ru,}R_C$)- and ($S_{Ru,}R_C$)-[CpRu(P-P')Hal] forming the 16-electron intermediates ($R_{Ru,}R_C$)- and ($S_{Ru,}R_C$)-[CpRu(P-P')]$^+$ which maintain their pyramidal structures. The Hal exchange reactions proceeded at 0 - 20 ^oC in first-order kinetics with half-lives of minutes/hours and occurred with predominant retention of the metal configuration accompanied by partial epimerization at the metal atom. Interestingly, the thermodynamically less stable ($R_{Ru,}R_C$)-diastereomer of [CpRu(Prophos)Cl] reacted about ten times faster then the thermodynamically more stable ($S_{Ru,}R_C$)-diastereomer. The change of the metal configuration in the epimerization of ($R_{Ru,}R_C$)- and ($S_{Ru,}R_C$)-[CpRu(P-P')Hal] took place in methanol containing solvents about 50 ^oC in first-order reactions with half-lives of minutes/hours. In $CDCl_3/CD_3OD$ mixtures the equilibrium composition ($R_{Ru,}R_C$)-/($S_{Ru,}R_C$)-[CpRu(Prophos)Cl] was 15:85. The rates of Hal exchange and epimerization increased by a factor of about 10 in going from $CDCl_3/CD_3OD$ 9:1 to 1:1 due to better solvation of the ions formed in the rate-determining step. Hal exchange reactions and epimerization studies indicated a high pyramidal stability of the 16-electron fragments ($R_{Ru,}R_C$)- and ($S_{Ru,}R_C$)-[CpRu(P-P')]$^+$ towards inversion. This is surprising because calculations had shown that 16-electron fragments [CpM(PH_3)$_2$]$^+$ with P-M-P angles around 100 ^{o} should have planar structures. Obviously, pyramidality of the fragments [CpRu(P-P')]$^+$ is enforced by the small P-Ru-P angles of 82 - 83 ^{o} observed in the X-ray analyses of the chelate compounds ($R_{Ru,}R_C$)- and ($S_{Ru,}R_C$)-[CpRu(P-P')Hal]. These small angles resist planarization of the intermediates ($R_{Ru,}R_C$)- and ($S_{Ru,}R_C$)-[CpRu(P-P')]$^+$ and thus inversion of the metal configuration. The results are in accord with a basilica-type energy profile which has a relatively high barrier between the pyramidal intermediates ($R_{Ru,}R_C$)- and ($S_{Ru,}R_C$)-[CpRu(P-P')]$^+$ (Schemes 4-3 and 4-4).

1.5 References

1. Ojima, I. *Catalytic Asymmetric Synthesis*, Wiley, New York, **2000**.
2. Morrison, J. D. *Asymmetric Synthesis, Vol. V*, Academic Press, Orlando, **1985**.
3. Brunner, H. *Adv. Organomet. Chem.* **1980**, *18*, 151.
4. Consiglio, G.; Morandini, F. *Chem. Rev.* **1987**, *87*, 761.
5. Brunner, H. *Angew. Chem., Int. Ed. Engl.* **1999**, *38*, 1194.

6. Brunner, H. *Angew. Chem., Int. Ed. Engl.* **1969**, *8*, 382.
7. Brunner, H; Schindler, H.-D. *J. Organomet. Chem.* **1970**, *24*, C7.
8. Horner, L.; Siegel, H.; Büthe, H. *Angew. Chem., Int. Ed. Engl.* **1968**, *7*, 942.
9. Knowles, W. S.; Sabacky, M. *J. Chem. Soc., Chem. Commun.* **1968**, 1445.
10. Brunner, H. *Angew. Chem., Int. Ed. Engl.* **1983**, *22*, 897.
11. Brunner, H.; Zettlmeier, W. *Handbook of Enantioselective Catalysis with Transition Metal Compounds*, VCH, Weinheim, **1993**.
12. Halterman, R. L. *Chem. Rev.* **1992**, *92*, 965.
13. Paley, R. S. *Chem. Rev.* **2002**, *102*, 1493.
14. Dodo, Matsushima, Y.; Uno, M.; Onitsuka, K.; Takahashi, S. *J. Chem. Soc., Dalton Trans.* **2000**, *35*.
15. Matsushima, Y.; Onitsuka, K.; Takahashi, S. *Dalton Trans.* **2004**, *547*.
16. Onitsuka, K.; Matsushima, Y.; Takahashi, S. *Organometallics* **2005**, *24*, 6472.
17. Therrien, B.; König, A.; Ward, T. R. *Angew. Chem., Int. Ed.* **1999**, *38*, 405.
18. Therrien, B.; König, A.; Ward, T. R. *Organometallics* **1999**, *18*, 1565.
19. Therrien, B.; Ward, T. R. *Acta Cryst. C:* **2000**, *C56*, e561.
20. Brunner, H. *J. Organomet. Chem.* **1974**, *94*, 189.
21. Hofmann, P. *Angew. Chem., Int. Ed. Engl.* **1977**, *16*, *536.*
22. Ward, T. R.; Schafer, O.; Claude, D.; Hofmann, P. *Organometallics* **1997**, *16*, 3207.
23. Campion, B. K.; Heyn, R. H.; Tilley, T. D.; Hofmann, P. *J. Chem. Soc., Chem. Commun.* **1988**, 278.
24. Joslin, F. L.; Johnson, M. P.; Maque, J. T.; Roundhill, D. M. *Organometallics* **1991**, *10*, 2781.
25. Cesarotti, E.; Angoletta, M.; Walker, N. P., C.; Hursthouse, M. B.; Vefghi, R.; Schofield, P. A.; White, C. *J. Organomet. Chem.* **1985**, *95*, 322.
26. Consiglio, G.; Morandini, F.; Bangerter, F. *Inorg. Chem.* **1982**, *21*, 455.
27. Morandini, F.; Consiglio, G.; Straub, B.; Ciani, G.; Sironi, A. *J. Chem. Soc., Dalton Trans.* **1983**, 2293.

2. Stabilization of the Labile Metal Configuration in Half-Sandwich Complexes [CpRh(PN)Hal]X

2.1 Abstract

PN ligands **1** and **2**, derived from 2-diphenylphosphanylmethylpyridine, were synthesized, to which in the backbone a tether to a cyclopentadiene system and for comparison an ^{i}Pr substituent were attached. The chiral compounds were resolved by introduction of a menthoxy substituent into the 2-position of the pyridine system. The tripod ligand **1** contains three different binding sites (Cp, P, and N) connected by a resolved chiral carbon atom. (S_C)-Configuration of this tripod ligand enforces (R_{Rh})-configuration at the metal atom in the half-sandwich rhodium complex (L_{Ment},S_C,R_{Rh})-**4**. The opposite metal configuration is inaccessible. Substitution of the chloro ligand in (L_{Ment},S_C,R_{Rh})-**4** by halide (Br, I) or pseudohalide (N_3, CN, SCN) ligands occurs with retention of configuration. However, in the reaction of (L_{Ment},S_C,R_{Rh})-**4** with PPh_3 the pyridine arm of the tripod ligand becomes detached from the metal atom. In the Cp*Rh and CpRh compounds of the bidentate PN ligands **2** and **3** both metal configurations are accessible and they equilibrate fast. The stereochemical assignments are corroborated by 4 X-ray analyses.

2.2 Introduction

In three-legged piano-stool complexes of the type [(η^n-Ar)M(LL')X], L-L' = unsymmetrical chelate ligand and X = monodentate ligand, the metal atom is a chiral center. With an enantiomerically pure chelate ligand, e.g. an ^{i}Pr-substituted (S_C)-configurated PN ligand, two diastereomers (S_C,R_{Rh}) and (S_C,S_{Rh}) arise in compounds of the type [(η^5-C_5H_5)Rh(PN)Cl]PF_6 (Scheme 2-1, top), which only differ in the metal configuration.[1-3] In solution these compounds epimerize by a change of the labile metal configuration initiated by dissociation of the monodentate ligand or by chelate ring opening.[4,5] Compounds of this type are catalysts in organic transformations, such as transfer hydrogenation, isomerization, Diels-Alder reactions, etc.[6-8]

As usually the epimerization at the metal atom is much faster than the catalytic reaction, two diastereomeric catalysts are present.[6,7] It is known that the stereochemistry of reactions occurring at a metal center strongly depend on the metal configuration.[9] Thus, reaction channels with diastereomeric catalysts differing in the metal configuration tend to produce products with opposite configuration. Diastereomer equilibria in chiral-at-metal half-sandwich complexes may

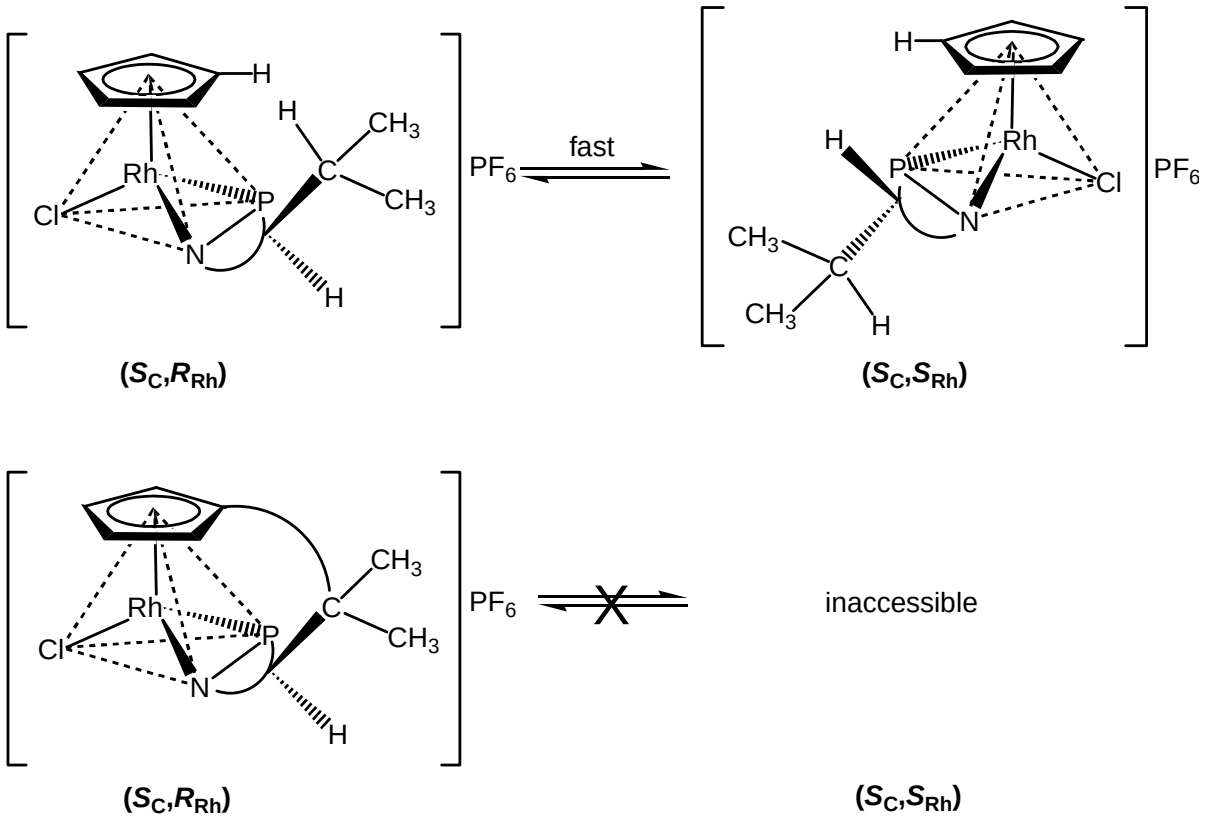

Scheme 2-1.

lie between 50:50 and 99:1.[10-13] However, although in a 99:1 equilibrium one of the two diastereomers is dominating by two powers of ten, this is no general solution of the problem, because the more stable isomer may be the less reactive catalyst and vice versa as shown for diastereomeric complexes of prochiral olefins bonded to Rh(LL*) fragments in asymmetric hydrogenations.[14] Therefore, it would be desirable to control the metal configuration such that only a catalyst with a single metal configuration is present during catalysis. This part of the Thesis deals with a new tripod ligand CpH(PN_{Ment}) which fix the metal chirality inhibiting any configurational change. This ligand has three different binding sites, a cyclopentadiene system (CpH), a diphenylphosphanyl group (P) and a pyridine ring (N_{Ment}) connected by an asymmetric carbon atom. This part also discloses the bidentate ligand PN_{Ment}. The tripod ligand CpH(PN_{Ment})

afforded cationic half-sandwich complexes with $RhCl_3 \cdot 3H_2O$ in which only one additional chloro ligand is bonded to the Rh atom. For comparison the corresponding complexes with a combination of the bidentate ligand PN_{Ment} with a separated Cp or Cp* ligand were synthesized. Due to the L-menthyl substituent diastereomers arise with respect to the configuration of the branching position (R_C)/(S_C) and the metal configuration (R_{Rh})/(S_{Rh}). Fortunately, these diastereomers differ in their ^1H and $^{31}P\{^1H\}$ NMR spectra allowing to monitor separation procedures and to determine diastereomer ratios. In addition, the synthesis of the ligands CpH(PN) and PN, devoid of the L-menthyl substituent and, thus, the source of diastereomerism, and their complexes is included in the present study.[15,16)]

2.3 Results and Discussion

2.3.1 Syntheses of Ligands

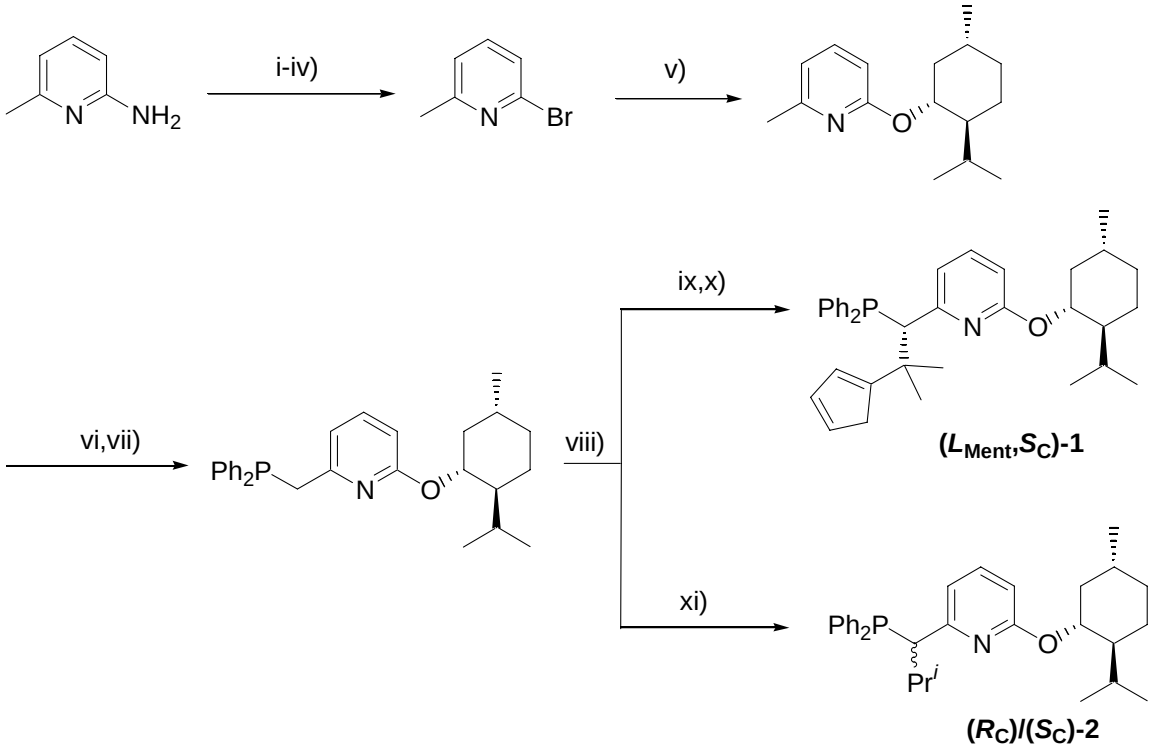

i) 48% HBr, 0 °C; ii) Br_2, 0 °C; iii) $NaNO_2$, < 5 °C; iv) NaOH(aq) < 20 °C; v) 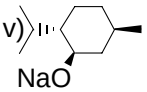 ;

vi) BuLi, Ether, -30 °C; vii) Ph_2PCl, Ether, -80 °C and then r.t. 20 h; viii) BuLi, 0 °C and then r.t. 1 h; ix) 6,6-dimethylfulvene, 20 °C, 20 h; x) recrystallization from pentane, -40 °C; xi) *i*-PrI, 20 °C, r.t.

Scheme 2-2.

The ligands **1** and **2** were prepared as a mixture of diastereomers according to Köllnberger's method (Scheme 2-2).[16,17] The tripod ligand **1** which has (*S*)-configuration at the branching position bonding three different coordination sites was obtained from recrystallization of pentane at -40 °C. The absolute configuration of **1** had been determined by X-ray crystallography.[16,17] Diastereomers **2** could not be separately isolated.

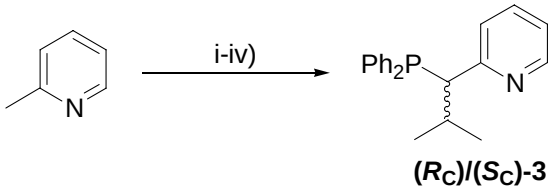

i) BuLi, Ether, -5 °C; ii) Ph_2PCl, Ether, -78 °C and then 20 °C, 10 h;
iii) BuLi, 0 °C; iv) *i*-PrI, full stop after 20 h

Scheme 2-3.

The racemic ligand **3** was prepared similar to ligand **2** (Scheme 2-3).

2.3.2 The Configurationally Stable Tripod Complex and the Substitution of Its Chloro Ligand with Retention of Configuration

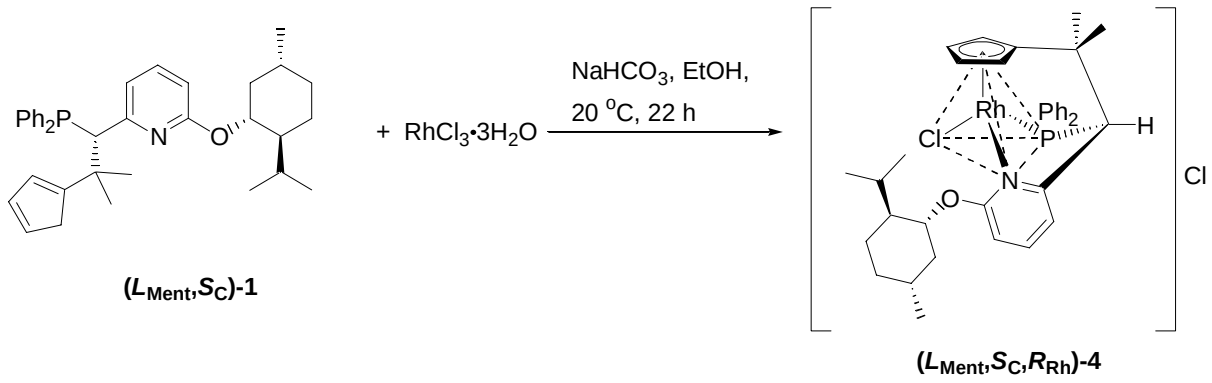

Scheme 2-4.

Complexation of (L_{Ment},S_C)-**1** with $RhCl_3 \cdot 3H_2O$ in ethanol at room temperature afforded the complex (L_{Ment},S_C,R_{Rh})-**4** (Scheme 2-4). After a few minutes an orange precipitate was formed, which dissolved within some hours indicating that ligand (L_{Ment},S_C)-**1** coordinated slowly and stepwise to the metal center. After 24 h the red-orange compound (L_{Ment},S_C,R_{Rh})-**4** was precipitated with pentane. It is soluble in polar solvents, such as alcohols or chlorinated solvents, and it is air-stable not only in the solid state but also in solution.

Interestingly, the cyclopentadiene isomerism present in ligand (L_{Ment},S_C)-**1** disappeared on complexation to (L_{Ment},S_C,R_{Rh})-**4**, because a cyclopentadienyl system without stereogenicity was formed. Consequently, the $^{31}P\{^1H\}$ NMR spectrum of (L_{Ment},S_C,R_{Rh})-**4** showed only one doublet at 72.6 ppm with a P-Rh coupling of 145 Hz. The configuration at the rhodium atom was assigned on the basis of the ligand priority sequence Cp > Cl > P > N.[18,19)]

Remarkably, the ligand (L_{Ment},S_C)-**1** can only form the complex (L_{Ment},S_C,R_{Rh})-**4**. The (S_{Rh})-configuration is inaccessible for the metal atom (Scheme 2-1 bottom). Thus, the (S_C)-configuration of the α-carbon of the ligand predetermines the (R_{Rh})-configuration of the metal center.[20)] Even if ligand arms dissociate from the metal center, the chirality at the metal atom does not get lost, because on coming back the original (R_{Rh})-configuration inevitably is restored. Heating a sample of (L_{Ment},S_C,R_{Rh})-**4** at 60 °C for 3 days did not show any epimerization,

whereas similar compounds lacking the ligand tether typical for (L_{Ment},S_C,R_{Rh})-**4** (see below) epimerized already under mild conditions by change of the metal configuration. Clearly, the opposite metal configuration (S_{Rh}) is only accessible with the other diastereomer (L_{Ment},R_C)-**1**. There has been a different approach to fix the metal configuration in (η^6-arene)ruthenium complexes using planar chirality.[21,22] The synthesis of chiral CpH(PP') and IndH(PP') ligands has been described.[23] However, they have been used in complexation studies unresolved with respect to the branching position.

Complex (L_{Ment},S_C,R_{Rh})-**4** is an air-stable, unreactive compound. Activation for catalysis should be possible by chloride abstraction to give a Lewis acidic fragment. Furthermore, the easily accessible ligand (L_{Ment},R_C)-**1** should form compounds similar to (L_{Ment},S_C,R_{Rh})-**4** with a variety of transition metal precursors. Here, a comparison of complexes of $CpPN_{Ment}$ systems with complexes containing a combination of a Cp and a PN_{Ment} ligand will demonstrate the value of a fixed metal configuration.

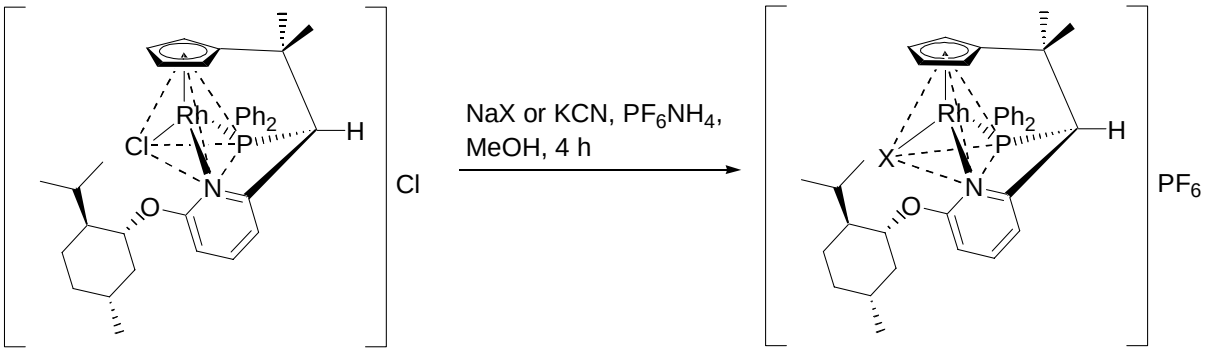

(L_{Ment},S_C,R_{Rh})-**4**

(L_{Ment},S_C,S_{Rh})-**5**: X = Br
(L_{Ment},S_C,S_{Rh})-**6**: X = I
(L_{Ment},S_C,S_{Rh})-**7**: X = N_3
(L_{Ment},S_C,R_{Rh})-**8**: X = CN
(L_{Ment},S_C,S_{Rh})-**9**: X = SCN

Scheme 2-5.

The predetermination of the metal configuration by the tripod ligand (L_{Ment},S_C)-**1** implies that substitution reactions of the chloro ligand in (L_{Ment},S_C,R_{Rh})-**4** must occur with retention of the metal configuration. Stirring (L_{Ment},S_C,R_{Rh})-**4** with an excess of NaBr or NaI in methanol at room

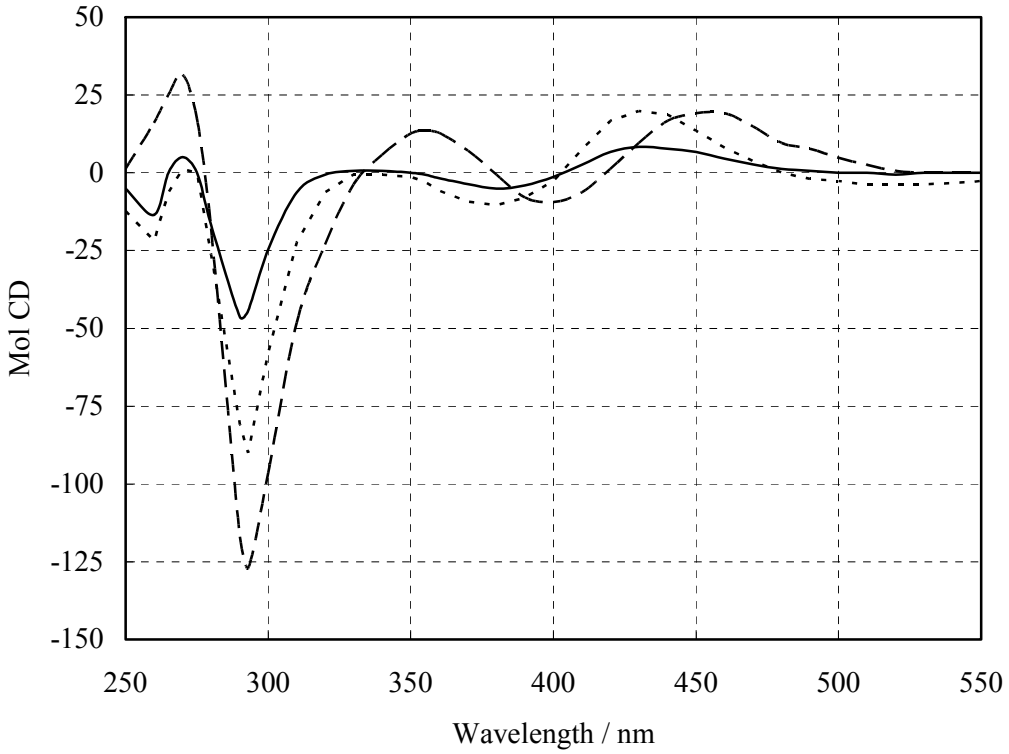

Figure 2-1. CD spectra of (L_{Ment},S_C,R_{Rh})-**4** (c = 2.4 × 10^{-4} mol L^{-1}: ———), of its Br analog (L_{Ment},S_C,S_{Rh})-**5** (c = 2.3 × 10^{-4} mol L^{-1}: – – – –) and of its I analog (L_{Ment},S_C,S_{Rh})-**6** (c = 2.2 × 10^{-4} mol L^{-1}: — — —) in CH_2Cl_2.

temperature and subsequent addition of NH_4PF_6 afforded the bromo and iodo derivatives (L_{Ment},S_C,S_{Rh})-**5** and (L_{Ment},S_C,S_{Rh})-**6** (Scheme 2-5). The priority sequence of the ligands for (L_{Ment},S_C,R_{Rh})-**4** was described above, whereas for the corresponding bromo and iodo compounds it is Br(I) > Cp > P > N which leads to different configurational symbols for the same relative configurations. Characteristic for the CD spectra is a strong negative Cotton effect around 280-290 nm. The similarity of the CD spectra of the chloro, bromo and iodo complexes in Fig. 2-1 is in accordance with the same configuration at the metal center.

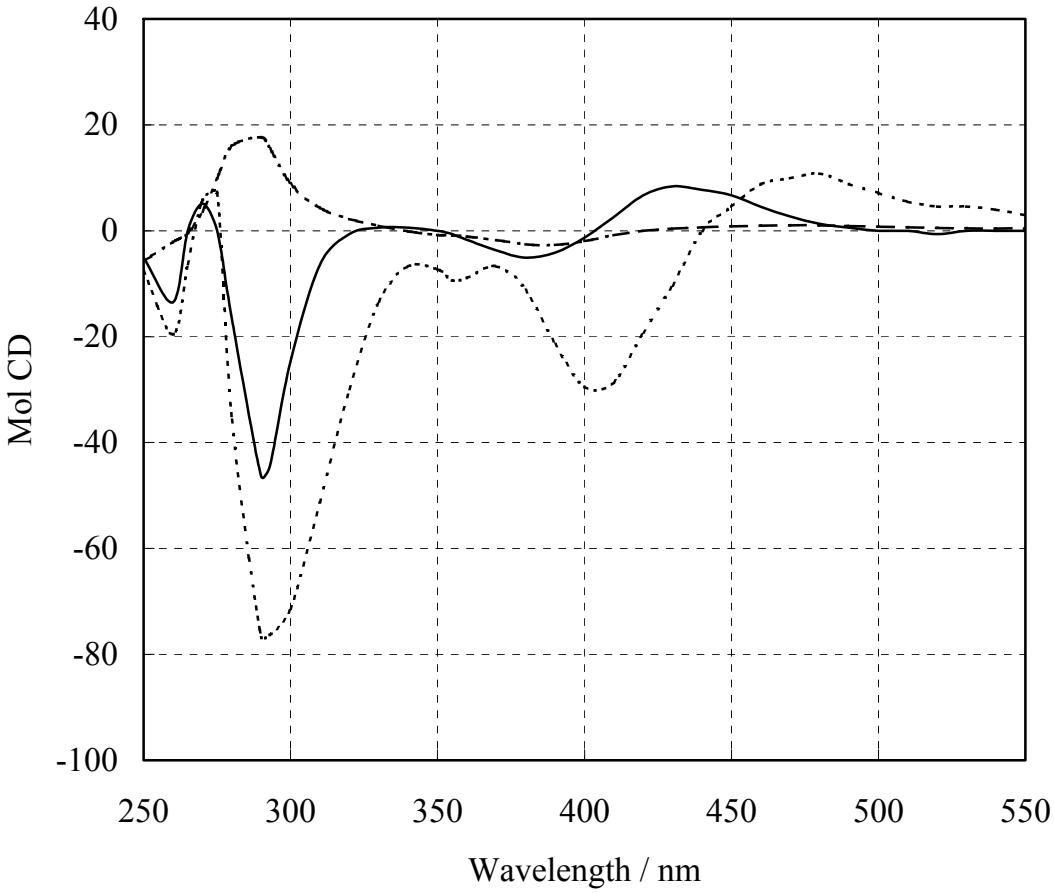

Figure 2-2. CD spectra of (L_{Ment},S_C,R_{Rh},)-**4** (c = 2.4 × 10^{-4} mol L^{-1}: ——), (L_{Ment},S_C,S_{Rh},)-**10** (c = 1.9 × 10^{-4} mol L^{-1}: – – – –), and (L_{Ment},S_C,R_{Rh},)-[Cp(PN_{Ment})Ru(PPh_3)Cl] (c = 1.4 × 10^{-4} mol L^{-1}: ———) in CH_2Cl_2.

Reaction of (L_{Ment},S_C,R_{Rh})-**4** with NaN_3, KCN and NaSCN, respectively, afforded the corresponding azido, cyano and thiocyanato substitution products (L_{Ment},S_C,S_{Rh})-**7**, (L_{Ment},S_C,R_{Rh})-**8** and (L_{Ment},S_C,R_{Rh})-**9** (Scheme 2-5). The configurations at rhodium atom were assigned on the bases of the ligand priority sequence Cp > S > P > N_3 > N > CN.[18,19] The CD spectra were similar to the chloro complex except the thiocyanato compound, the 290 nm CD band of which had the same position but double intensity. This is interpreted as an indication that the ambidentate SCN^- ligand binds via the soft sulfur atom and not the hard nitrogen atom as, e.g. in the azido complex. Increase of the band intensity is also observed in Fig. 2-1 in going from the hard chloro ligand to the soft iodo ligand.

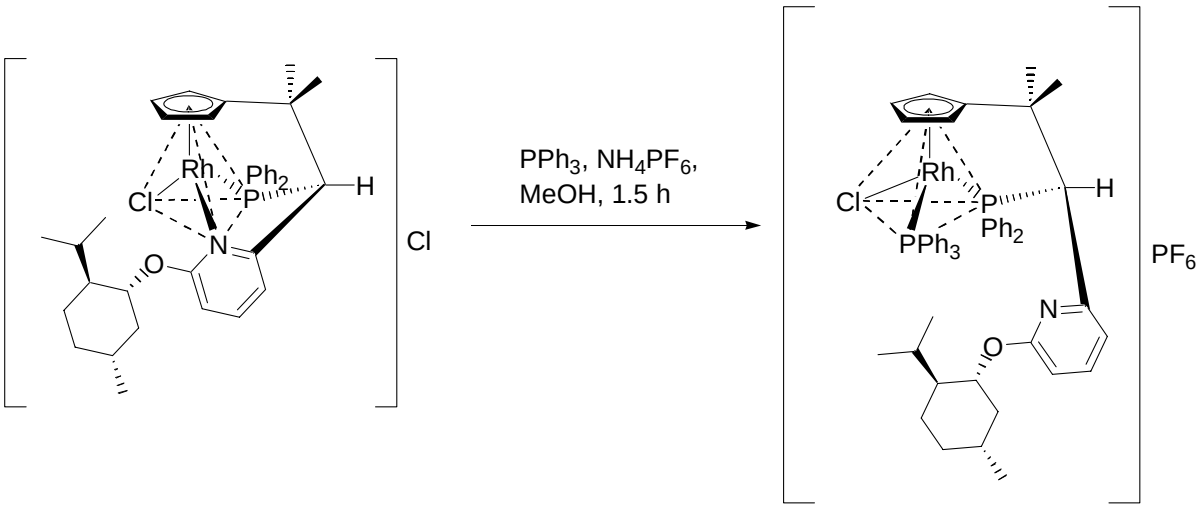

(L_{Ment},S_C,R_{Rh})-4 (L_{Ment},S_C,S_{Rh})-10

Scheme 2-6.

The chloro complex (L_{Ment},S_C,R_{Rh})-**4** underwent clean substitution with PPh_3 in the presence of NH_4PF_6 to produce complex **10** in quantitative yield (Scheme 2-6). The CD spectrum of the orange substitution product was similar to the chloro complex (Fig. 2-2). However, the mass spectrum (ESI in CH_2Cl_2) of substitution product **10** showed the peak for the cation at *m/z* 936 and not as expected for a Cl^- substitution at *m/z* 901 which indicated the presence of a chlorine atom along with a PPh_3 ligand in the cation. Therefore, on the basis of the mass spectral data as well as the elemental analysis which also showed the presence of Cl, it had to be assumed that during the substitution the pyridine-rhodium bond broke resulting in the formation of **10** having the central rhodium atom coordinated to Cp and P only of the tripod together with the two monodentate ligands Cl and PPh_3 (Scheme 2-6). The chloro ligand remained a constituent of the cation. Thus, in this case it was not the chloro ligand which was replaced but the pyridine system of the tripod ligand. In the CD spectrum of the complex **10** a negative Cotton effect was observed at 290 nm in CH_2Cl_2, whereas (L_{Ment},S_C,R_{Ru})-[Cp(PN_{Ment})Ru(PPh_3)Cl] (Chart 2-1), which was characterized by an X-ray analysis, showed a positive Cotton effect at 286 nm (Fig. 2-2).[24] The CD spectra suggest that complex **10** has the opposite metal configuration compared to (L_{Ment},S_C,R_{Ru})-[Cp(PN_{Ment})Ru(PPh_3)Cl], i.e., the chirality of rhodium is (S_{Rh}). The ligand priority sequence of complexes of the type [Cp(PN_{Ment})M(PPh_3)Cl] is Cp > Cl > PPh_3 > PPh_2. In this Thesis the chemistry of the chiral-at-metal half-sandwich complexes of ruthenium involving (L_{Ment},S_C,R_{Ru})-[Cp(PN_{Ment})Ru(PPh_3)Cl] will be fully discussed in Part 3.

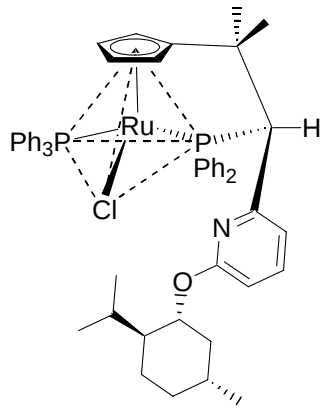

(L_{Ment},S_C,R_{Ru})-[Cp(PN$_{Ment}$)Ru(PP$_3$)Cl]

Chart 2-1.

2.3.3 Half-Sandwich Rh Complexes with Bidentate PN Ligands

Formal cleavage of the C-C bond between the cyclopentadienyl ring and the CMe_2 group of the tether to the branching position in (L_{Ment},S_C,R_{Rh})-**4** results in a combination of a Cp ligand and the bidentate PN_{Ment} (L_{Ment},S_C)-**2**. As shown in Scheme 2-7, for such a ligand combination two different metal configurations (R_{Rh}) and (S_{Rh}) are accessible. Therefore, compounds of type (L_{Ment},S_C)(R_{Rh})- and (L_{Ment},S_C)(S_{Rh})-[CpRh(PN$_{Ment}$)Cl]X (both metal configurations possible) should be prepared and contrasted with tripod complexes (L_{Ment},S_C,R_{Rh})-[(CpPN$_{Ment}$)RhCl]X (fixed metal configuration) such as (L_{Ment},S_C,R_{Rh})-**4**. As the pentamethylcyclopentadienyl (η^5-C_5Me_5 = Cp*) compounds of rhodium are more stable than the cyclopentadienyl (η^5-C_5H_5 = Cp) compounds, the Cp*-derivatives are included in the present study.

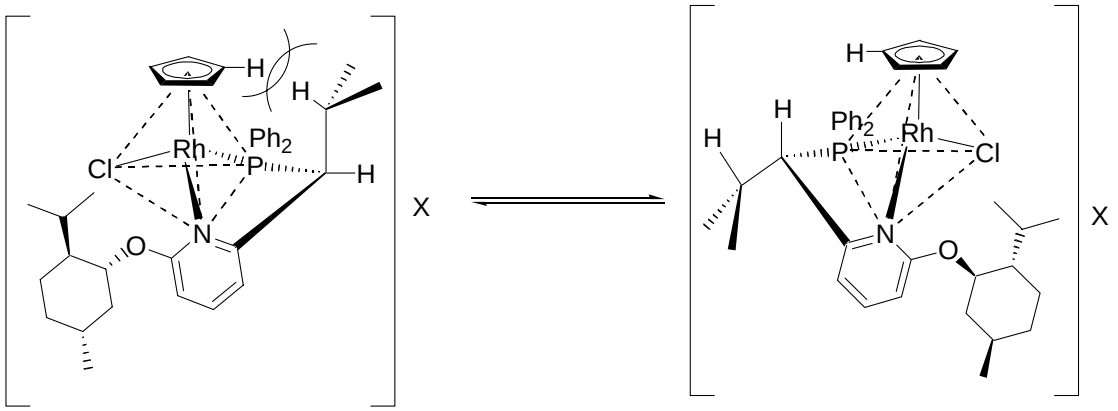

(L_{Ment},S_C)(R_{Rh})-[CpRh(PN$_{Ment}$)Cl]X **(L_{Ment},S_C)(S_{Rh})-[CpRh(PN$_{Ment}$)Cl]X**

Scheme 2-7.

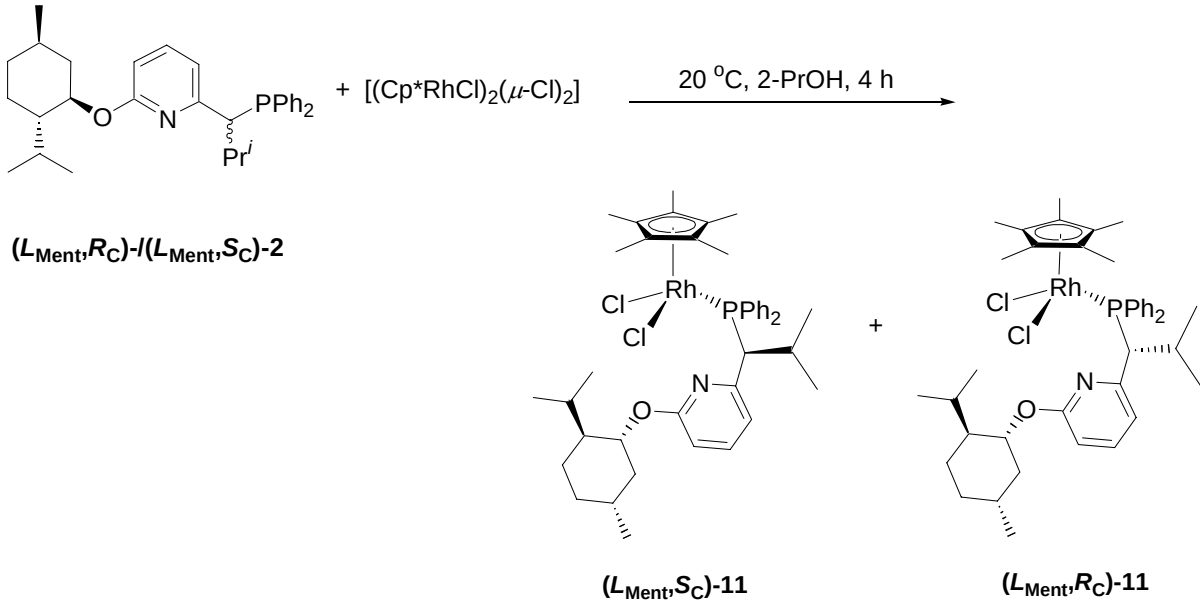

Scheme 2-8.

Reaction of $[(Cp^*RhCl)_2(\mu\text{-}Cl)_2]$ with a 1 : 1 mixture of the diastereomers (L_{Ment},R_C)- and (L_{Ment},S_C)-**2** afforded two products (Scheme 2-8). One of the products was isolated in pure form as a sparingly soluble material by washing the mixture of diastereomers with ether. The other was obtained purely by silica gel chromatography of the concentrated mother liquor. ESI-MS

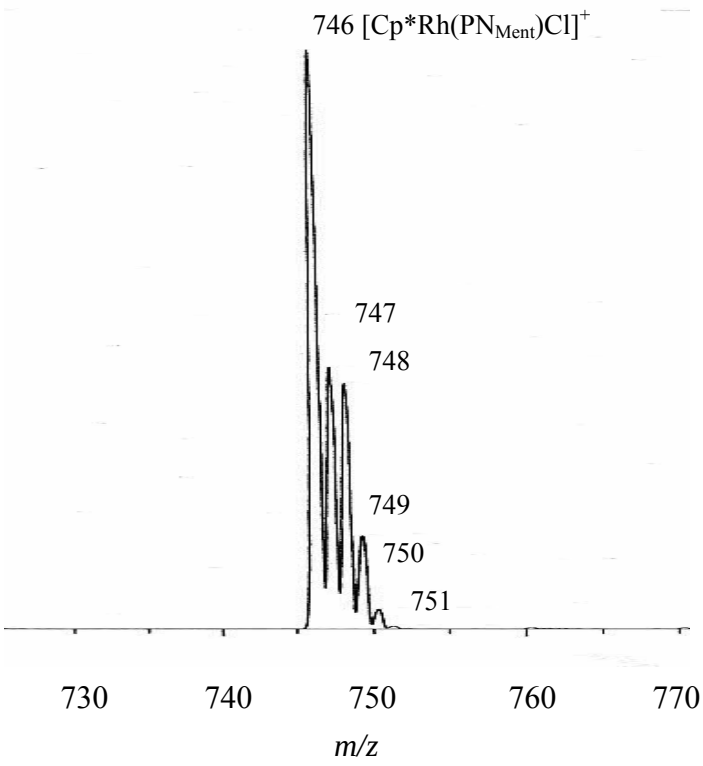

Figure 2-3. ESI-MS spectrum of (L_{Ment},R_C)-**11**.

spectra of both diastereomers exhibited an envelope of peaks with *m/z* 746-751 (Fig. 2-3), having the maximum relative intensity at *m/z* 746 characteristic of $[Cp^*Rh(PN_{Ment})Cl]^+$.

The ^1H and $^{31}P\{^1H\}$ NMR spectra of these products are shown in Figs. 2-4 and 2-5, respectively. As they are diastereomers, their NMR spectra are very similar. The phosphorus signals of the diastereomers appeared at ca. 30 ppm as doublets having $^1J_{P\text{-}Rh}$ = 141 Hz, while that of (L_{Ment},S_C,R_{Rh})-**4** was observed at 72.6 ppm ($^1J_{P\text{-}Rh}$ = 145 Hz). Thus, in the $^{31}P\{^1H\}$ NMR spectra of the diastereomers, the phosphorus signals displayed an upfield shift (ca. 43 ppm) as compared to that in (L_{Ment},S_C,R_{Rh})-**4**. It has been reported that the phosphorus, which is coordinated at rhodium in neutral complexes of the type $[Cp^*Rh(Ph_2PR)Cl_2]$, exhibited its signal at 24.4-32.5 ppm in the $^{31}P\{^1H\}$ NMR spectrum (Chart 2-2).[25-28] By comparison of the chemical shifts of the phosphorus in the complexes, it is obvious that the new diastereomers are neutral complexes $[Cp^*Rh(PN_{Ment})Cl_2]$ with a dangling pyridinyl moiety.

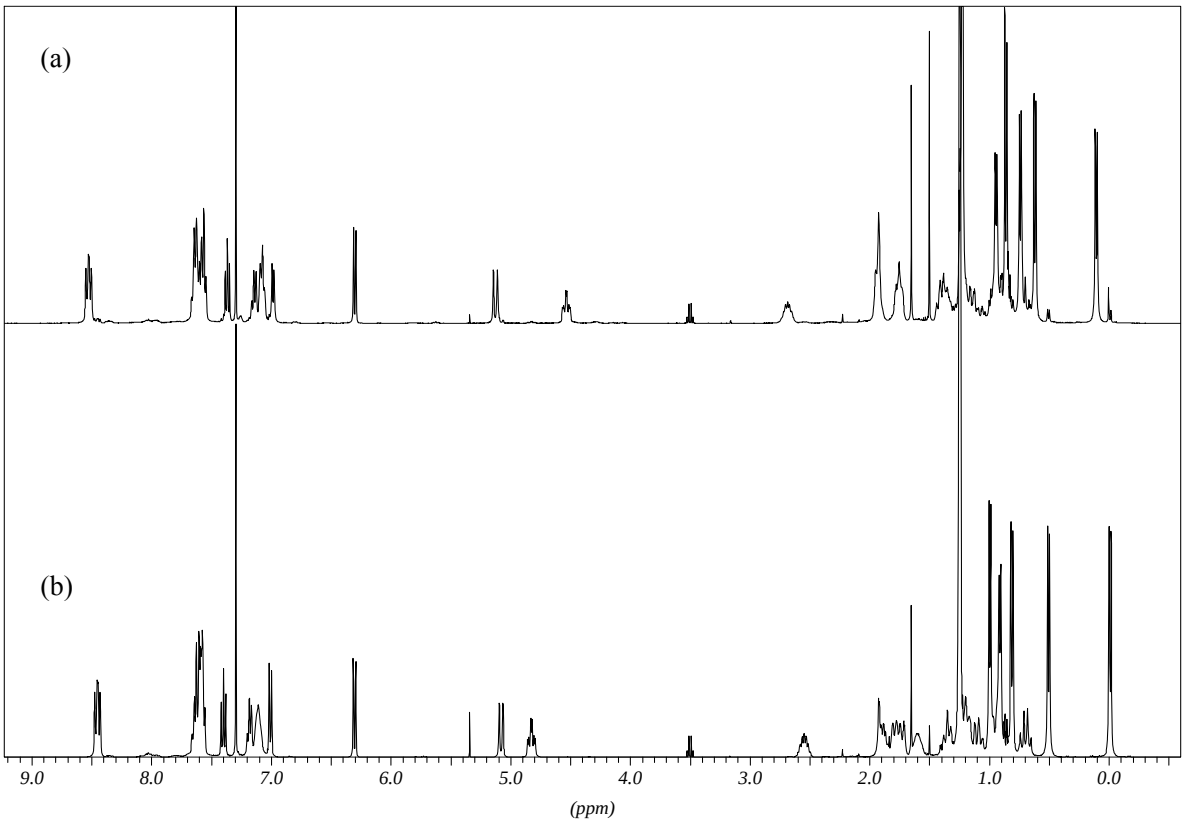

Figure 2-4. ^1H NMR spectra of (L_{Ment},R_C)-**11** (a) and (L_{Ment},S_C)-**11** (b) in $CDCl_3$ at 253 K.

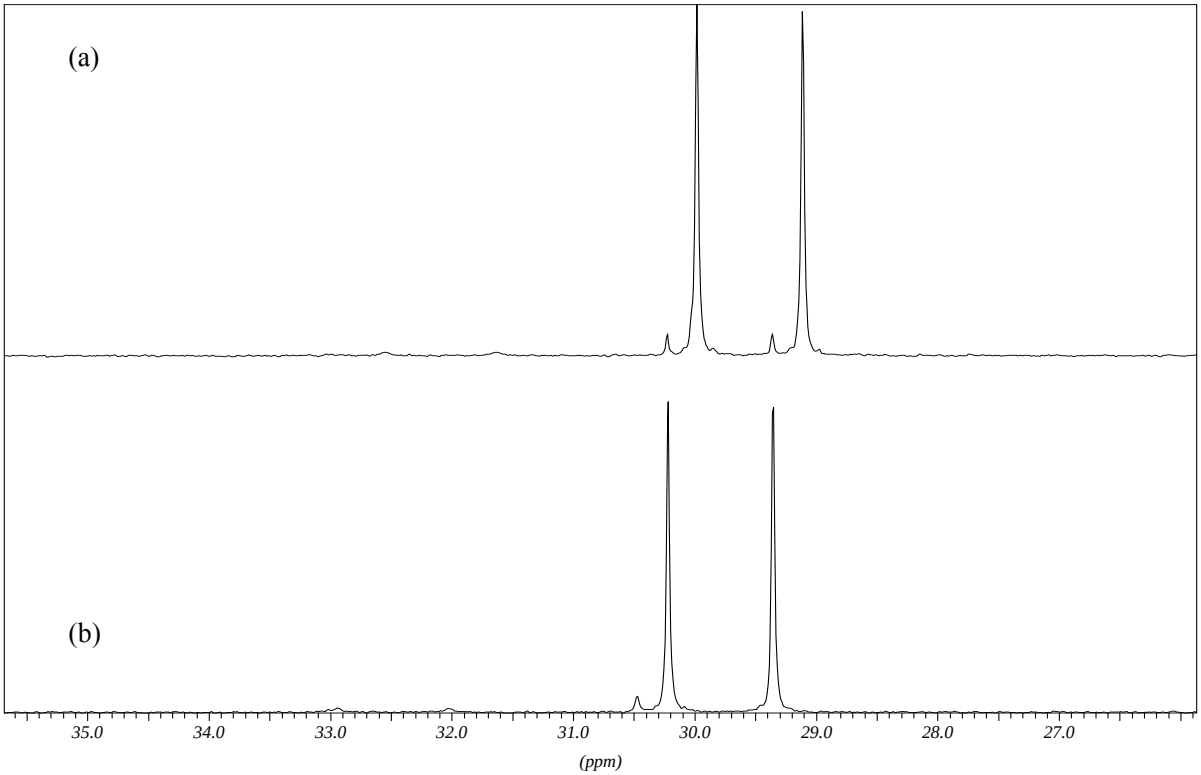

Figure 2-5. $^{31}P\{^{1}H\}$ NMR spectra of (L_{Ment},R_C)-**11** (a) and (L_{Ment},S_C)-**11** (b) in $CDCl_3$ at 253 K.

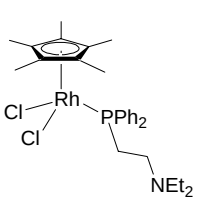

δ = 25.7 (d, $^{1}J_{P\text{-}Rh}$ = 145 Hz) Ref. (25)

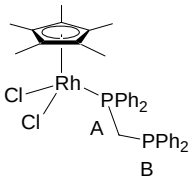

δ = -26.8 (d, P_B), 30.1 (dd, P_A) Ref. (26)

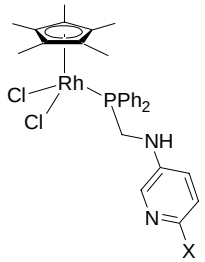

X = Cl δ = 24.5 (d, $^{1}J_{P\text{-}Rh}$ = 146 Hz) Ref. (27)
X = Br δ = 24.4 (d, $^{1}J_{P\text{-}Rh}$ = 145 Hz) Ref. (27)

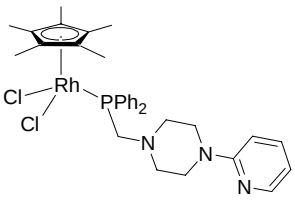

δ = 32.5 (d, $^{1}J_{P\text{-}Rh}$ = 139 Hz) Ref. (28)

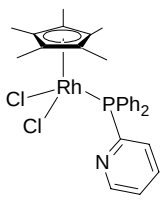

δ = 28.9 (d, $^{1}J_{P\text{-}Rh}$ = 141 Hz) Ref. (28)

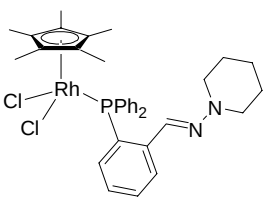

δ = 30.5 (d, $^{1}J_{P\text{-}Rh}$ = 145 Hz) Ref. (28)

Chart 2-2.

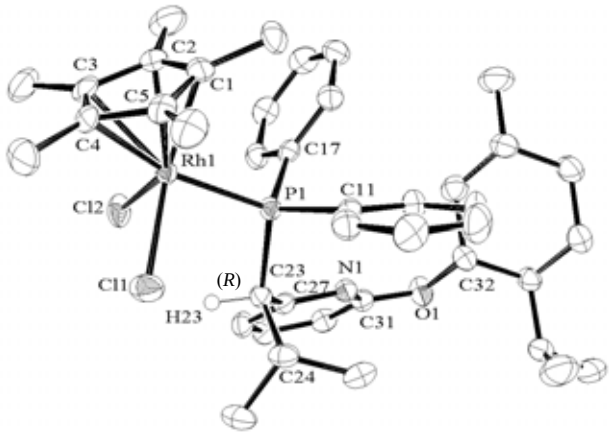

Figure 2-6. Molecular structure of (L_{Ment},R_C)-**11**. Hydrogen atoms omitted except of α-carbon atom. Selected bond lengths [Å] and angles [°]: Rh1-Cl1 2.4124(10), Rh1-Cl2 2.4057(9), Rh1-P1 2.3476(7), Rh1-C1 2.1922(2), Rh1-C2 2.178(3), Rh1-C3 2.207(3), Rh1-C4 2.213(3), Rh1-C5 2.173(3); Cl1-Rh1-Cl2 91.77(3), Cl1-Rh1-P1 91.84(3), Cl2-Rh1-P1 84.90(3), Rh1-P1-C11 117.17(10).

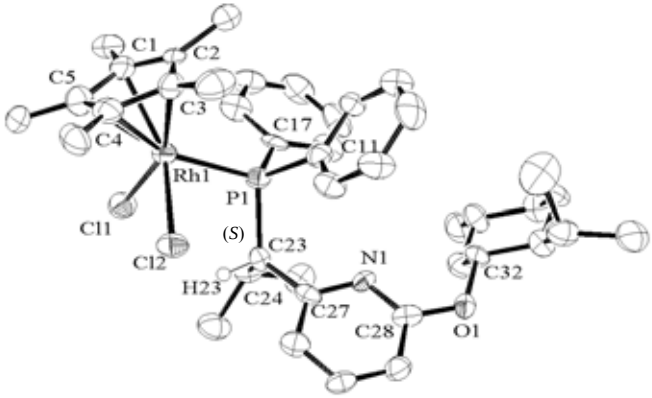

Figure 2-7. Molecular structure of (L_{Ment},S_C)-**11**. Hydrogen atoms omitted except of α-carbon atom. Selected bond lengths [Å] and angles [°]: Rh1-Cl1 2.404(2), Rh1-Cl2 2.404(2), Rh1-P1 2.354(2), Rh1-C1 2.189(9), Rh1-C2 2.193(5), Rh1-C3 2.151(8), Rh1-C4 2.232(9), Rh1-C5 2.227(8); Cl1-Rh1-Cl2 92.97(7), Cl1-Rh1-P1 87.77(7), Cl2-Rh1-P1 87.03(8), Rh1-P1-C11 110.4(3).

The stereochemistries of both diastereomers were determined by X-ray analyses (Figs. 2-6 and 2-7). The less soluble complex is (L_{Ment},R_C)-**11**. Although the complexes (L_{Ment},R_C)-**11** and (L_{Ment},S_C)-**11** are diastereomers, their CD spectra are similar but opposite to each other (Fig. 2-8).

They are dominated by the asymmetric center in the ligand backbone. Thus, the products of the first complexation step could be isolated here, whereas in the synthesis of (L_{Ment},S_C,R_{Rh})-**4** in the isolated product the P, N and Cp ligand parts coordinated simultaneously.

Surprisingly, the reaction of [(Cp*RhCl)$_2$(μ-Cl)$_2$] with the racemic ligand (R_C)/(S_C)-**3** was different from that with the menthylated ligand **2**, in which no ionic species were detected. Scheme 2-9 shows the reaction of (S_C)-**3** with [(Cp*RhCl)$_2$(μ-Cl)$_2$] and the ratios of the products at 193 – 273 K. The molecular dichloro complex **12** could be observed in the NMR spectrum at low temperatures (Fig. 2-9). In addition, however, there were the salt-like chelate complexes (R_C)(R_{Rh})/(S_C)(S_{Rh})- and (R_C)(S_{Rh})/(S_C)(R_{Rh})-**13** in which the metal atom is a chiral center (Scheme 2-9). In these ionic species chloride is the counter-ion. The $^{31}P\{^1H\}$ NMR spectrum of **12**/**13** in CD_2Cl_2 at 193 K showed three phosphorus signals at 75.0 (br d, $J_{Rh\text{-}P}$ = 125.1 Hz), 59.9 (d, $^1J_{Rh\text{-}P}$ = 141.9 Hz) and 31.0 (d, $^1J_{Rh\text{-}P}$ = 141.9 Hz) ppm, respectively (Fig. 2-9). It is assumed that the 31.0 ppm signal is the dichloride complex **12**, the other two signals are due to the two diastereomers (R_C)(R_{Rh})/(S_C)(S_{Rh})- and (R_C)(S_{Rh})/(S_C)(R_{Rh})-**13**. The ratios (R_C)(R_{Rh})/(S_C)(S_{Rh})-**13**:(R_C)/(S_C)-**12**:(R_C)(S_{Rh})/(S_C)(R_{Rh})-**13** were temperature dependent (see

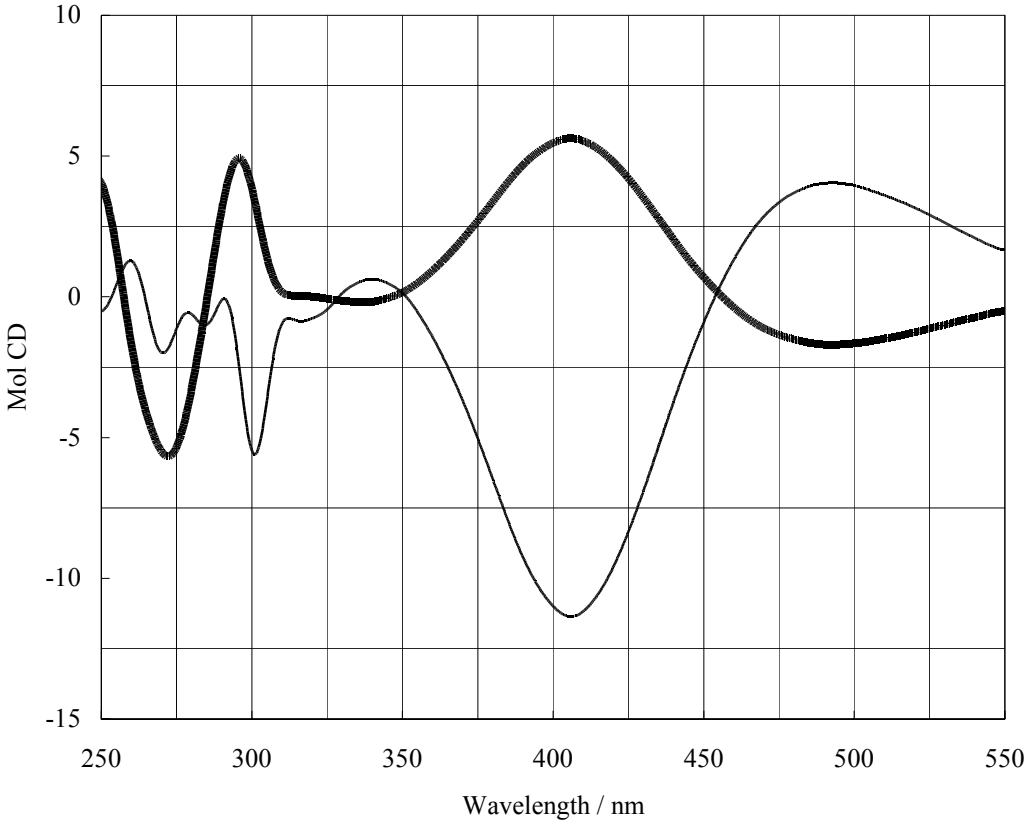

Figure 2-8. CD spectra of (L_{Ment},R_C)-**11** (c = 2.3 × 10^{-4} mol L^{-1}: ▬▬) and (L_{Ment},S_C)-**11** (c = 2.4 × 10^{-4} mol L^{-1}: ——) in CH_2Cl_2 at room temperature.

bottom of Scheme 2-9 and Fig. 2-9). With increasing temperature, the signal at 31.0 ppm disappeared and the ratios $(R_C)(R_{Rh})/(S_C)(S_{Rh})$-**13**:$(R_C)(S_{Rh})/(S_C)(R_{Rh})$-**13** increased. This suggested that equilibration between **12** and the diastereomers of **13** was fast. Assignment of configurations to the signals in the $^{31}P\{^1H\}$ NMR spectra of the chloride diastereomers of **13** was made by comparison with the hexafluorophosphate diastereomers of $[Cp^*Rh(PN_{Ment})Cl]PF_6$ for which the stereochemistry was established by X-ray analyses (see below).

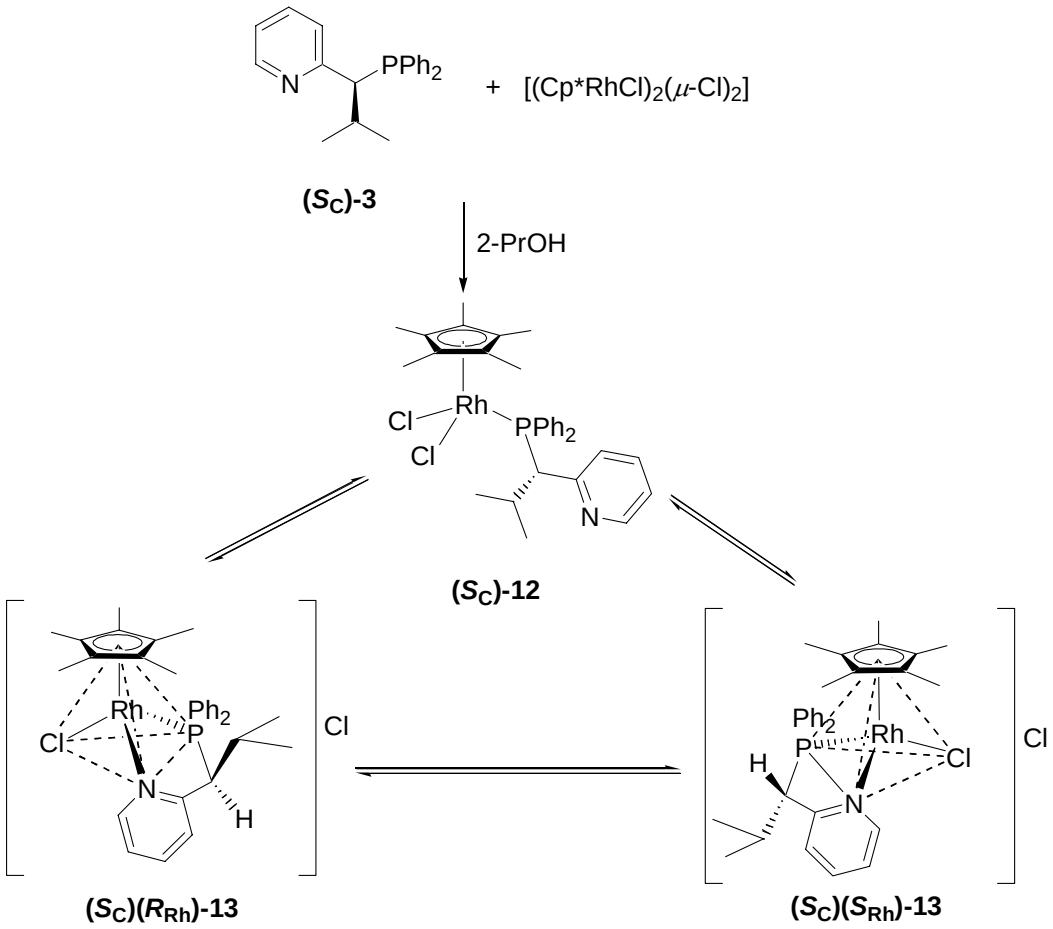

Temp./K	$(R_C)(R_{Rh})/(S_C)(S_{Rh})$-**13**		$(R_C)/(S_C)$-**12**		$(R_C)(S_{Rh})/(S_C)(R_{Rh})$-**13**
193	75	:	13	:	12
213	66	:	11	:	23
233	71	:	3	:	26
253	69	:	0	:	31
273	72	:	0	:	28

Scheme 2-9.

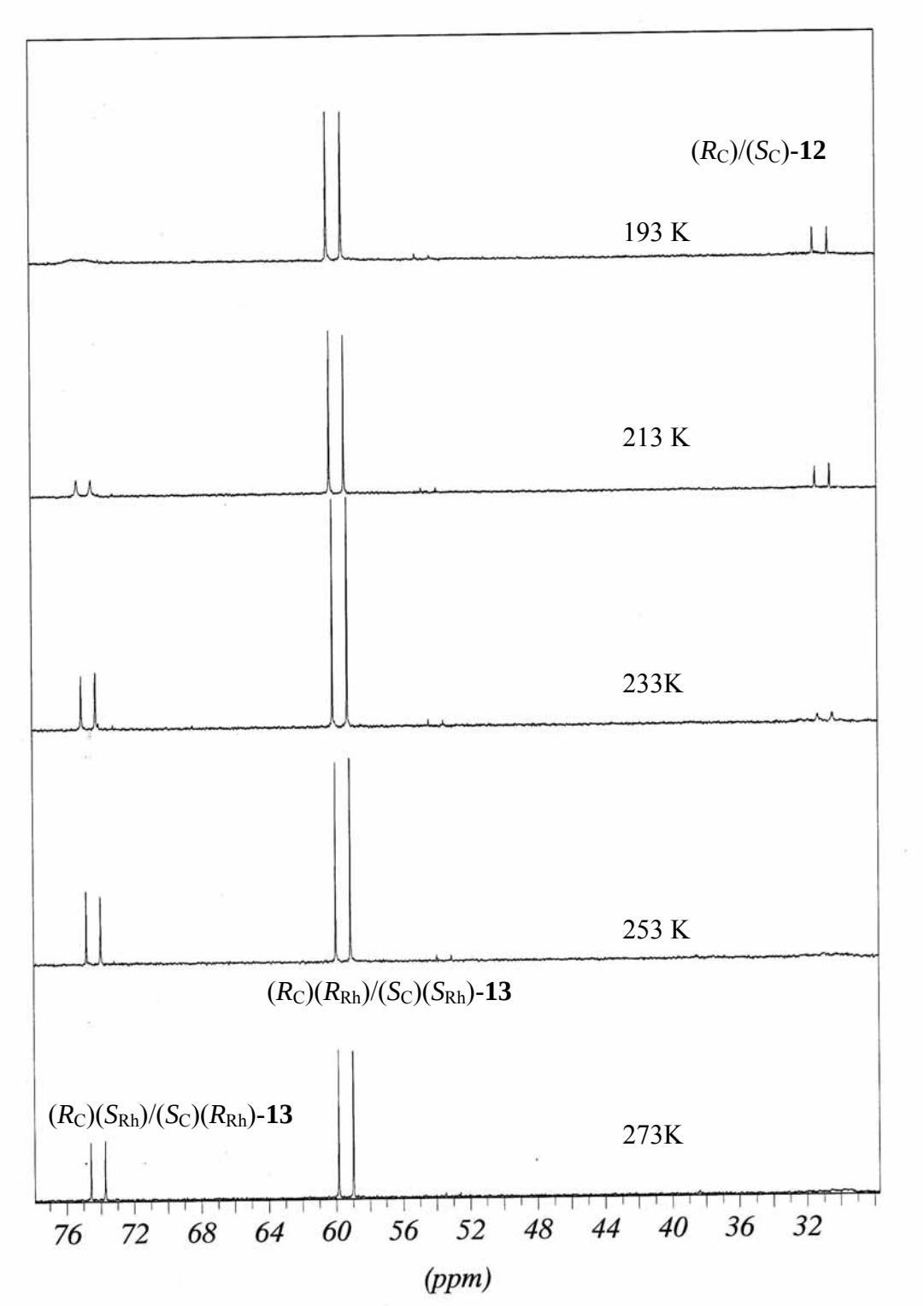

Figure 2-9. $^{31}P\{^{1}H\}$ NMR spectra of the mixture of $(R_C)/(S_C)$-**12**, $(R_C)(R_{Rh})/(S_C)(S_{Rh})$-**13**, and $(R_C)(S_{Rh})/(S_C)(R_{Rh})$-**13** in CD_2Cl_2.

Reaction of **13** with NH_4PF_6 in THF afforded the chiral-at-metal PF_6 salts **14**. Scheme 2-10 shows only (S_C)-enantiomer **12** and (S_C)-diastereomers **13** and **14**. The ratio was (R_C)(R_{Rh})/(S_C)(S_{Rh})-**14** : (R_C)(S_{Rh})/(S_C)(R_{Rh})-**14** = 74 : 26.

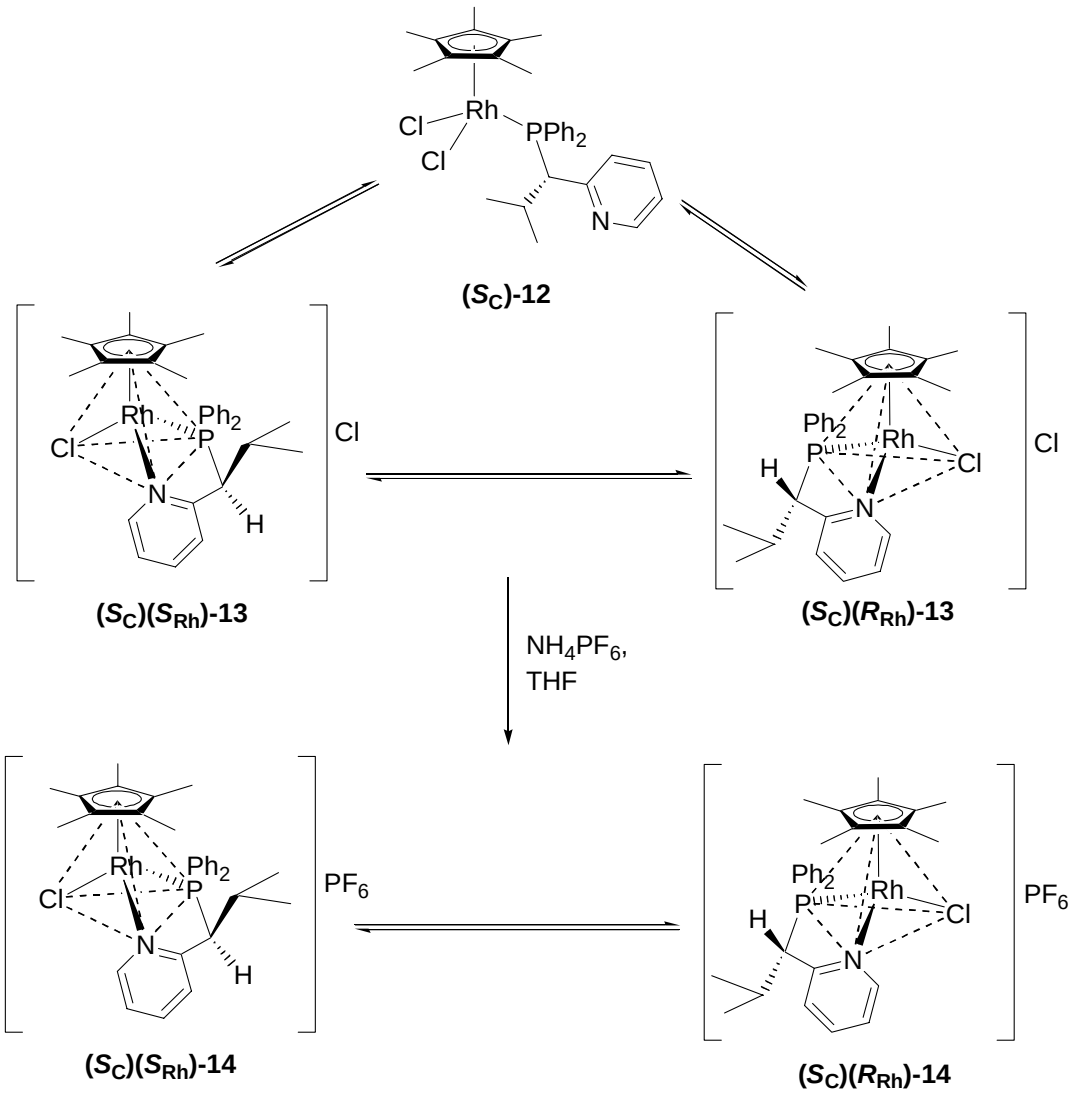

Scheme 2-10.

Similarly, treatment of the pure isomer (L_{Ment},S_C)-**11** with NH_4PF_6 in THF gave the diastereomers (L_{Ment},S_C)(R_{Rh})- and (L_{Ment},S_C)(S_{Rh})-**15** (Scheme 2-11). Thus, in the presence of NH_4PF_6 both in **14** and **15** the PN ligands **2** and **3** coordinated in a bidentate way. The $^{31}P\{^1H\}$ NMR spectrum at 193 K showed the signals of two diastereomers at 52.7 (main; $^1J_{Rh\text{-}P}$ = 143.6 Hz) and 61.3 (minor; $^1J_{Rh\text{-}P}$ = 130.3 Hz) ppm in the ratio 96 : 4 (Fig. 2-10, top). The $^{31}P\{^1H\}$ NMR spectrum was temperature dependent. In the range between 213 K and 273 K the minor

phosphorus signal disappeared, whilst the major broadened appreciably. At 300 K there was one phosphorus signal at 53.2 ppm as a sharp doublet having $^{1}J_{Rh\text{-}P}$ = 131.8 Hz (Fig. 2-10, bottom). Similar tendencies were also observed in the ^{1}H NMR spectra. Processes underlying this temperature dependency were the sterically hindered rotation of the menthyl substituent and the inversion within the puckered chelate ring. Single crystals of the major isomer were obtained by recrystallization using acetone/petroleum ether. X-ray analysis established (L_{Ment},S_C)(S_{Rh})-configuration (Fig. 2-11). On dissolution of the crystals in CD_2Cl_2 at 193 K the $^{31}P\{^{1}H\}$ NMR spectrum showed the equilibrium (L_{Ment},S_C)(S_{Rh})-**15** : (L_{Ment},S_C)(R_{Rh})-**15** = 96 : 4. Thus equilibration between (L_{Ment},S_C)(R_{Rh})-**15** and (L_{Ment},S_C)(S_{Rh})-**15** took place rapidly.

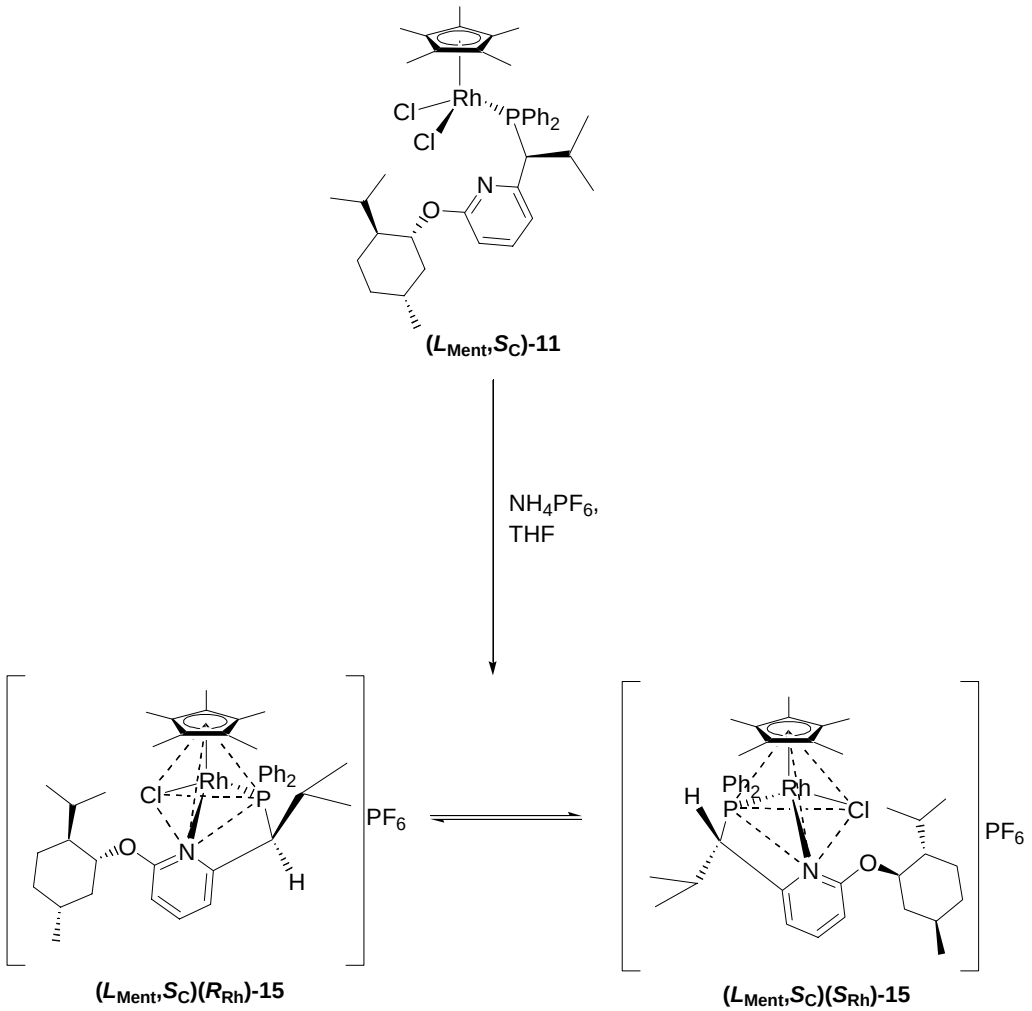

Scheme 2-11.

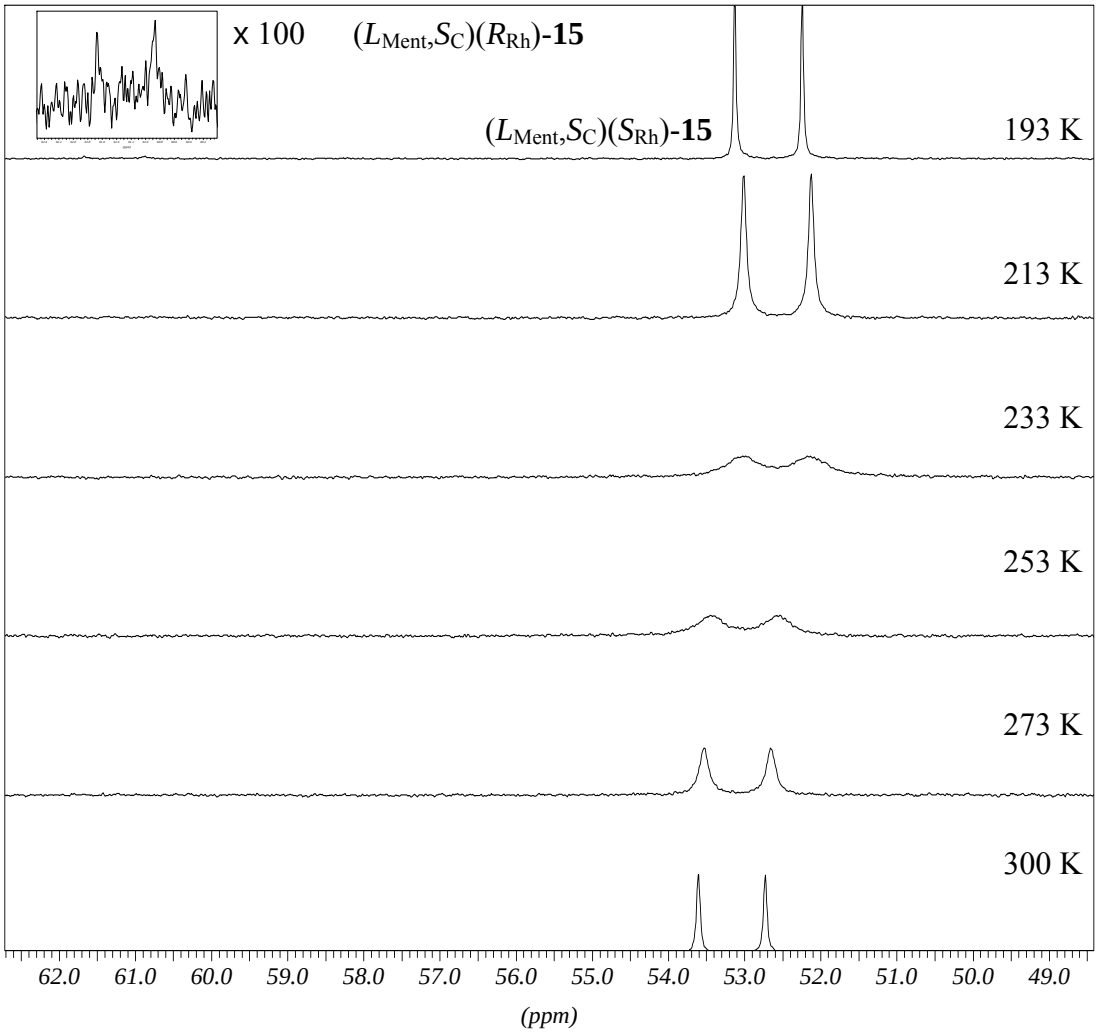

Figure 2-10. $^{31}P\{^1H\}$ NMR spectra of (L_{Ment},S_C)(R_{Rh})- and (L_{Ment},S_C)(S_{Rh})-**15** in CD_2Cl_2.

Similar to (L_{Ment},S_C)-**11** (Scheme 2-11), reaction of (L_{Ment},R_C)-**11** with NH_4PF_6 afforded the diastereomers (L_{Ment},R_C)(R_C)- and (L_{Ment},R_C)(S_C)-**15** (Scheme 2-12). The $^{31}P\{^1H\}$ NMR spectrum showed the presence of two diastereomers [major: 55.8 ppm ($^1J_{Rh\text{-}P}$ = 139.0 Hz), minor: 61.6 ppm ($^1J_{Rh\text{-}P}$ = 142.1 Hz) at 300 K in CD_2Cl_2] in temperature dependent ratios. At 193 K the major : minor ratio of the diastereomers was 76:24, whereas at 300 K it was 92 : 8 (Fig. 2-12). By comparison with the $^{31}P\{^1H\}$ NMR spectra of (L_{Ment},S_C)(S_{Rh})-**15** and (L_{Ment},S_C)(R_{Rh})-**15**, the main diastereomer is (L_{Ment},R_C)(R_{Rh})-**15**, while the minor one is (L_{Ment},R_C)(S_{Rh})-**15**.

The ratios of diastereomers indicates that the stabilities of **15** are in order of (L_{Ment},S_C)(R_{Rh})- < (L_{Ment},R_C)(S_{Rh})- <(L_{Ment},R_C)(R_{Rh})- <(L_{Ment},S_C)(S_{Rh})-configuration.

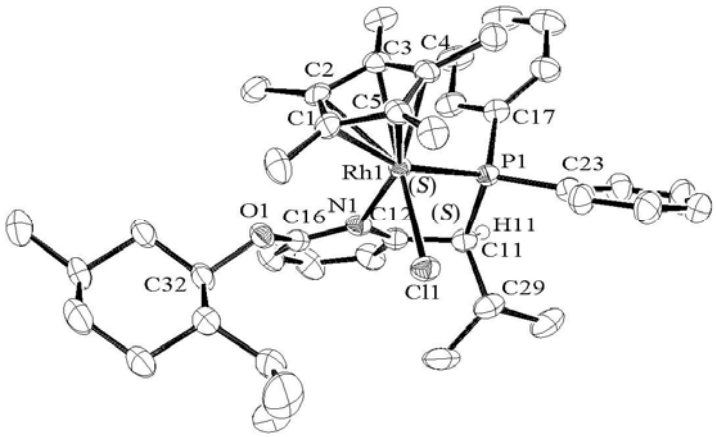

Figure 2-11. Molecular structure of (L_{Ment},S_C)(S_{Rh})-**15**. Hydrogen atoms (except of α-carbon atom), PF_6 anion and two acetone molecules omitted. Selected bond lengths [Å], angles and torsion angles [°]: Rh1-Cl1 2.3993(12), Rh1-P1 2.3028(10), Rh1-N1 2.1781(3), Rh1-C1 2.240(4), Rh1-C2 2.252(5), Rh1-C3 2.202(4), Rh1-C4 2.168(4), Rh1-C5 2.170(4); Cl1-Rh1-P1 93.02(4), Cl1-Rh1-N1 86.88(9), P1-Rh1-N1 81.58(8), Rh1-P1-C11 102.10(13), Rh1-N1-C12 118.62(2), Rh1-N1-C16 124.01(3), P1-C11-C12 107.41(3), N1-C12-C11 117.71(3), P1-C11-H11 108.04, C12-C11-H11 107.95; Rh-N1-C12-C11 26.4(4), N1-C12-C11-P1 –39.5(4), C12-C11-P1-Rh1 32.5(3), C11-P1-Rh1-N1 –16.13(15), P1-Rh1-N1-C12 –2.1(2).

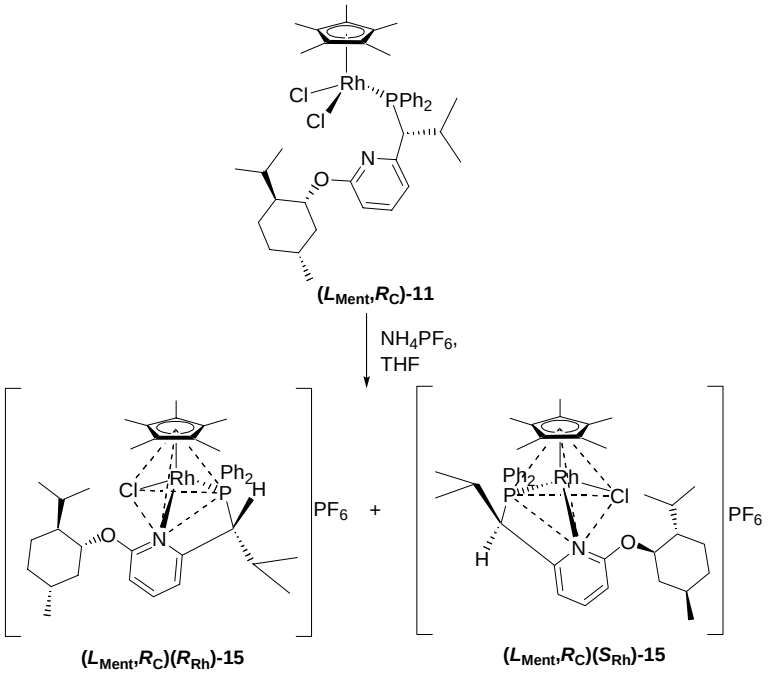

Scheme 2-12.

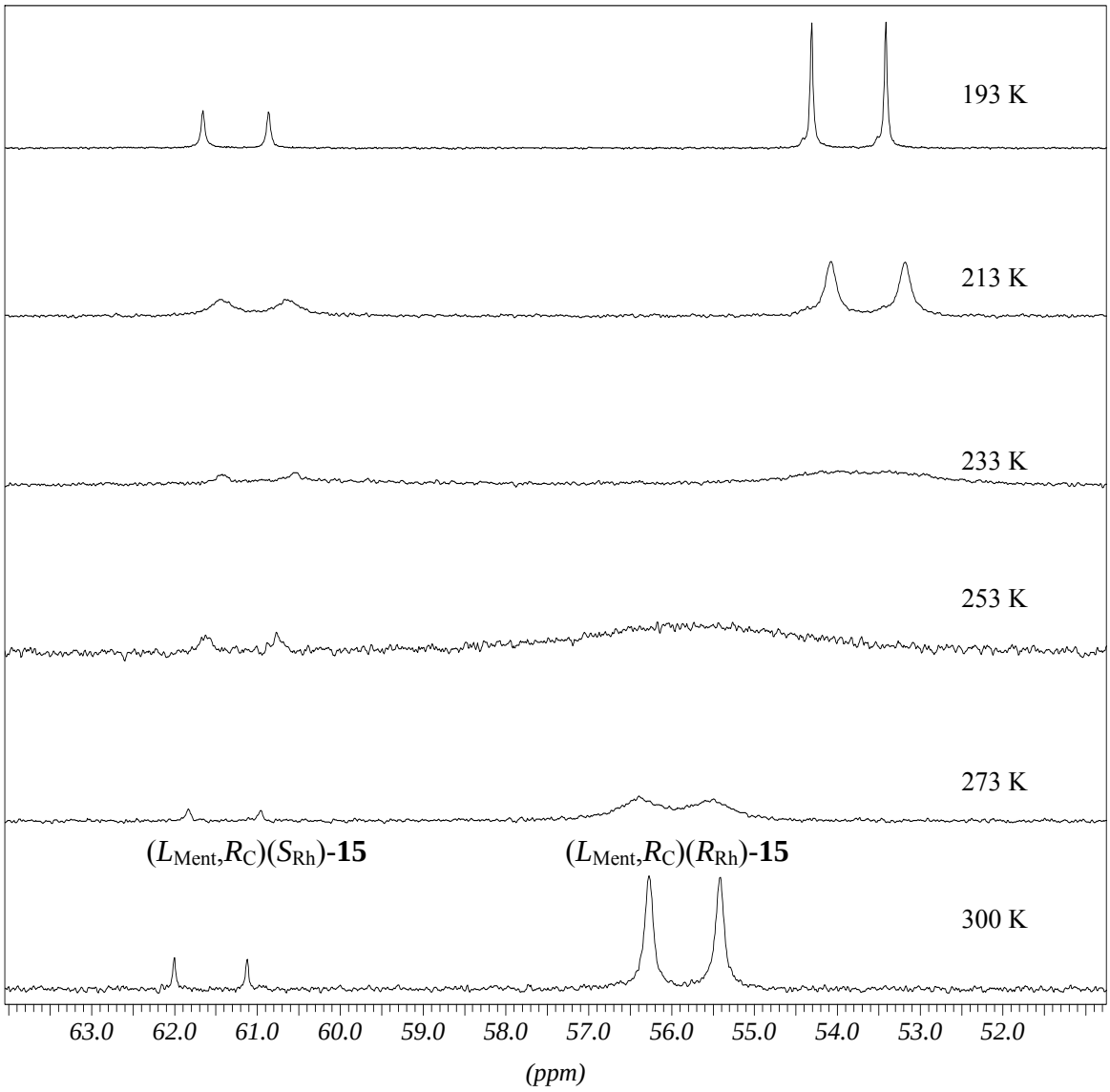

Figure 2-12. $^{31}P\{^1H\}$ NMR spectra of (L_{Ment},R_C)(R_{Rh})- and (L_{Ment},R_C)(S_{Rh})-**15** in CD_2Cl_2.

Reaction of the diastereomer mixture (L_{Ment},R_C)- and (L_{Ment},S_C)-**11** with NH_4PF_6 led to a single crystal containing a 1:1 mixture of the diastereomers (L_{Ment},R_C)(R_{Rh})-**15** and (L_{Ment},S_C)(S_{Rh})-**15** (Fig. 2-13).

To switch to the unsubstituted Cp compounds [$(CpRhCl)_2(\mu$-$Cl_2)$] was reacted with the 1:1 diastereomer mixture of **3** in THF in the presence of NH_4PF_6. As expected there were the signals of four diastereomers of **16** (Scheme 2-13) at 300 K the $^{31}P\{^1H\}$ NMR spectra, in addition to the

PF_6 signal (Fig. 2-14). By comparison with the diastereomers of **15** the two low field signals were assigned to (L_{Ment},R_C)(R_{Rh})- and (L_{Ment},S_C)(S_{Rh})-**16** (isopropyl group towards Cp), while the two high field signals were due to (L_{Ment},S_C)(R_{Rh})- and (L_{Ment},R_C)(S_{Rh})-**16**. The main product was the (L_{Ment},S_C)(S_{Rh})-isomer. Thus, surprisingly, compared to the tripod complex (L_{Ment},S_C,R_{Rh})-**4** the "less stable" Rh configuration was stabilized in the Cp and Cp* series with the bidentate PN_{Ment} ligand **2**.

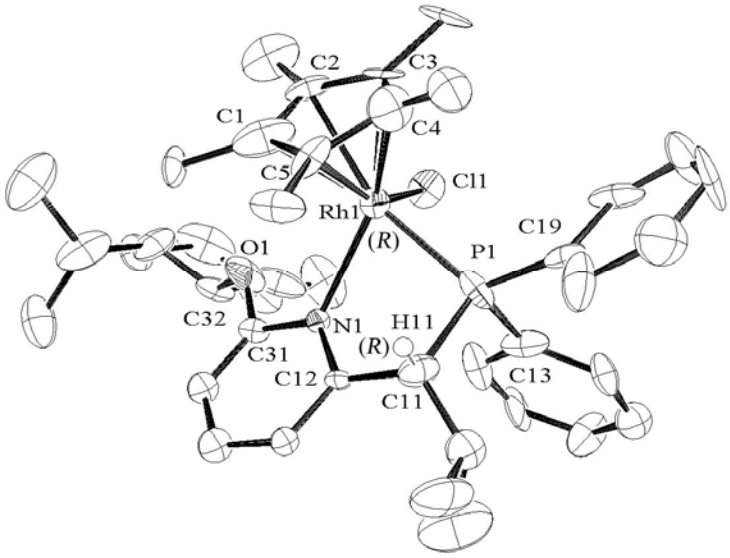

Figure 2-13. Molecular structure of the 1:1 diastereomer mixture of (L_{Ment},R_C)(R_{Rh})- and (L_{Ment},S_C)(S_{Rh})-**15** (only (L_{Ment},R_C)(R_{Rh})-diastereomer shown). Hydrogen atoms (except of α-carbon atom) and PF_6 anion omitted. Selected bond lengths [Å], angles and torsion angles [°]: Rh1-Cl1 2.3810(10), Rh1-P1 2.2697(10), Rh1-N1 2.214(2), Rh1-C1 2.165(4), Rh1-C2 2.225(3), Rh1-C3 2.162(3), Rh1-C4 2.223(4), Rh1-C5 2.196(3); Cl1-Rh1-P1 91.51(4), Cl1-Rh1-N1 100.09(7), P1-Rh1-N1 76.90(6), Rh1-P1-C11 100.22(11), Rh1-N1-C12 115.02(18), Rh1-N1-C31 122.23(18), P1-C11-C12 107.9(2), N1-C12-C11 118.3(3), P1-C11-H11 104.84, C12-C11-H11 104.88; Rh1-N1-C12-C11 –22.3(3), N1-C12-C11-P1 –13.3(3), C12-C11-P1-Rh1 39.2(2), C11-P1-Rh1-N1 –37.26(2), P1-Rh1-N1-C12 38.2(2).

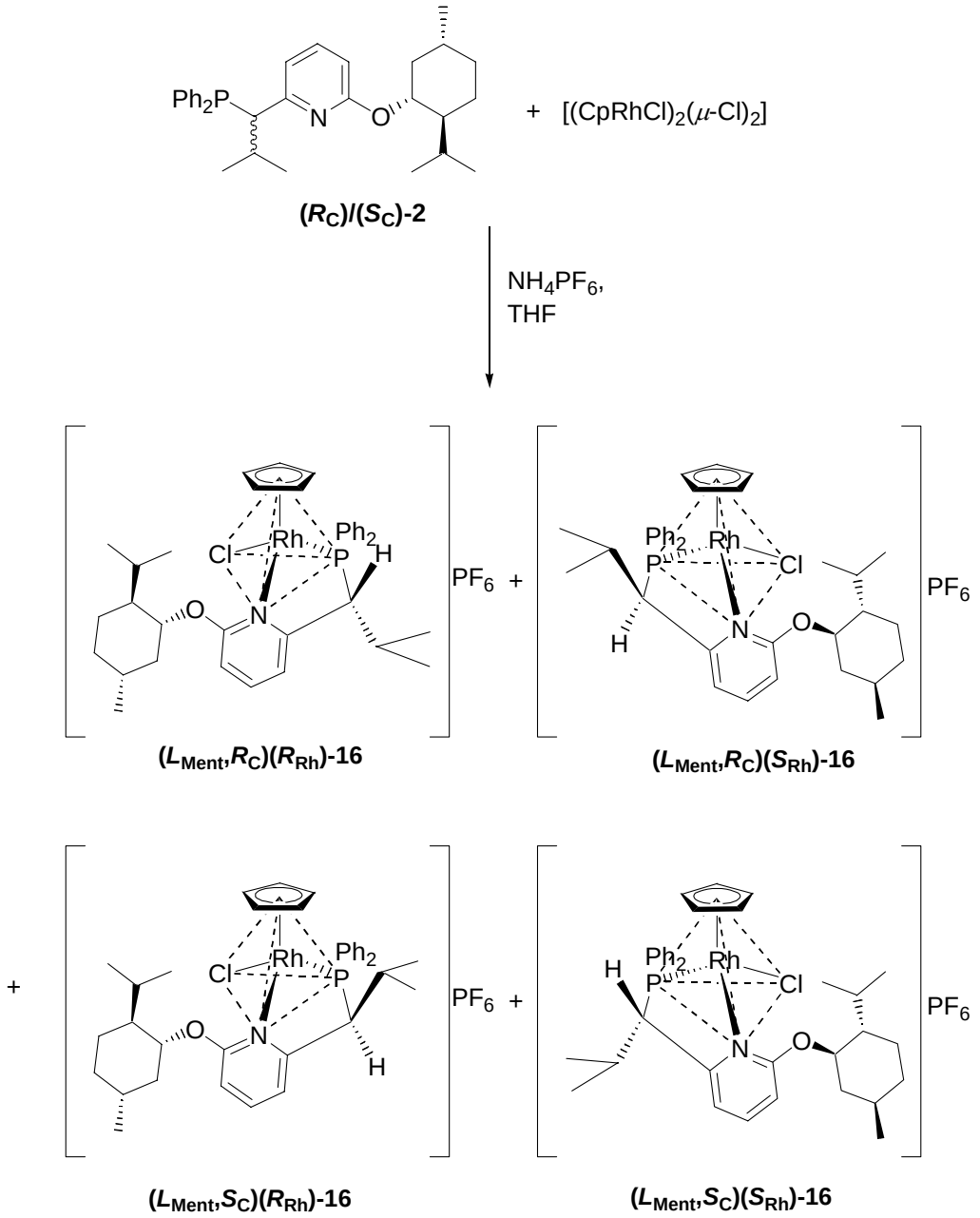

Scheme 2-13.

The complex (L_{Ment},S_C,R_{Rh})-**4** is air-stable, relatively unreactive, and, thus, not a good catalyst precursor. Addition of $AgPF_6$ might create a Lewis acidic site at the metal atom. Dissociation of the hemilabile pyridine arm might open a second vacant site. For catalyses requiring three empty coordination sites metal atoms with coordination numbers higher than Rh(III), e.g., lanthanides, could be used. At any rate, tripod ligands such as (L_{Ment},S_C)-**1** fix a specific metal configuration and in enantioselective catalysis should maintain it throughout all the catalytic cycles, preventing participation of diastereomers with opposite metal configurations which would open other reaction channels to probably give the opposite product configurations.[9] Similar to the PN ligands described in this part, many bidentate ligands can be metalated and additional tripod legs such as the cyclopentadienyl system can be introduced by reaction with fulvenes. Thus, a broad

extension of the concept of the chiral tripod ligands and the consequences for the metal configuration is possible. Control of the metal configuration could be a promising improvement in the field of enantioselective catalysis.

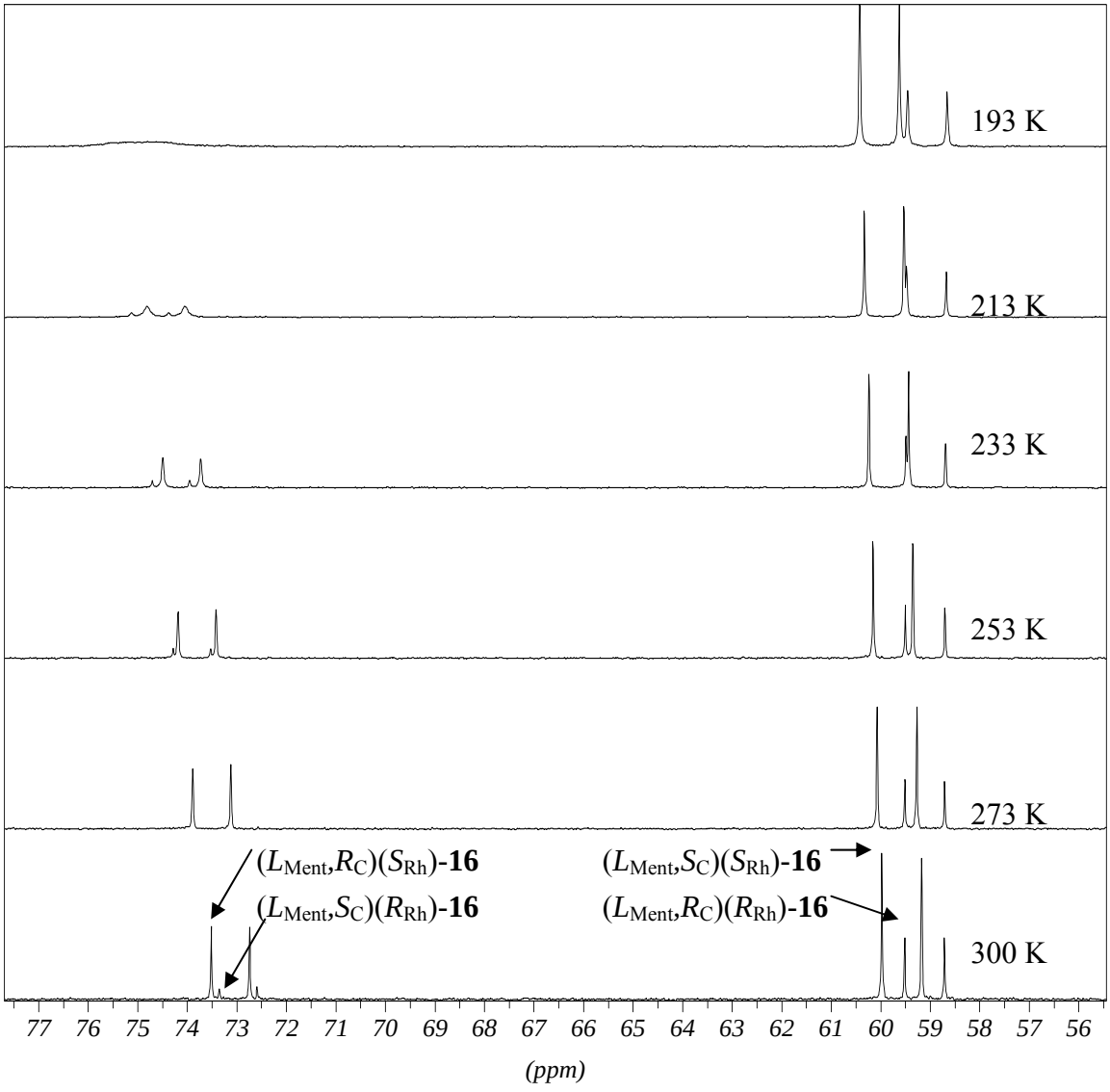

Figure 2-14. $^{31}P\{^{1}H\}$ NMR spectra of (L_{Ment},S_C)(R_{Rh})-/(L_{Ment},S_C)(S_{Rh})-/(L_{Ment},R_C)(R_{Rh})-/(L_{Ment},R_C)(S_{Rh})-**16** in CD_2Cl_2.

2.4 Experimental

2.4.1 General

Synthetic conditions: The syntheses of ligands (when necessary) and complexes were carried out under an inert atmosphere of dry nitrogen or argon using standard Schlenk techniques.

Solvents: Solvents were dried by standard methods and distilled prior to use:

acetone	$KMnO_4$
ethanol, methanol, 2-propanol	Mg with I_2
tetrahydrofuran	$LiAlH_4$
dichloromethane, chloroform	CaH_2
diethyl ether, petroleum ether 40/60, hexane, pentane, toluene, benzene	Na/K

Chromatography: The silica gel used for column chromatography was Merck Kieselgel 60 (63-200 mesh) which was dried on a mantle heater under dry nitrogen.

2.4.2 Spectra

^{1}H, ^{13}C{^{1}H}, and ^{31}P{^{1}H} NMR spectra: ^{1}H, ^{13}C{^{1}H}, and ^{31}P{^{1}H} NMR spectra were measured in $CDCl_3$, CD_2Cl_2, or Toluene-d_8 using an Avance 300 or an Avance 400 spectrometer. TMS was used as an internal standard for ^{1}H and ^{13}C{^{1}H} NMR, while H_3PO_4 was used as an external standard for ^{31}P{^{1}H} NMR.

IR spectra: IR spectra were measured as KBr disks using a Beckman IR 4240 or a BIO-RAD FTS-60A spectrophotometer.

Mass spectra: MS spectra were obtained with a Finnigan MAT 95, Finnigan MAT 311, or Thermoquest TSQ 7000 spectrometer (ESI = electron spray ionization). Only the most intense peak of a cluster is given.

CD spectra: The samples were dissolved in dichloromethane (Uvasol® of Merck) and their CD

spectra were measured on a JASCO J-710 spectrophotometer using a quartz cell (10 cm).

2.4.3 Analysis

Melting points: Melting points were determined on a Büchi SMP 20 or a micro hot-stage Yazawa apparatus and are uncorrected.

Optical rotations: The samples were dissolved in dichloromethane (Uvasol® of Merck) and their optical rotations were measured on a Perkin-Elmer 241 polarimeter using a quartz cell (10 cm).

Elemental analyses: Element analyses were obtained with an Elementar Vario EL III or a YANAKO CHN corder MT-5.

X-Ray structure analyses: STOE-IPDS diffractometer (Mo-Kα radiation, 173 K, l = 0.71073 Å, Oxford cryosystems cooler, graphite monochromator) or Rigaku RAXIS-RAPID diffractometer (Cu-Kα radiation, 296 K, l = 1.5419 Å).

2.4.4 Chemicals

2-Amino-6-methylpyridine, $RhCl_3 \cdot 3H_2O$, and diphenylphosphanyl chloride were commercially available. Di-μ-chlorodichlorobis(η^5-1,2,3,4,5-pentamethylcyclopentadienyl)dirhodium $[(Cp^*RhCl)_2(\mu\text{-}Cl)_2]$[29], di-$\mu$-chlorodichlorobis($\eta^5$-cyclopentadienyl)dirhodium $[(CpRhCl)_2(\mu\text{-}Cl)_2]$[30], 6,6'-dimethylfulvene[31] were prepared as published.

2.4.5 Syntheses

2-Bromo-6-methylpyridine: 2-Amino-6-methylpyridine (43.1 g, 0.399 mol) was put in a 1 L three-necked round-bottom flask equipped with a thermometer, a dropping funnel, and a gas inlet-adaptor and cooled to 0 °C in an ice bath. Hydrobromic acid (170 mL, 47%) was slowly dropped from the funnel to the flask. To the solution was added bromine (56 mL, 1.10 mol)

dropwise with stirring below 5 °C. A solution of $NaNO_2$ (69 g, 1.0 mol) in water (100 mL) was added to the red-orange solution below 5 °C. Next, a solution of NaOH (174 g, 4.3 mol) in water (330 ml) was poured to the reaction mixture below 20 °C. The layers were separated. The aqueous layer was extracted with ether (50 mL x 3). The combined organic fractions were dried over Na_2SO_4 and evaporated in vacuo. The residual oil was distilled under reduced pressure.

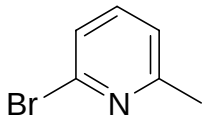

Yield: 46.8 g (68%).

Bp.: 64-67 °C (0.1 Torr) [Lit.[17] 82-85 °C (2 Torr), Lit.[32] 102-103 (20 Torr)].

2-(1*R*,2*S*,5*R*)-Menthoxy-6-methylpyridine: Sodium hydride (6.8 g, 0.28 mol), washed with pentane, was added to L-menthol (100 g, 0.64 mol) in a three-necked flask equipped with a condenser, a dropping funnel, and a gas-inlet-adaptor under dry nitrogen. The mixture was warmed to 60 °C in an oil bath and stirred for 1 h. 2-Bromo-6-methylpyridine (46.7 g, 0.269 mol) was slowly added from the dropping funnel to the mixture. The temperature of the oil bath was raised to 100 °C and the mixture was stirred for 20 h. After cooling, water (100 mL) was poured into the reaction mixture. The solution was extracted with ether (100 mL x 3). The combined organic fractions were dried over Na_2SO_4 and evaporated in vacuo. The unreacted L-menthol in the residue was sublimed at 100 °C under 2 Torr. The residual oil was chromatographed on silica gel using petroleum ether 40/60.

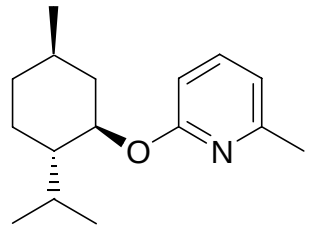

Yield: 35.4 g (53%).

Spectroscopic data corresponded with authentic data.[17]

2-(2-Cyclopentadienyl-1-diphenylphosphanyl-2-methylprop-1-yl)-6-[(1*R*,2*S*,5*R*)-menthoxy]pyridine 1: 2-(1*R*,2*S*,5*R*)-Menthoxy-6-methylpyridine (3.01 g, 12.2 mmol) in 60 mL of Et_2O was slowly added to a solution of BuLi (12.3 mmol, 7.7 mL of a 1.6 mol L^{-1} solution in hexane) at –10 °C under dry nitrogen. The red-orange solution was warmed up to 20 °C and stirred for 1 h. The mixture was cooled to –78 °C and then a solution of PPh_2Cl (2.23 mL, 12.2 mmol) in 40 mL of Et_2O was slowly added. The solution was allowed to warm up and stirred for 20 h at room temperature. BuLi (12.3 mmol, 7.7 mL of a 1.6 mol L^{-1} solution in hexane) was added at 0 °C and stirring was continued for 1 h at 20 °C. 6,6´-Dimethylfulvene (1.63 mL, 12.2 mmol) was added and the reaction mixture was stirred overnight at room temperature. The reaction mixture was quenched with a solution of NH_4Cl (651 mg, 12.2 mmol) in H_2O (20 mL) and the layers were separated under nitrogen. The organic layer was dried over Na_2SO_4 and the solvent was removed in vacuo to give the two diastereomers (L_{Ment},S_C)-**1** and (L_{Ment},R_C)-**1** as a

honey-like oil (ratio in the range 40:60~45:55). The diastereomers were very air-sensitive.
Yield: 5.7 g (87%).

(L_{Ment},S_C)-1: The mixture of diastereomers was dissolved in 30 mL of pentane. At –40 °C only the (L_{Ment},S_C)-diastereomer of **1** crystallized. Its crystals were washed 3 times with 10 mL of cold pentane (–40 °C) under dry nitrogen.

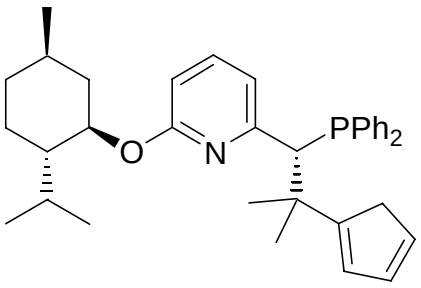

(L_{Ment},R_C)-**1**

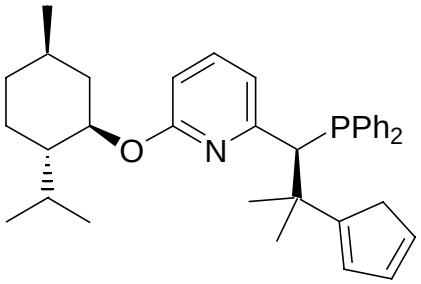

(L_{Ment},S_C)-**1**

Yield: 1.60 g (61%).
Mp.: 100-104 °C.
Spectroscopic data corresponded with authentic data.[17)]

2-(1-Diphenylphosphanyl-2-methylprop-1-yl)pyridine 3: BuLi (0.03 mol, 20 mL of a 1.6 M solution in hexane) was mixed with absolute ether (30 mL). At –5 °C an ether solution of 3.2 mL (3.0 g, 0.03 mol) of 2-methylpyridine was added dropwise. The color of the solution changed to yellow-orange after a few min. The reaction mixture was stirred for 1 h at 20 °C. The solution was added dropwise to a cooled solution (–78 °C) of PPh_2Cl (5.5 mL, 0.03 mol) in ether. The mixture was warmed to 20 °C and stirred for 10 h. To the reaction mixture was added another 20 mL of BuLi at 0 °C and stirred for 1 h at 20 °C. To the orange-red reaction mixture was added dropwise 2-iodopropane (3.0 mL, 0.03 mol) and stirred for 20 h. Hydrolysis was performed with NH_4Cl (1.6 g, 0.03 mol) in 20 mL of water. The organic layer was dried over Na_2SO_4. The solvent was removed to give an oily product.

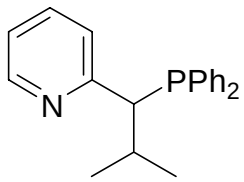

3

Yield 7.7 g (75%).

$C_{21}H_{22}NP$: 319.4 g mol^{-1}.
$^1H\{^{31}P\}$ NMR (400 MHz, $CDCl_3$): δ = 8.35-8.33 (m, 1H, Py-H^6), 7.95-7.90 (m, 1H, Ph), 7.67-7.61 (m, 4H, Ph, Py), 7.46-7.39 (m, 6H, Ph), 7.23-7.18 (m, 1H, Py), 6.99-6.98 (m, 1H, Py-H^5), 3.83-3.79 (m, 1H, PCHPy), 2.58-2.51 (m, 1H, C*H*$(CH_3)_2$), 1.14 (d, ^3J = 6.8 Hz, 3H, CH_3), 0.96 (d, J = 6.7 Hz, 3H, CH_3).
$^{31}P\{^1H\}$ NMR (162 MHz, $CDCl_3$): δ = –6.33 (br s, 1P).

MS (CI, NH_3): *m/z* (%) = 320 (MH, 27), 247 (100).

2-(1-Diphenylphosphanyl-2-methylprop-1-yl)-6-(1*R*,2*S*,5*R*)-menthoxypyridine 2: To a solution of 2-(1*R*,2*S*,5*R*)-menthoxy-6-methylpyridine (6.03 g, 24.4 mmol) in dry ether (60 mL) was slowly added BuLi (24.5 mmol, 15.3 ml of a 1.6 mol L^{-1} solution in hexane) at –30 °C under dry nitrogen. The orange mixture was stirred for 1 h at room temperature and then cooled to –80 °C. Ph_2PCl (4.50 mL, 24.5 mmol) was added to the mixture at –80 °C. The mixture was stirred for 1 h at room temperature and then cooled to –10 °C. To the mixture was slowly added BuLi (24.5 mmol, 15.3 ml of a 1.6 mol L^{-1} solution in hexane) at –10 °C. To the red-orange mixture was added isopropyl iodide (2.43 mL, 24.4 mmol) at –10 °C. After raising the temperature to room temperature, the mixture was stirred for 1 h. Then, a solution of NH_4Cl (1.4 g, 26.2 mmol) in degassed water (30 mL) was added. The layers were separated. The organic layer was dried over Na_2SO_4 and evaporated in vacuo. The residual oil was chromatographed on SiO_2 using petroleum ether 40/60 as an eluent to give 2-(1-diphenylphosphanyl-2-methylprop-1-yl)-6-(1*R*,2*S*,5*R*)-menthoxypyridine.

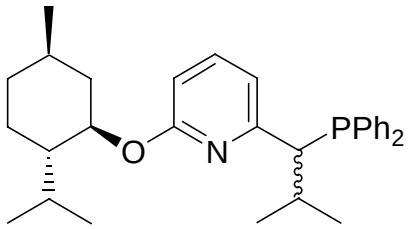

2

Yield: 4.2 g (36%).

$C_{31}H_{40}NOP$: 473.6 g mol^{-1}.

^{1}H NMR (400 MHz, $CDCl_3$, signals of the 45%-diastereomer in parentheses if distinguishable from the 55%-diastereomer): δ = 7.78-7.68 (m, 1H, Ph), 7.66-7.56 (m, 1H, Ph), 7.54-7.22 (m, 8H, Ph, Py-H^4), 7.13-7.03 (m, 1H, Ph), [6.70 (m, 1H, Py-H$^{3/5}$)], 6.63 (d, ^3J = 7.2 Hz, 1H, Py-H$^{3/5}$), [6.37 (ddd, ^3J = 8.2 Hz, J = 1.3 Hz, ^4J = 0.7 Hz, 1H, Py-H$^{3/5}$)], 6.35 (ddd, ^3J = 8.2 Hz, J = 1.3 Hz, ^4J = 0.7 Hz, 1H, Py-H$^{3/5}$), 5.12-5.05 (m, 1H, OCH), 3.60-3.57 (m, 1H, PCHPy), 2.09-1.98 (m, 2H, Ment, C*H*$(CH_3)_2$), 1.74-1.63 (m, 2H, Ment), 1.61-0.72 (m, 5H, Ment), 0.93 (d, ^3J = 6.3 Hz, 3H, CH_3), [0.90 (d, ^{3}J = 6.9 Hz, 3H, CH_3)], 0.86 (d, ^{3}J = 6.9 Hz, 6H, CH_3), [0.91 (d, ^{3}J = 6.9 Hz, 6H, CH_3)], 0.78 (d, ^3J = 7.4 Hz, 3H, CH_3), [0.77 (d, ^3J = 6.6 Hz, 3H, CH_3)].

^{31}P NMR (162 MHz, $CDCl_3$): δ = –6.83 (s, 1P), [–7.50 (s, 1P)].

MS (PI–DCI, NH_3): *m/z* (%) = 474 (MH, 100).

(R_{Rh})-Chloro[1-[(2*S*)-2-(diphenylphosphanyl-κ*P*)-1,1-dimethyl-2-[6-[(1*R*,2*S*,5*R*)-menthoxy]-2-pyridinyl-κ*N*]ethyl]-η^5-cyclopentadienyl]rhodium(III) chloride

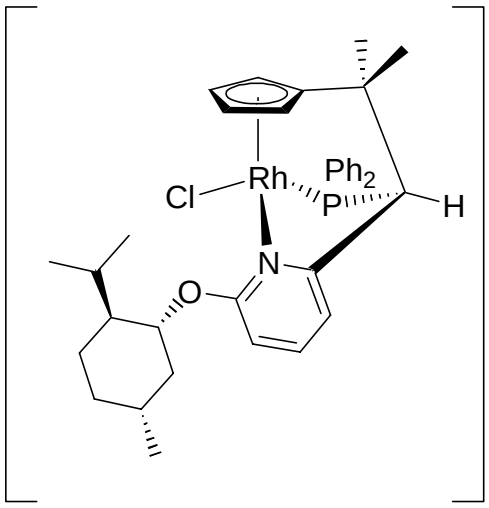

(L_{Ment},S_C,R_{Rh})-**4**

(L_{Ment},S_C,R_{Rh})-4: (L_{Ment},S_C)-**1** (336 mg, 0.63 mmol) was dissolved in 20 mL of ethanol. $RhCl_3 \cdot 3H_2O$ (165 mg, 0.452 mmol), dissolved in 20 mL of ethanol, and $NaHCO_3$ (57.5 mg, 1.04 mmol) were added. After stirring at 20 °C for 22 h the solvent was removed. The residue was chromatographed on SiO_2 with CH_2Cl_2-acetone (1:1) as an eluent.

Yield: 175 mg (54%).

Mp.: > 200 °C.

Spectroscopic data corresponded with authentic data.[17)]

Substitution of the Cl ligand in (L_{Ment},S_C,R_{Rh})-4 by halides (Br, I) and pseudohalides (N_3, CN ,SCN) 5-9: Compounds **5-9** were prepared as published.

Chloro[1-[(2*S*)-2-(diphenylphosphanyl-κ*P*)-1,1-dimethyl-2-[6-[(1*R*,2*S*,5*R*)-menthoxy]-2-pyridinyl]ethyl]-η^5-cyclopentadienyl](triphenylphosphine)rhodium(III) hexafluorophosphate (L_{Ment},S_C,S_{Rh})-10: Compound **10** was prepared as published.

Dichloro[2-[(1*R*/1*S*)-1-(diphenylphosphanyl-κ*P*)-2-methylprop-1-yl]-6-(1*R*,2*S*,5*R*)-menthoxypyridine](η^5-1,2,3,4,5-pentamethylcyclopentadienyl)rhodium(III) (L_{Ment},R_C)-1 and (L_{Ment},S_C)-1: To a solution of a 1:1 mixture of (L_{Ment},R_C)- and (L_{Ment},S_C)-**2** (374 mg, 0.788 mmol) in 2-propanol (40 mL) was added $[(Cp^*RhCl)_2(\mu\text{-}Cl)_2]$[29)] (242 mg, 0.392 mmol) under nitrogen at 20 °C. The mixture was stirred for 4 h and then evaporated. Ether (40 mL) was added to the residue. The mixture was vigorously stirred and filtered. From the insoluble part (L_{Ment},R_C)-**1** was obtained in 53% (164 mg) yield based on (L_{Ment},R_C)-**1**. The filtrate was evaporated. The residue was chromatographed on silica gel using CH_2Cl_2/EtOAc (1:3) to give (L_{Ment},S_C)-**1** in 42% (129 mg) yield based on (L_{Ment},S_C)-**1**.

$C_{41}H_{55}Cl_2NOPRh$: 782.7 g mol^{-1}.

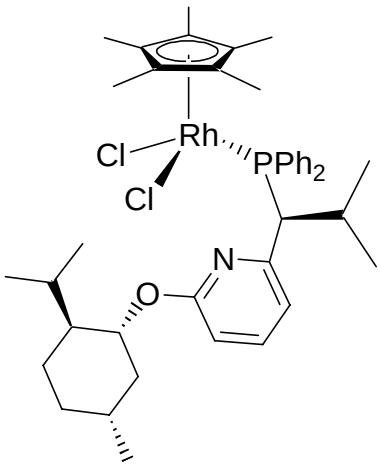

(L_{Ment},S_C)-**11**

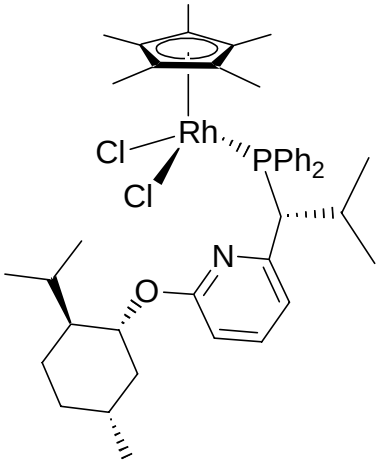

(L_{Ment},R_C)-**11**

(L_{Ment},R_C)-11:

Mp.: 197.5-201 °C.

^{1}H NMR (400 MHz, 253 K, $CDCl_3$): δ = 8.45 (dd, ^3J = 7.2 Hz, ^3J = 9.6 Hz, 2H, Ph), 7.66-7.55 (m, 6H, Ph), 7.40 (t, ^3J = 7.8 Hz, 1H, Py-H^4), 7.18 (br t, J = 6.6 Hz, 1H, Ph), 7.10 (br s, 1H, Ph), 7.00 (d, ^3J = 7.2 Hz, 1H, Py-H$^{3/5}$), 6.30 (d, ^3J = 8.2 Hz, 1H, Py-H$^{3/5}$), 5.08 (d, $^2J_{P\text{-}H}$ = 12.3 Hz, 1H, PCHPy), 4.82 (dt, ^3J = 4.3 Hz, ^3J = 10.7 Hz, 1H, OCH), 2.55 (sept, ^3J = 6.6 Hz, 1H, C*H*$(CH_3)_2$), 1.92-0.65 (m, 8H, Ment), 1.24 (d, $^4J_{P\text{-}H}$ = 3.3 Hz, 15H, Cp-CH_3), 0.99 (d, ^3J = 6.4 Hz, 3H, CH_3), 0.91 (d, ^3J = 6.4 Hz, 3H, CH_3), 0.81 (d, ^3J = 7.0 Hz, 3H, CH_3), 0.50 (d, ^3J = 6.9 Hz, 3H, CH_3), –0.01 (d, ^3J = 6.8 Hz, 3H, CH_3).

^{31}P{^{1}H} NMR (162 MHz, 253 K, $CDCl_3$): δ = 29.8 (d, $^1J_{Rh\text{-}P}$ = 140.3 Hz, 1P).

MS (ESI, CH_2Cl_2): *m/z* (%) = 746 (M–Cl, 100).

CD (c = 2.3×10^{-4} mol L^{-1}, CH_2Cl_2): λ_{max} (nm) = 272 ($\Delta\varepsilon$ = –5.7), 296 ($\Delta\varepsilon$ = 4.9), 337 ($\Delta\varepsilon$ = –0.2), 406 ($\Delta\varepsilon$ = 5.6), 492 ($\Delta\varepsilon$ = –1.7).

Elemental analysis: Calcd. C 62.92, H 7.08, N 1.79
Found C 62.38, H 6.59, N 1.67.

(L_{Ment},S_C)-11:

Mp.: 229-231 °C.

^{1}H NMR (400 MHz, 253 K, $CDCl_3$): δ = 8.52 (dd, ^3J = 8.4 Hz, ^3J = 9.8 Hz, 2H, Ph), 7.66-7.54 (m, 5H, Ph), 7.36 (t, ^3J = 7.6 Hz, 1H, Py-H^4), 7.18-7.05 (m, 3H, Ph), 6.98 (br d, ^3J = 7.2 Hz, 1H, Py-H$^{3/5}$), 6.29 (d, ^3J = 8.2 Hz, 1H, Py-H$^{3/5}$), 5.12 (d, $^2J_{P\text{-}H}$ = 13.3 Hz, 1H, PCHPy), 4.53 (dt, ^3J = 3.5 Hz, ^3J = 10.6 Hz, 1H, OCH), 2.68 (sept, ^3J = 6.6 Hz, 1H, C*H*$(CH_3)_2$), 1.97-1.87 (m, 2H, Ment), 1.81-1.70 (m, 2H, Ment), 1.44-0.65 (m, 8H, Ment), 1.22 (d, $^4J_{P\text{-}H}$ = 3.3 Hz, 15H, Cp-CH_3),

0.94 (d, ^3J = 6.5 Hz, 3H, CH_3), 0.86 (d, ^3J = 6.4 Hz, 3H, CH_3), 0.74 (d, ^3J = 7.0 Hz, 3H, CH_3), 0.62 (d, ^3J = 7.0 Hz, 3H, CH_3), 0.10 (d, ^3J = 6.8 Hz, 3H, CH_3).

$^{31}P\{^1H\}$ NMR (162 MHz, 253 K, $CDCl_3$): δ = 29.5 (d, $^1J_{Rh\text{-}P}$ = 140.8 Hz, 1P).

MS (ESI, CH_2Cl_2): *m/z* (%) = 746 (M–Cl, 100).

CD (c = 2.4×10^{-4} mol L^{-1}, CH_2Cl_2): λ_{max} (nm) = 263 ($\Delta\varepsilon$ = –2.3), 301 ($\Delta\varepsilon$ = –5.6), 340 ($\Delta\varepsilon$ = 0.63), 406 ($\Delta\varepsilon$ = –11.4), 493 ($\Delta\varepsilon$ = 4.0).

Elemental analysis: Calcd. C 62.92, H 7.08, N 1.79
Found C 62.84, H 6.70, N 1.74.

(R_{Rh})/(S_{Rh})-Chloro[2-[(1*R*/1*S*)-1-(diphenylphosphanyl-κP)-2-methylprop-1-yl]-6-(1*R*,2*S*,5*R*)-menthoxypyridine-κN](η^5-1,2,3,4,5-pentamethylcyclopentadienyl) rhodium(III) hexafluorophosphate (L_{Ment},R_C)(R_{Rh})-15 and (L_{Ment},S_C)(S_{Rh})-15 as well as (L_{Ment},S_C)(S_{Rh})-15: A 1:1 mixture of (L_{Ment},R_C)- and (L_{Ment},S_C)-**2** (87.4 mg, 0.111 mmol) was reacted with NH_4PF_6 (85.7 mg, 0.526 mmol). The residue was dissolved in ethanol. The ethanolic solution was diluted with ether and allowed to stand at room temperature to deposit a 1:1 mixture of the diastereomers (L_{Ment},R_C)(R_{Rh})- and (L_{Ment},S_C)(S_{Rh})-**15** (26.5 mg, 27%) as red-orange prism. After filtration, further standing at room temperature afforded (L_{Ment},S_C)(S_{Rh})-**15** as orange needles in 40 % (19.8 mg) yield.

(R_{Rh})/(S_{Rh})-Chloro[2-[(1*R*)-1-(diphenylphosphinanyl-κP)-2-methylprop-1-yl]-6-(1*R*,2*S*,-5*R*)-menthoxypyridine-κN](η^5-1,2,3,4,5-pentamethylcyclopentadienyl)rhodium(III) hexafluorophosphate (L_{Ment},R_C)(R_{Rh})- and (L_{Ment},R_C)(S_{Rh})-15: (L_{Ment},R_C)-**2** (116 mg, 0.148 mmol) and NH_4PF_6 (1.26 g, 7.7 mmol) were dissolved in THF (30 mL) under nitrogen at 20 °C. The mixture was stirred for 16 h and then evaporated. Chloroform was added to the residue. The suspension was vigorously stirred and then filtered. The filtrate was evaporated in vacuo. The red residue was chromatographed on a short silica gel column using acetone as an eluent. The red fraction was evaporated and the residue was washed with ether to give an orange powder of (L_{Ment},R_C)(R_{Rh})-**15**:(L_{Ment},R_C)(S_{Rh})-**15** = 91:9 (by $^{31}P\{^1H\}$ NMR integration at 300 K).

Yield: 68.4 mg (51%).

Mp.: 164-166 °C.

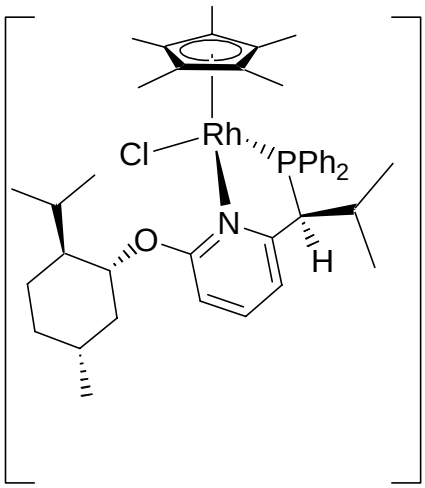

(L_{Ment},S_C)(R_{Rh})-**15**

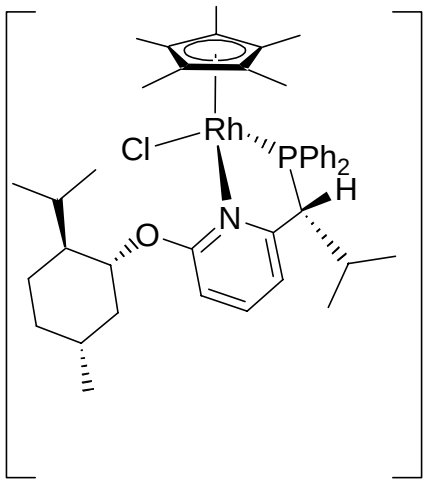

(L_{Ment},R_C)(R_{Rh})-**15**

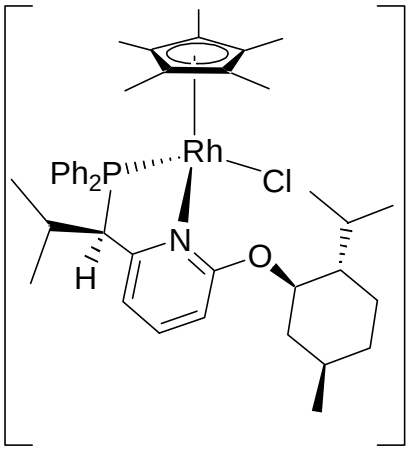

(L_{Ment},R_C)(S_{Rh})-**15**

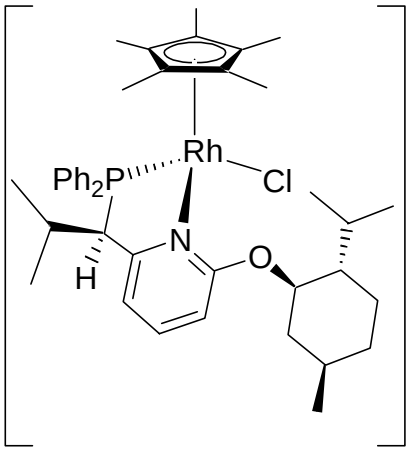

(L_{Ment},S_C)(S_{Rh})-**15**

^{1}H NMR (400 MHz, CD_2Cl_2, major diastereomer (L_{Ment},R_C)(R_{Rh})-**15**, minor diastereomer (L_{Ment},R_C)(S_{Rh})-**15** in brackets): δ = 7.96 (t, ^3J = 7.4 Hz, 1H, Py-H^4), [8.17 (br t, ^3J = 8.5 Hz, 1H, Py-H^4)], 7.75-7.56 (m, 6H, Ph), 7.48-7.41 (m, 4H, Ph), 7.26 (d, ^3J = 7.4 Hz, 1H, Py-H$^{3/5}$), [7.04 (br d, ^3J = 8.5 Hz, 1H, Py-H$^{3/5}$)], 7.16 (d, ^3J = 8.4 Hz, 1H, Py-H$^{3/5}$), [7.02 (br d, ^3J = 8.5 Hz, 1H, Py-H$^{3/5}$)], 4.41 (br q, ^3J = 9.6 Hz, 1H, OCH), 4.01 (dd, $^2J_{P\text{-}H}$ = 13.5 Hz, ^3J = 3.1 Hz, 1H, PCHPy), 2.42-2.32 (m, 2H, C*H*(CH_3)$_2$), 1.97-0.95 (m, 8H, Ment), 1.30 (d, $^4J_{P\text{-}H}$ = 3.7 Hz, 15H, Cp-CH_3), [1.35 (d, $^4J_{P\text{-}H}$ = 3.9 Hz, 15H, Cp-CH_3)], 1.06 (d, ^3J = 7.0 Hz, 3H, CH_3), 1.03 (d, ^3J = 6.8 Hz, 6H, CH_3), 0.94 (d, ^3J = 6.4 Hz, 3H, CH_3), 0.36 (d, ^3J = 6.8 Hz, 3H, CH_3), [0.73 (d, ^3J = 7.0 Hz, 3H, CH_3)], 0.05 (d, ^3J = 6.8 Hz, 3H, CH_3), [0.43 (d, ^3J = 7.0 Hz, 3H, CH_3)].

^{31}P{^{1}H} NMR (162 MHz, CD_2Cl_2): δ = 55.8 (d, $^1J_{Rh\text{-}P}$ = 139.0 Hz, 1P), [61.6 (d, $^1J_{Rh\text{-}P}$ = 142.1 Hz, 1P)], –143.9 (sept, $^1J_{F\text{-}P}$ = 710.6 Hz, 1P, PF_6).

CD (c = 2.3×10^{-4} mol L^{-1}, CH_2Cl_2): λ_{max} (nm) 289 ($\Delta\varepsilon$ = –2.9), 314 ($\Delta\varepsilon$ = 14.5), 373 ($\Delta\varepsilon$ = –8.3), 477 ($\Delta\varepsilon$ = 3.3).

MS (ESI, CH_2Cl_2): *m/z* (%) = 746 (cation, 100).

HRMS (LSI, MeOH-glycerol): $C_{41}H_{55}ClOPRh$ (cation). Calcd. 746.2758.
Found 746.2744.

(S_{Rh})-Chloro[2-[(1*S*)-1-(diphenylphosphanyl-κP)-2-methylprop-1-yl]-6-(1*R*,2*S*,5*R*)-menthoxypyridine-κN](η^5-1,2,3,4,5-pentamethylcyclopentadienyl)rhodium(III) hexafluorophosphate (L_{Ment},S_C)(S_{Rh})-15: In the above manner the reaction of (L_{Ment},S_C)-**2** (38.9 mg, 0.0497 mmol) with NH_4PF_6 (228 mg, 1.34 mmol) in THF (15 mL) gave (L_{Ment},S_C)(S_{Rh})- and (L_{Ment},S_C)(R_{Rh})-**15** in 41% (18.6 mg) yield. Recrystallization of the mixture using acetone-petroleum ether (40/60) afforded pure (L_{Ment},S_C)(S_{Rh})-**15**, isolated as orange needles.

Mp.: 167-171 °C.

^{1}H NMR (400 MHz, CD_2Cl_2): δ = 7.96-7.90 (m, 3H, Ph, Py-H^4), 7.71-7.50 (m, 6H, Ph), 7.35-7.30 (m, 2H, Ph), 7.18 (d, ^3J = 7.2 Hz, 1H, Py-H$^{3/5}$), 7.03 (d, ^3J = 8.4 Hz, 1H, Py-H$^{3/5}$), 4.28 (dt, ^3J = 4.1 Hz, ^3J = 10.4 Hz, 1H, OCH), 3.93 (dd, $^2J_{P-H}$ = 13.3 Hz, ^3J = 4.3 Hz, 1H, PCHPy), 2.70 (dsept, ^3J = 2.4 Hz, ^3J = 6.8 Hz, 1H, Ment-C*H*(CH_3)$_2$), 2.42-2.24 (m, 2H, Ment, PCHC*H*(CH_3)$_2$), 1.81 (d, ^3J = 6.1 Hz, 3H, CH_3), 1.85-1.59 (m, 5H, Ment), 1.43-1.38 (m, 1H, Ment), 1.32 (d, $^4J_{P-H}$ = 3.9 Hz, 15H, Cp-CH_3), 1.11-1.01 (1H, m, Ment), 0.90 (d, ^3J = 6.8 Hz, 3H, CH_3), 0.80 (d, ^3J = 6.8 Hz, 3H, CH_3), 0.36 (d, ^3J = 6.8 Hz, 3H, CH_3), 0.11 (d, ^3J = 6.8 Hz, 3H, CH_3).

^{31}P{^{1}H} NMR (162 MHz, CD_2Cl_2): δ = 53.2 (d, $^1J_{Rh-P}$ = 142.3 Hz, 1P, PH), –143.9 (sept, $^1J_{F-P}$ = 710.6 Hz, 1P, PF_6).

MS (ESI, CH_2Cl_2): *m/z* (%) = 746 (cation, 100).

CD (c = 2.4×10^{-4} mol L^{-1}, CH_2Cl_2): λ_{max} (nm) = 280 ($\Delta\varepsilon$ = 4.8), 316 ($\Delta\varepsilon$ = –29.7), 373 ($\Delta\varepsilon$ = 14.6), 465 ($\Delta\varepsilon$ = –3.91).

HRMS (LSI, MeOH-glycerol): $C_{41}H_{55}ClNOPRh$ (cation). Calcd. 746.2758.
Found 746.2747.

(R_{Rh})/(S_{Rh})-Chloro[2-[(1*R*/1*S*)-1-(diphenylphosphanyl-κP)-2-methylprop-1-yl]pyridine-κN](η^5-1,2,3,4,5-pentamethylcyclopentadienyl)rhodium(III) chloride (R_C)(R_{Rh})/ (S_C)(S_{Rh})- and (R_C)(S_{Rh})/(S_C)(R_{Rh})-13: To a solution of racemic **3** (284 mg, 0.893 mmol) in ethanol (30 mL) was added [(Cp*RhCl)$_2$(μ-Cl)$_2$] (256 mg, 0.414 mmol) under nitrogen at 20 °C. The mixture was stirred for 5 h and then evaporated. The residue was washed with 10% dichloromethane/ether to give (R_C)(R_{Rh})/(S_C)(S_{Rh})- and (R_C)(S_{Rh})/(S_C)(R_{Rh})-**13** as an orange powder.

Yield: 487 mg (94%).

Mp.: 168-174 °C.

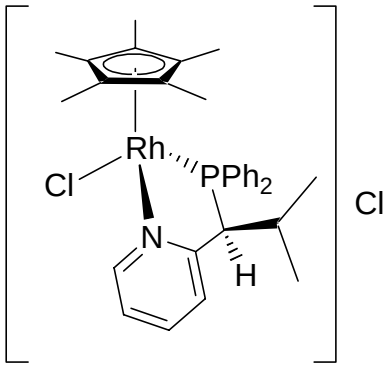

(S_C)(R_{Rh})-**13**

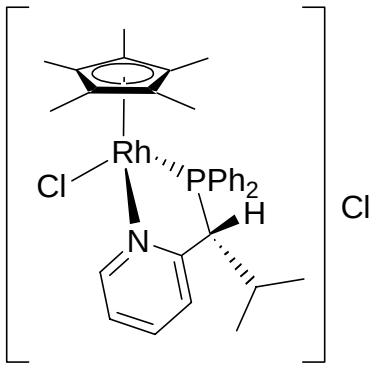

(R_C)(R_{Rh})-**13**

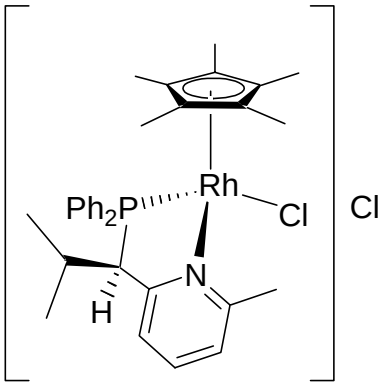

(R_C)(S_{Rh})-**13**

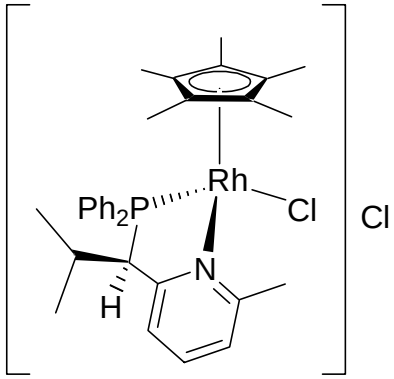

(S_C)(S_{Rh})-**13**

^{1}H NMR (400 MHz, CD_2Cl_2, major isomers (R_C)(R_{Rh})/(S_C)(S_{Rh}), minor isomers (S_C)(R_{Rh})/(R_C)(S_{Rh}) in brackets): δ = 8.66 (br d, ^3J = 5.8 Hz, 1H, Py-H^6), [8.87 (br d, ^3J = 6.4 Hz, 1H, Py-H^6)], 8.13-7.17 (m, 13H, Ph, Py-H$^{3-5}$), 3.99 (dd, $^3J_{P-H}$ = 15.2 Hz, ^3J = 5.3 Hz, 1H, PCHPy), [5.01 (br d, J_{P-H} = 16.0 Hz, 1H, PCHPy)], 2.36-2.20 (m, 1H, C*H*(CH_3)$_2$), [2.56-2.42 (m, 1H, C*H*(CH_3)$_2$)], 1.41 (d, $^4J_{P-H}$ = 3.5 Hz, 15H, Cp-CH_3), [1.53 (d, ^3J = 3.7 Hz, 15H, Cp-CH_3)], 0.75 (d, ^3J = 6.8 Hz, 3H, CH_3), [1.11 (d, ^3J = 7.2 Hz, 3H, CH_3)], 0.32 (d, ^3J = 6.8 Hz, 3H, CH_3), [0.38 (d, ^3J = 7.0 Hz, 3H, CH_3).

^{31}P{^{1}H} NMR (162 MHz, CD_2Cl_2): δ = [73.9 (d, $^1J_{Rh-P}$ = 135.8 Hz, 1P, R_C,S_{Rh}/S_C,R_{Rh}-P)], 59.3 (d, $^1J_{Rh-P}$ = 141.9 Hz, 1P, R_C,R_{Rh}/S_C,S_{Rh}-P).

MS (ESI, CH_2Cl_2): *m/z* (%) = 592 (cation, 100).

Elemental analysis: Calcd. C 59.25, H 5.93, N 2.23.
Found C 59.36, H 6.08, N 2.27.

(R_{Rh})/(S_{Rh})-Chloro[2-[(1*R*/1*S*)-1-(diphenylphosphanyl-*κP*)-2-methylprop-1-yl]pyridine-*κN*](η^5-1,2,3,4,5-pentamethylcyclopentadienyl)rhodium(III) hexafluorophosphate (R_C)(R_{Rh})/(S_C)(S_{Rh})- and (R_C)(S_{Rh})/(S_C)(R_{Rh})-14: (R_C)(R_{Rh})/(S_C)(S_{Rh})- and (R_C)(S_{Rh})/(S_C)(R_{Rh})-**13** (174 mg, 0.277 mmol) were dissolved in THF (30 mL) under nitrogen at

20 °C. NH_4PF_6 (1.08 g, 6.63 mmol) was added. After stirring for 15 h the solvent was evaporated. Dichloromethane was added to the residue and the suspension was filtered. The filtrate was evaporated and the residue was washed with ether to give (R_C)(R_{Rh})/(S_C)(S_{Rh})- and (R_C)(S_{Rh})/(S_C)(R_{Rh})-**14** as an orange powder. Isomer composition: (R_C)(R_{Rh})/(S_C)(S_{Rh}): (R_C)(S_{Rh})/(S_C)(R_{Rh}) = 74:26 by $^{31}P\{^1H\}$ NMR integration at 300 K.

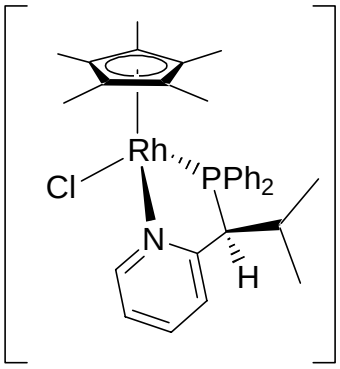

(S_C)(R_{Rh})-**14**

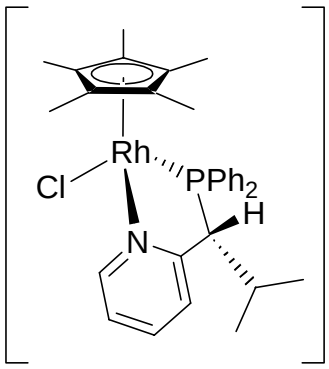

(R_C)(R_{Rh})-**14**

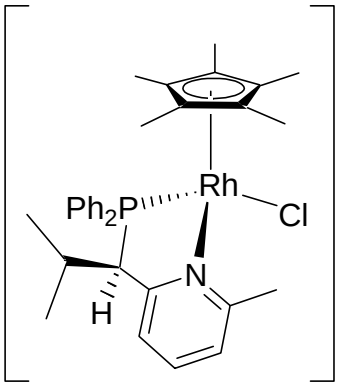

(R_C)(S_{Rh})-**14**

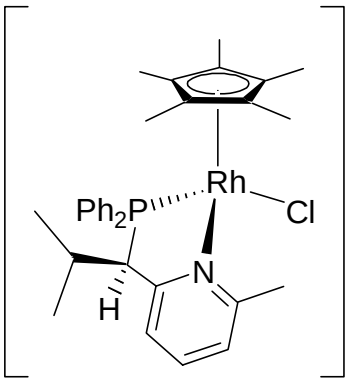

(S_C)(S_{Rh})-**14**

Yield: 163 mg (80%).

Mp.: 145-155 °C.

^1H NMR (400 MHz, CD_2Cl_2, major isomers (R_C)(R_{Rh})/(S_C)(S_{Rh}), minor isomers (R_C)(S_{Rh})/(S_C)(R_{Rh}) in brackets): δ = 8.59 (br d, ^3J =5.8 Hz, 1H, Py-H^6), [8.80 (br d, ^3J = 5.4 Hz, 1H, Py-H^6)], 8.06-7.17 (m, 13H, Ph, Py-H$^{3-5}$), 3.91 (dd, $^2J_{P-H}$ = 15.1 Hz, ^3J = 5.3 Hz, 1H, PCHPy), [4.99 (br d, $^2J_{P-H}$ = 15.0 Hz, 1H, PCHPy)], 2.37-2.21 (m, 1H, C*H*(CH_3)$_2$), [2.54-2.40 (m, 1H, C*H*(CH_3)$_2$)], 1.40 (d, $^4J_{P-H}$ = 3.7 Hz, 15H, Cp-CH_3), [1.51 (d, ^3J = 3.7 Hz, 15H, Cp-CH_3)], 0.74 (d, ^3J = 6.7 Hz, 3H, CH_3), [1.11 (d, ^3J = 7.2 Hz, 3H, CH_3)], 0.32 (d, ^3J = 6.9 Hz, 3H, CH_3), [0.38 (d, ^3J = 7.0 Hz, 3H, CH_3).

$^{31}P\{^1H\}$ NMR (162 MHz, CD_2Cl_2): δ = 73.6 (d, $^1J_{Rh-P}$ = 135.8 Hz, 1P, R_C,S_{Rh}/S_C,R_{Rh}-P), 59.3 (d, $^1J_{Rh-P}$ = 143.5 Hz, 1P, R_C,R_{Rh}/S_C,S_{Rh}-P), –143.8 (sept, $^1J_{F-P}$ = 712.6 Hz, 1P, PF_6).

MS (ESI, CH_2Cl_2): *m/z* (%) = 592 (cation, 100).

Elemental analysis: Calcd. C 50.46, H 5.05, N 1.90.
Found C 50.59, H 5.65, N 1.86.

(R_{Rh})/(S_{Rh})-Chloro(η^5-cyclopentadienyl)[2-[(1*R*/1*S* and 1*S*/1*R*)-1-(diphenylphosphanyl-κP)-2-methylprop-1-yl]-6-(1*R*,2*S*,5*R*)-menthoxypyridine-κN]rhodium(III) hexafluorophosphate (L_{Ment},R_C)(R_{Rh})-, (L_{Ment},R_C)(S_{Rh})-, (L_{Ment},S_C)(R_{Rh})-, and (L_{Ment},S_C)(S_{Rh})-16: To a 1:1 mixture of the diastereomers of **2** (52.6 mg, 0.111 mmol) in THF (20 mL) was added $[(CpRhCl)_2(\mu\text{-}Cl)_2]$[30] (32.6 mg, 0.0682 mmol) under nitrogen at 20 °C. The mixture was stirred for 2 h and then NH_4PF_6 (383 mg, 2.35 mmol) was added. The orange solution was stirred for 17 h and evaporated. Dichloromethane was added to the residue and the suspension was filtered to remove inorganic salts. The filtrate was evaporated and the residue was subjected to silica gel chromatography using 25% EtOH-benzene as an eluent to give a mixture of (L_{Ment},R_C)(R_{Rh})-, (L_{Ment},R_C)(S_{Rh})-, (L_{Ment},S_C)(R_{Rh})- and (L_{Ment},S_C)(S_{Rh})-**16**. Isomer composition: L_{Ment},S_C,S_{Rh}:L_{Ment},S_C,R_{Rh}:L_{Ment},R_C,R_{Rh}:L_{Ment},R_C,S_{Rh} = 50:5:20:25 by $^{31}P\{^1H\}$ NMR integration.

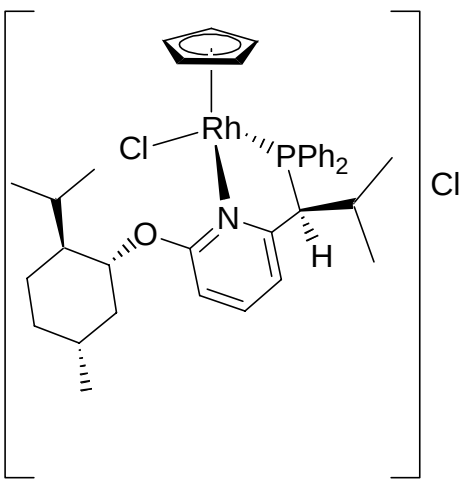

(L_{Ment},S_C)(R_{Rh})-**16**

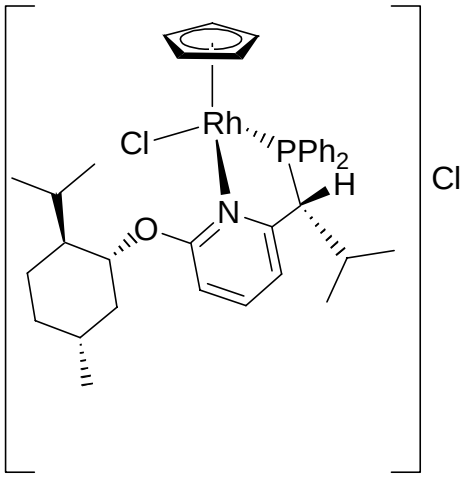

(L_{Ment},R_C)(R_{Rh})-**16**

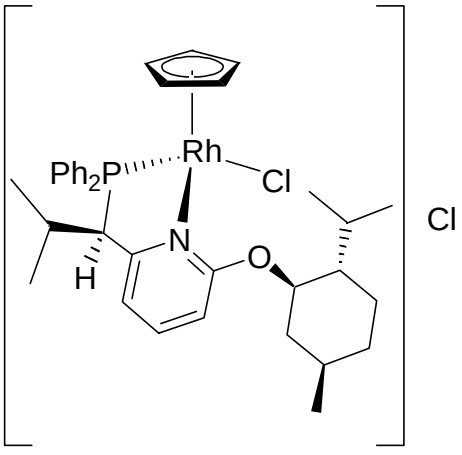

(L_{Ment},R_C)(S_{Rh})-**16**

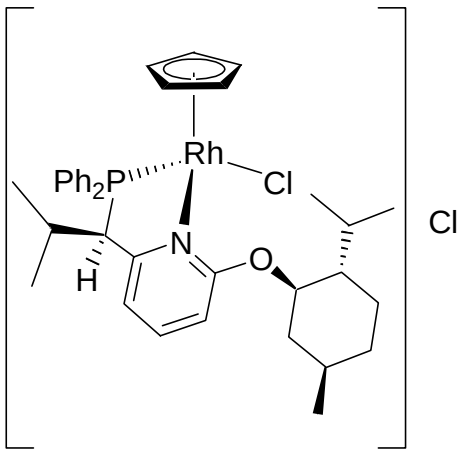

(L_{Ment},S_C)(S_{Rh})-**16**

Yield: 68.0 mg (75%).

Mp.: 138-145 °C.

^{1}H NMR (400 MHz, $CDCl_3$): δ = 8.14-7.20 (m, 13H, Ph, Py-H$^{3-5}$), 5.36 (d, $^3J_{P\text{-}H}$ = 1.2 Hz, 5H, L_{Ment},S_C,S_{Rh}-Cp-H), 5.67 (d, $^3J_{P\text{-}H}$ = 1.6 Hz, 5H, L_{Ment},S_C,R_{Rh}-Cp-H), 5.63 (d, $^3J_{P\text{-}H}$ = 1.6 Hz, 5H, L_{Ment},R_C,S_{Rh}-Cp-H), 5.38 (d, $^3J_{P\text{-}H}$ = 1.2 Hz, 5H, L_{Ment},R_C,R_{Rh}-Cp-H), 4.35 (dt, ^3J = 3.9 Hz, ^3J = 11.0 Hz, 1H, L_{Ment},S_C,S_{Rh}-OCH), 4.67-4.59 (m, 1H, L_{Ment},S_C,R_{Rh}-OCH), 4.57-4.50 (m, 1H, L_{Ment},R_C,S_{Rh}-OCH), 4.42 (dt, ^3J = 3.9 Hz, ^3J = 10.9 Hz, 1H, L_{Ment},R_C,R_{Rh}-OCH), 4.10 (dd, $^2J_{P\text{-}H}$ = 16.8 Hz, ^3J = 5.3 Hz, 1H, L_{Ment},S_C,S_{Rh}-PCHPy), 4.87 (br d, $^2J_{P\text{-}H}$ = 16.2 Hz, L_{Ment},S_C,R_{Rh}-PCHPy), 4.79 (br d, $^2J_{P\text{-}H}$ = 16.2 Hz, L_{Ment},R_C,S_{Rh}-PCHPy), 4.21 (dd, $^2J_{P\text{-}H}$ = 16.6 Hz, ^3J = 5.3 Hz, 1H, L_{Ment},R_C,R_{Rh}-PCHPy), 2.65-0.80 (m, 10H, Ment, CHC*H*$(CH_3)_2$), 1.04 (d, ^3J = 6.4 Hz, 3H, L_{Ment},S_C,S_{Rh}-CH_3), 1.08 (d, ^3J = 6.4 Hz, 3H, L_{Ment},R_C,R_{Rh}-CH_3), 1.17 (d, ^3J = 7.2 Hz, 3H, L_{Ment},R_C,S_{Rh}-CH_3), 0.99 (d, ^3J = 7.0 Hz, 3H, L_{Ment},S_C,S_{Rh}-CH_3), 0.98 (d, ^3J = 7.0 Hz, 3H, L_{Ment},R_C,R_{Rh}-CH_3), 1.05 (d, ^3J = 7.0 Hz, 3H, L_{Ment},R_C,S_{Rh}-CH_3), 0.74 (d, ^3J = 6.8 Hz, 3H, L_{Ment},S_C,S_{Rh}-CH_3), 0.93 (d, ^3J = 6.4 Hz, 3H, L_{Ment},R_C,R_{Rh}-CH_3), 0.91 (d, ^3J = 7.4 Hz, 3H, L_{Ment},R_C,S_{Rh}-CH_3), 0.59 (d, ^3J = 6.8 Hz, 3H, L_{Ment},S_C,S_{Rh}-CH_3), 0.92 (d, ^3J = 6.4 Hz, 3H, L_{Ment},S_C,R_{Rh}-CH_3), 0.76 (d, ^3J = 7.4 Hz, 3H, L_{Ment},R_C,R_{Rh}-CH_3), 0.91 (d, ^3J = 6.6 Hz, 3H, L_{Ment},R_C,S_{Rh}-CH_3), 0.33 (d, ^3J = 6.8 Hz, 3H, L_{Ment},S_C,S_{Rh}-CH_3), 0.39 (d, ^3J = 7.2 Hz, 3H, L_{Ment},S_C,R_{Rh}-CH_3), 0.36 (d, ^3J = 6.8 Hz, 3H, L_{Ment},R_C,R_{Rh}-CH_3), 0.48 (d, ^3J = 7.0 Hz, 3H, L_{Ment},R_C,S_{Rh}-CH_3).

^{31}P{^{1}H} NMR (162 MHz, $CDCl_3$): δ = 73.0 (d, $^1J_{Rh\text{-}P}$ = 125.1 Hz, 1P, L_{Ment},R_C,S_{Rh}-P), 72.3 (d, $^1J_{Rh\text{-}P}$ = 123.6 Hz, 1P, L_{Ment},S_C,R_{Rh}-P), 59.6 (d, $^1J_{Rh\text{-}P}$ = 131.24 Hz, 1P, L_{Ment},S_C,S_{Rh}-P), 58.7 (d, $^1J_{Rh\text{-}P}$ = 129.7 Hz, 1P, L_{Ment},R_C,R_{Rh}-P), –143.9 (sept, $^1J_{F\text{-}P}$ = 710.6 Hz, 1P, PF_6).

MS (ESI, CH_2Cl_2): *m/z* (%) = 676 (cation, 100).

Elemental analysis: $C_{36}H_{45}F_6ClNOP_2Rh\cdot(C_6H_6)_{1/2}$ (861.1):

Calcd. C 54.40, H 5.62, N 1.63.

Found C 53.92, H 5.79, N 1.55.

2.5 References

1. Brunner, H. *Adv. Organomet. Chem.* **1980**, *18*, 151.
2. Brunner, H. *Angew. Chem., Int. Ed.* **1999**, *38,* 1194.
3. Brunner, H. *Eur. J. Inorg. Chem.* **2001**, 905.
4. Brunner, H.; Köllnberger, A.; Burgemeister, T.; Zabel. M. *Polyhedron* **2000**, *19*, 1519.
5. Brunner, H.; Köllnberger, A.; Zabel. M. *Polyhedron* **2003**, *22*, 2639.
6. Brunner, H.; Zwack, T.; Zabel. M.; Beck, W.; Böhm, A. *Organometallics* **2003**, *22*, 1741.
7. Brunner, H.; Henning, F.; Weber, M.; Zabel, M.; Carmona, D.; Lahoz, F. J. *Synthesis* **2003**, 1091.
8. Carmona, D.; Lamata, M. P.; Oro, L. A. *Eur. J. Inorg. Chem.* **2002**, 2239.
9. Brookhart, M.; Timmers, D.; Tucker, J. R.; Williams, G. D.; Husk, G. R.; Brunner, H.; Hammer, B. *J. Am. Chem. Soc.* **1983**, *105*, 6721.
10. Brunner, H.; Lukas, R. *Chem. Ber.* **1979**, *112*, 2528.
11. Brunner, H. *Acc. Chem. Res.* **1979**, *12*, 250.
12. Haack, K. J.; Hashiguchi, S.; Fujii, A.; Ikariya, T.; Noyori, R. *Angew. Chem., Int. Ed. Engl.* **1997**, *36*, 285.
13. Kaulen, C.; Pala, C.; Hu, C.; Ganter, C. *Organometallics* **2001**, *20*, 1614.
14. Halpern, J. In *Asymmetric Synthesis*, Vol. 5, Morrison, J. Ed., Academic Press, Orlando, 1985, pp. 41-69.
15. Brunner, H.; Köllnberger, A.; Mehmood, A.; Tsuno, T.; Zabel, M. *Organometallics* **2004**, *23*, 4006.
16. Brunner, H.; Köllnberger, A.; Mehmood, A.; Tsuno, T.; Zabel, M. *J. Organomet. Chem.* **2004**, *689*, 4244.
17. Köllnberger, A. Ph.D. Thesis, University of Regensburg, 2002.
18. Lecomte, C.; Dusausoy, Y.; Protas, J.; Tirouflet, J.; Dormond, A. *J. Organomet. Chem.* **1974**, *73*, 67.
19. Brunner, H. *Enantiomer* **1997**, *2*, 133.
20. Knof, U.; von Zelewsky, A. *Angew. Chem., Int. Ed.* **1999**, *38*, 303.
21. Therrien, B.; Ward, T. R. *Angew. Chem., Int. Ed.* **1999**, *38*, 405.
22. Therrien, B.; König, A.; Ward, T. R. *Organometallics* **1999**, *18*, 1565.
23. Vogelgesang, J.; Frick, A.; Huttner, G.; Kircher, P. *Eur. J. Inorg. Chem.* **2001**, 949.
24. Tsuno, T.; Brunner, H.; Katano, S.; Kinjyo, N.; Zabel, M. *J. Organomet. Chem.* **2006**, *691*, 2739.
25. Stoppioni, P.; Di Vaira, M.; Maitlis, P. M. *J. Chem. Soc., Dalton Trans.* **1982**, 1147.

26. Valderrama, M.; Contreras, R.; Bascuňan, M.; Alegria, S.; Boys, D. *Polyhedron* **1995**, *14*, 2239.
27. Durran, S. E.; Smith, M. B.; Dale, S. H.; Coles, S. J.; Hursthouse, M. B.; Light, M. E. *Inorg. Chim. Acta* **2006**, *359*, 2980.
28. Clarke, M. L.; Slawin, A. M. Z.; Wheatley, M. V.; Woollins, J. D. *J. Chem. Soc., Dalton Trans.* **2001**, 3421.
29. White, C.; Yates, A.; Maitlis, P. M.; Heinekey, D. M. *Inorg. Synth.* **1992**, *29*, 228.
30. Lyatifov, I. R.; Dzhafarov, G. M.; Kurbanov, T. Kh. *J. Gen. Chem. USSR* **1989**, *59*, 1606; Zh. *Obsh. Khim.* **1989**, *59*, 1803.
31. Ragauskas, A. J.; Stothers, J. B. *Can. J. Chem.* **1985**, *63*, 2961.
32. Ashimori, A.; Ono, T.; Uchida, T.; Ohtaki, Y.; Fukaya, C.; Watanabe, M.; Yokoyama, K. *Chem. Pharm. Bull.* **1990**, *38*, 2446.

3 Synthesis of Chiral-at-Metal Half-Sandwich Ruthenium(II) Complexes with the CpH(PN_{Ment}) Tripod Ligand

3.1 Abstract

Treatment of the chiral tripod ligand (L_{Ment},S_C)-CpH(PN_{Ment}) **1** with $(Ph_3P)_3RuCl_2$ in ethanol afforded the two chiral-at-metal diastereomers (L_{Ment},S_C,R_{Ru})- and (L_{Ment},S_C,S_{Ru})-[Cp(PN_{Ment})Ru(PPh_3)Cl] (70% de) in which the cyclopentadienyl group and the P atom of the ligand coordinated at the metal center. The (L_{Ment},S_C,R_{Ru})-diastereomer was isolated by crystallization from ethanol-pentane and its structure was established by X-ray crystallography. The (L_{Ment},S_C,R_{Ru})-diastereomer epimerized in $CDCl_3$ solution at 60 °C in a first-order reaction with a half-life of 56.6 h. In alcoholic solution epimerization occurred at room temperature. Substitution of the chloride ligand in (L_{Ment},S_C,R_{Ru})- and (L_{Ment},S_C,S_{Ru})-[Cp(PN_{Ment})Ru(PPh_3)Cl] by nitriles NCR (R = Me, Ph, CH_2Ph) in the presence of NH_4PF_6 gave mixtures of the diastereomers (L_{Ment},S_C,R_{Ru})- and (L_{Ment},S_C,S_{Ru})-[Cp(PN_{Ment})Ru(PPh_3)NCR]PF_6. Treatment of (L_{Ment},S_C,R_{Ru})- and (L_{Ment},S_C,S_{Ru})-[Cp(PN_{Ment})Ru(PPh_3)Cl] with piperidine or morpholine in the presence of NH_4PF_6 led to the chiral-at-metal diastereomers (L_{Ment},S_C,R_{Ru})- and (L_{Ment},S_C,S_{Ru})-[Cp(PN_{Ment})Ru(PPh_3)NH_3]PF_6 (6% de).

3.2 Introduction

Due to the recent progress in asymmetric organometallic catalysis, enantioselective synthesis has become one of the most effective methods for the preparation of enantiomerically enriched compounds and alternative strategies in this field are highly desired. In three-legged piano-stool complexes of the type [(η^n-Ar)M(LL')X] (LL' = unsymmetrical chelate ligand and X = monodentate ligand) the metal atom is a chiral center. These compounds have attracted much study in terms of the stereochemistry of substitution reactions at the chiral metal center.[1-4] In particular, there are many chiral-at-metal ruthenium compounds [(η^5-Cp)Ru(LL')X] some of which can be used as catalysts in organic transformations. As usually the epimerization at the

metal center is faster than the catalytic reaction, two diastereomeric catalysts participate in product formation. Hence, it would be desirable to control the metal configuration in such complexes during catalysis.

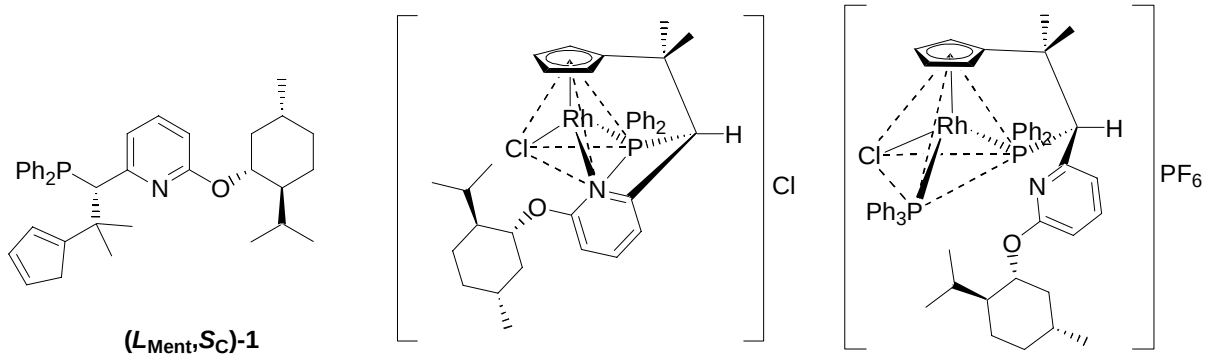

(*L*$_{Ment}$,*S*$_C$)-**1** (*L*$_{Ment}$,*S*$_C$,*R*$_{Rh}$)-**4** (*L*$_{Ment}$,*S*$_C$,*S*$_{Rh}$)-**10**

Chart 3-1

As described in the Part 2, the tripod ligand CpH(PN$_{Ment}$) = (L$_{Ment}$,*S*$_C$)-**1** (Chart 3-1) has three different binding sites, a cyclopentadiene system (CpH), a diphenylphosphanyl group (P), and a 2-menthoxy-substituted pyridine ring (N$_{Ment}$) connected by an asymmetric carbon atom. Separation of the CpH(PN$_{Ment}$)-diastereomers (L$_{Ment}$,*S*$_C$) and (L$_{Ment}$,*R*$_C$) by fractional crystallization gave (L$_{Ment}$,*S*$_C$)-**1** resolved with respect to the asymmetric carbon atom at the branching position.[5)] The synthesis of the half-sandwich rhodium complex (L$_{Ment}$,*S*$_C$,*R*$_{Rh}$)-**4** in which the ligand coordinated with Cp, P and N$_{Ment}$ to the metal atom (Chart 3-1), was reported. The (*S*$_C$)-configuration of the tripod ligand (L$_{Ment}$,*S*$_C$)-**1** enforced (*R*$_{Rh}$)-configuration at the metal center and inhibited any configuration change at the metal atom including substitution reactions of the Cl ligand by other halogen and pseudohalogen ligands.[5,6)] However, the attempt to replace the Cl ligand by PPh$_3$ resulted in a decoordination of the pyridine part of the ligand which in the product (L$_{Ment}$,*S*$_C$,*S*$_{Rh}$)-**10** was only bound to the metal atom by Cp and P (Chart 3-1). This part deals with the synthesis of chiral-at-metal ruthenium complexes with the tripod ligand (L$_{Ment}$,*S*$_C$)-**1** resolved at the branching asymmetric carbon atom.

3.3 Results and Discussion

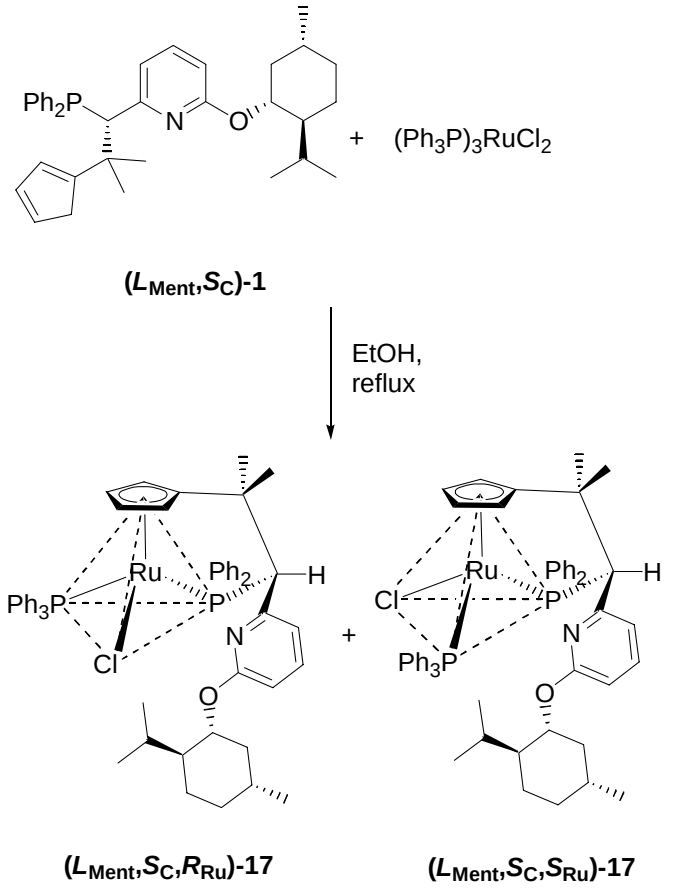

Scheme 3-1

The reaction of (L_{Ment},S_C)-**1** with $(Ph_3P)_3RuCl_2$ in ethanol afforded orange crystals in 54% yield. The ^1H NMR spectrum of a solution of the crystals in $CDCl_3$ showed two sets of signals which are assigned to be the two diastereomers (L_{Ment},S_C,R_{Ru})- and (L_{Ment},S_C,S_{Ru})-**17** differing only in the Ru-configuration (Scheme 3-1). This assignment was corroborated by the appearance of two signals in the $^{31}P\{^1H\}$ NMR spectrum for a coordinated PPh_3 ligand at 42.8 (d, $^2J_{P\text{-}P}$ = 35.1 Hz) and 43.6 ppm (d, $^2J_{P\text{-}P}$ = 35.1 Hz) and the coordinated PPh_2 group of the tripod ligand at 75.0 (d, $^2J_{P\text{-}P}$ = 35.1 Hz) and 62.8 ppm (d, $^2J_{P\text{-}P}$ = 35.1 Hz), respectively (ratio 85 : 15). In boiling benzene the reaction of (L_{Ment},S_C)-**1** with $(Ph_3P)_3RuCl_2$ gave the two diastereomers also in the ratio 85 : 15.

In the reaction of (L_{Ment},S_C)-**1** with $(Ph_3P)_3RuCl_2$ the cyclopentadiene system of the tripod was transformed into the π-bonded cyclopentadienyl ligand occupying three coordination sites at the Ru atom in (L_{Ment},S_C,R_{Ru})- and (L_{Ment},S_C,S_{Ru})-**17**. According to the $^{31}P\{^1H\}$ NMR spectrum

another two coordination sites in the half-sandwich complexes were occupied by P atoms. The sixth coordination position, however, was crucial. The ligand for this coordination site could have been the relatively nucleophilic chloride giving the neutral complex [Cp(PN_{Ment})Ru(PPh_3)Cl] **17** (similar to **10** in Chart 3-1) or the pyridine arm of the tripod ligand giving the ionic complex [Cp(PN_{Ment})Ru(PPh_3)]Cl **18** (Chart 3-2 and similar to **4** in Chart 3-1). A decision was possible on the basis of the mass spectra. The ESI-MS spectrum in dichloromethane-acetonitrile showed peaks at *m/z* 900 for $[Cp(PN_{Ment})Ru(PPh_3)]^+$ and at *m/z* 941 for $[Cp(PN_{Ment})Ru(PPh_3)NCMe]^+$ [Fig. 3-1 (a)]. These ions do not contain chlorine.

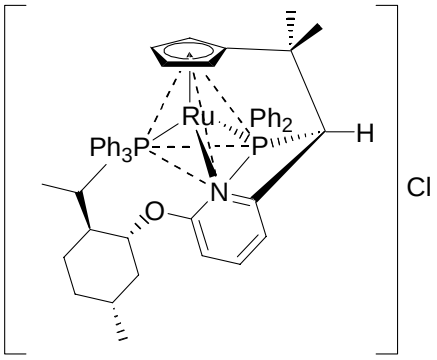

(L_{Ment},S_C,R_{Ru})-18

Chart 3-2.

However, when the solvent was changed to dichloromethane only, a peak at 935 for $[Cp(PN_{Ment})Ru(PPh_3)Cl]^+$ was observed [Fig. 3-1 (b)] indicating that complexes (L_{Ment},S_C,R_{Ru})- and (L_{Ment},S_C,S_{Ru})-**17** do contain a coordinated chloride ligand at the metal center. It has been reported that the reaction of **19** with $(Ph_3P)_3RuCl_2$ had given an ionic complex [Cp(PN)Ru(PPh_3)]Cl **20** with the tripod ligand binding by Cp, P and N (Scheme 3-2, top).[7] As in the FD mass spectrum in CH_2Cl_2 a peak at *m/z* 781 had been present this complex must be reformulated as the neutral complex [Cp(PN)Ru(PPh_3)Cl] **21** with a coordinated chloride ligand and the tripod ligand binding by Cp and P only similar to the complexes **17** of the present study.

Fortunately, slow diffusion of pentane into an ethanol or CH_2Cl_2 solution of the diastereomers **17** afforded single crystals of the main diastereomer of **17** which an X-ray analysis proved to have (L_{Ment},S_C,R_{Ru})-configuration (Fig. 3-2). The X-ray analysis corroborated the presence of the coordinated chloride ligand and the binding of the tripod ligand by Cp and P only. In Part 5, data of the X-ray analysis will be given.

In the CD spectrum of (L_{Ment},S_C,R_{Ru})-**17** a positive Cotton effect was observed at 286 nm in CH_2Cl_2 (Fig. 3-3, solid line) which has the same intensity but opposite sign compared to (L_{Ment},S_C,S_{Rh})-**4** probably due to the opposite metal configurations (see Fig. 2-2 in Part 2).

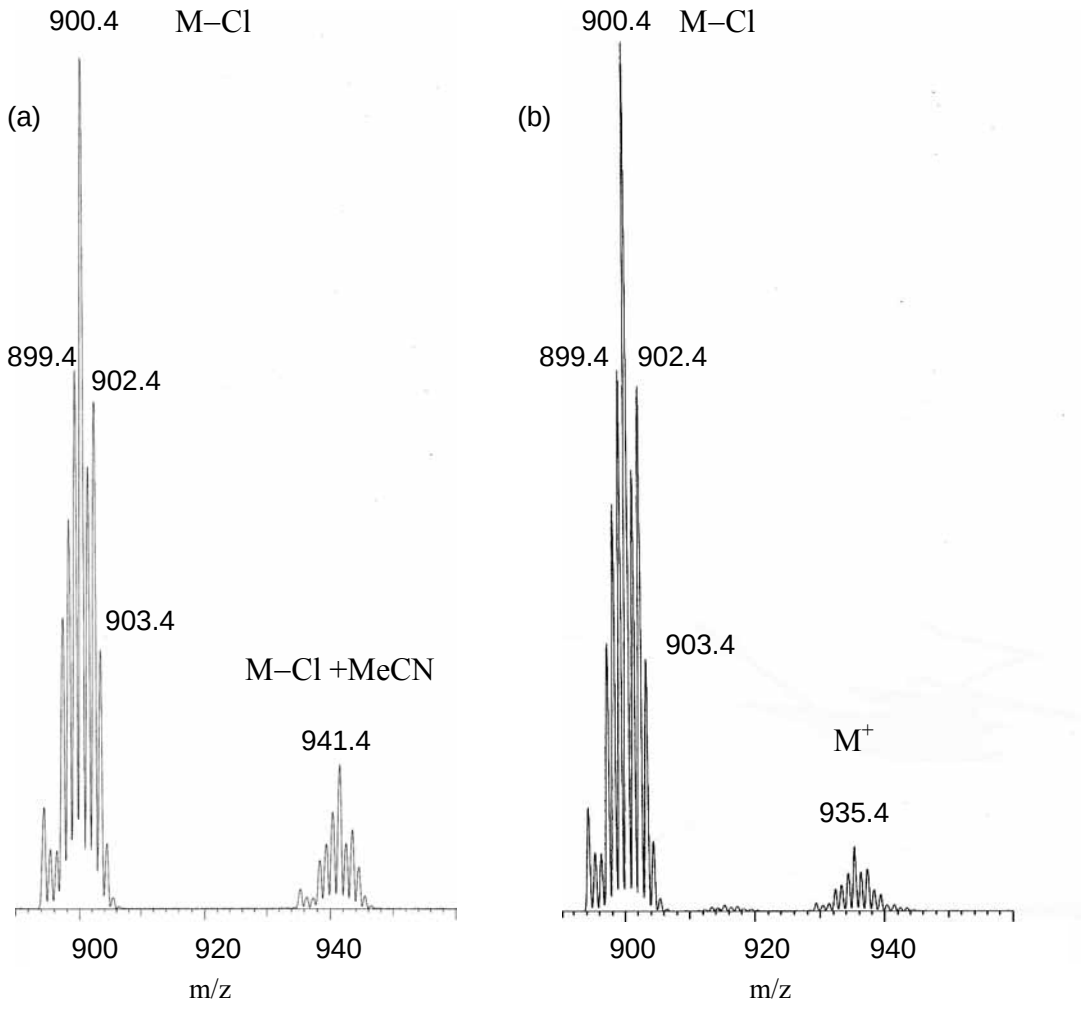

Figure 3-1. ESI-MS spectra of **17**: (a) in CH_2Cl_2-MeCN, (b) in CH_2Cl_2.

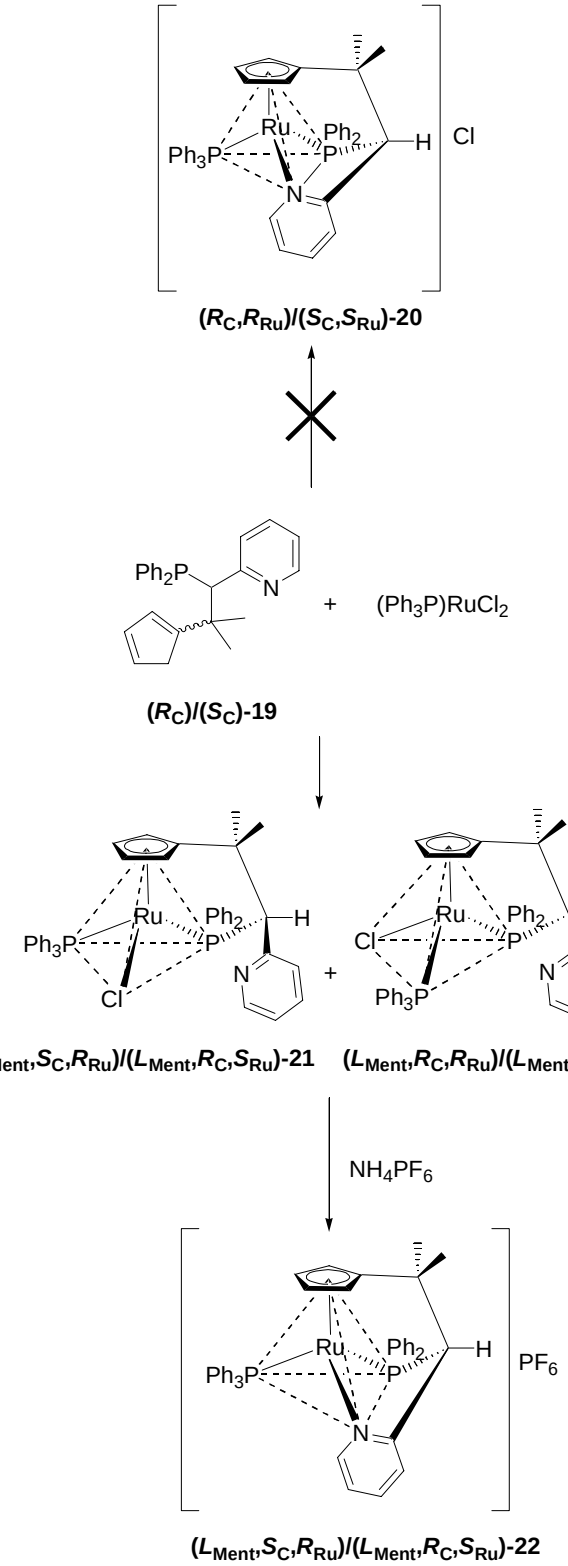
Ru
Ph2
Ph3P
P
H
Cl
N
(RC,RRu)/(SC,SRu)-20
Ph2P
N
+
(Ph3P)RuCl2
(RC)/(SC)-19
Ru
Ph2
H
Ph3P
P
N
Cl
+
Ru
Ph2
H
Cl
P
N
Ph3P
(LMent,SC,RRu)/(LMent,RC,SRu)-21
(LMent,RC,RRu)/(LMent,SC,SRu)-21
NH4PF6
Ru
Ph2
H
Ph3P
P
N
PF6
(LMent,SC,RRu)/(LMent,RC,SRu)-22

Scheme 3-2.

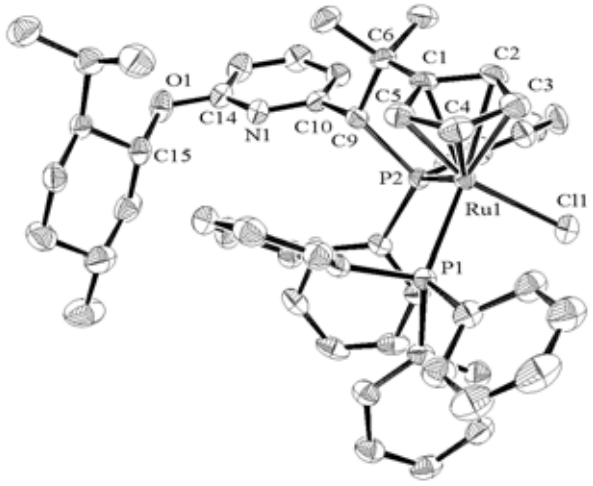

Figure 3-2. Molecular structure of (L_{Ment},S_C,R_{Ru})-**17**. Hydrogen atoms are omitted for clarity. Selected bond lengths [Å], angles and torsion angles [°]: Ru1-Cl1 2.4626(8), Ru1-P1 2.3219(7), Ru1-P2 2.3056(6), Ru1-C1 2.170(3), Ru1-C2 2.210(3), Ru1-C3 2.230(3), Ru1-C4 2.227(3), Ru1-C5 2.167(3); Cl1-Ru1-P1 91.85(3), Cl1-Ru1-P2 97.17(2), P1-Ru1-P2 100.87 (2), Ru1-P2-C9 101.08(8); Cl1-Ru1-P2-C(9) -159.90(8), P1-Ru1-P2-C9 106.81(8), Ru1-P2-C9-C6 42.66(18), Ru1-P2-C9-C10 179.20(19).

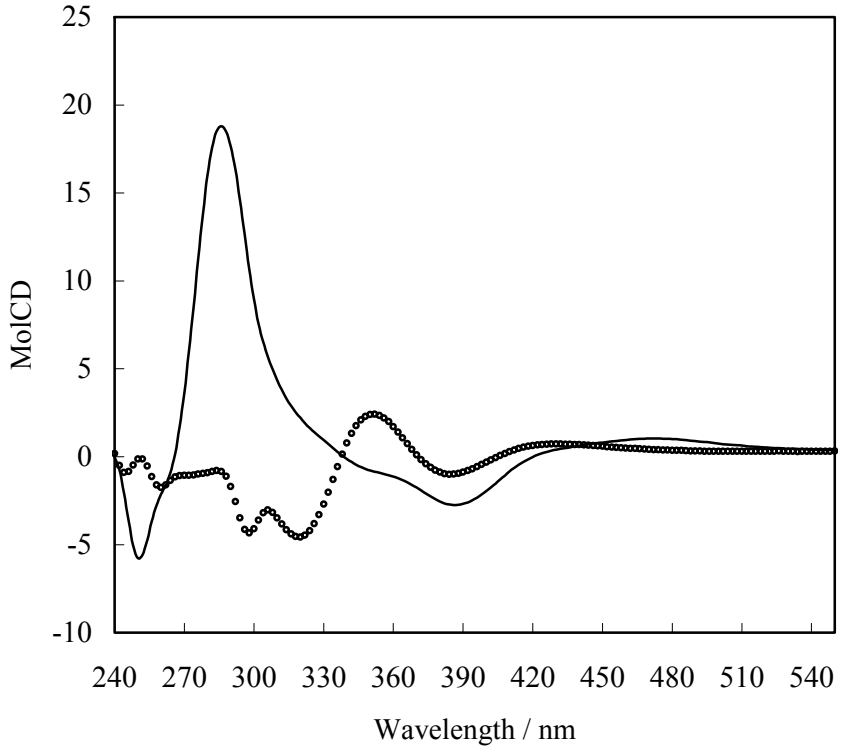

Figure 3-3. CD spectra of (L_{Ment},S_C,R_{Ru})-**17** (——) and a mixture (88 : 12) of (L_{Ment},S_C,R_{Ru})- and (L_{Ment},S_C,S_{Ru})-**23** (·····) in CH_2Cl_2.

The diastereomer (L_{Ment},S_C,R_{Ru})-**17** was configurationally stable in the solid state. In solution, however, epimerization occurred. When the equilibration of (L_{Ment},S_C,R_{Ru})-**17** (1.02×10^{-3} mol L^{-1}) with respect to the Ru-configuration to give the 85 : 15-mixture of (L_{Ment},S_C,R_{Ru})- and (L_{Ment},S_C,S_{Ru})-**17** was monitored by ^{1}H NMR in $CDCl_3$ at 60 °C, a rate constant *k* was calculated as 3.4×10^{-6} s^{-1} [half-life τ = 56.6 h] (Fig. 3-4). The cyclopentadienyl proton at ca. 3 ppm and the methine proton on the chiral carbon atom of (L_{Ment},S_C,R_{Ru})-**17** were observed as broad peaks (Fig. 3-4, bottom) Surprisingly, although both proton signals shifted to lower magnetic field during isomerization to (L_{Ment},S_C,S_{Ru})-**17**, the signals of these protons appeared as sharp peaks shifted to higher magnetic field with the methine proton resolved as a doublet ($^1J_{P\text{-}H}$ = 10.1 Hz) after 2 weeks at room temperature (Fig. 3-4, top). In the $^{31}P\{^1H\}$ NMR spectra a signal change of broad doublets to sharp doublets was also observed. Probably this signal broadening is caused by the paramagnetic species $[Cp(PN_{Ment})Ru(PPh_3)Cl]^+$ which were produced by the reaction of (L_{Ment},S_C,R_{Ru})-**17** with traces of oxygen. This will be fully discussed in Part 4. Furthermore, when CD_3OD was added to a solution of (L_{Ment},S_C,R_{Ru})-**17** in $CDCl_3$ at room temperature, the ratio of (L_{Ment},S_C,R_{Ru})- and (L_{Ment},S_C,S_{Ru})-**17** immediately reached the equilibrium state of 85 : 15.

The configurational lability of (L_{Ment},S_C,R_{Ru})-**17** found in the present study contrasts with the configurational stability of (R_C,R_{Ru})- and (R_C,S_{Ru})-[CpRu(Prophos)Cl], Prophos = (*R*)-1,2-bis(diphenylphosphanyl)propane.[8,9] Both compounds have the same coordination frame Cp, P, P', Cl with the chelate bridge in our complex between Cp and P and in the Prophos complex between P and P'. Whereas in our case the diastereomer ratio in the synthesis both in ethanol and in benzene was under thermodynamic control (see above), Consiglio et al. assigned the diastereomer ratio of 60 : 40 in their synthesis in refluxing benzene to kinetic control.[8] They state that their complexes did not show epimerization in toluene at 80 °C for 96 h, but they claim epimerization in C_6D_5Cl at 80 °C. Furthermore, Consiglio et al. used their Prophos complexes in methanol solution as the starting material for substitution reactions, which overwhelmingly occurred with retention of configuration at the Ru atom.[10,11] In contrast, our compound (L_{Ment},S_C,R_{Ru})-**17** epimerized readily in alcoholic solution at room temperature probably due to the ancillary effect of the dangling pyridine ligand**.** An alternative explanation of the higher configurational stability of Consiglio's Prophos complex (R_C,S_{Ru})-[CpRu(Prophos)Cl] could be the small chelate angle P-Ru-P' of 82.9° resisting widening necessary in any transition state for a change of the Ru configuration. As shown in Fig. 3-2, the P1-Ru-P2 angle in (L_{Ment},S_C,R_{Ru})-**17** is 100.87°. Conversely, in (L_{Ment},S_C,R_{Ru})-**17** the Cp-Ru-P2 (Cp = ring centroid) angle to the tethered

PPh_2 group and the Cp-Ru-P1 angle to the PPh_3 ligand are 113.16° and 117.90°, respectively. These angles are smaller than the Cp-Ru-P and Cp-Ru-P' angles in the Prophos complex (129.5° and 131.3°).[8] These problems will be addressed in Part 4 of this Thesis.

The reaction of the racemic tripod CpH(PN)-**19** lacking the 2-menthoxy substituent with $(Ph_3P)_3RuCl_2$ in the presence of NH_4PF_6 had given the complex $[Cp(PN)Ru(PPh_3)]PF_6$ **22** in which the tripod was bonded by Cp, P and N (Scheme 3-2, bottom).[7] We tried to synthesize the same type of complex with the resolved tripod $CpH(PN_{Ment})$ (L_{Ment},S_C)-**1**. However, the reaction of the diastereomers (L_{Ment},S_C,R_{Ru})- and (L_{Ment},S_C,S_{Ru})-**17** with NH_4PF_6 in CH_2Cl_2 afforded yellow-black powders the ^1H NMR spectrum of which showed only broad signals. Obviously, the N_{Ment} part of the tripod cannot coordinate at the metal center due to steric repulsion between the bulky 2-menthoxy moiety and the triphenylphosphane ligand.

Next, the reaction of diastereomerically pure (L_{Ment},S_C,R_{Ru})-**17** and NH_4PF_6 in the presence of acetonitrile was investigated. The monodentate ligand gave mixtures of the diastereomers (L_{Ment},S_C,R_{Ru})- and (L_{Ment},S_C,S_{Ru})-$[Cp(PN_{Ment})Ru(PPh_3)NCMe]PF_6$ **23** in 91% yield (76% de) (Scheme 3-3). The CD spectrum of the mixture of (L_{Ment},S_C,R_{Ru})- and (L_{Ment},S_C,S_{Ru})-**23** is shown in Fig. 3-3 (dotted line). It has been reported that both (S_C,R_{Ru})- and (S_C,S_{Ru})-$[CpRu(Prophos)NCMe]PF_6$ were stereospecifically obtained by substitution of the corresponding diastereomers (S_C,R_{Ru})- and (S_C,S_{Ru})-[CpRu(Prophos)Cl] with acetonitrile in the presence of NH_4PF_6.[10,11] However, in this case complex **17** was isolated as a mixture of diastereomers. When benzonitrile and phenylacetonitrile were used as monodentate ligands and reacted with the mixture of the diastereomers (L_{Ment},S_C,R_{Ru})- and (L_{Ment},S_C,S_{Ru})-**17** and NH_4PF_6, a mixture of the diastereomers of (L_{Ment},S_C,R_{Ru})- and (L_{Ment},S_C,S_{Ru})-$[Cp(PN_{Ment})Ru(PPh_3)NCR]PF_6$ **24** (R = Ph) and **25** (R = CH_2Ph) was obtained. The diastereomeric excess decreased in the order **23** (76% de) > **24** (56% de) > **25** (44% de). In the ESI-MS spectra of these nitrile complexes a cation peak containing the corresponding coordinated nitrile was observed, when dichloromethane was used as the solvent. Small amounts of single crystals of **25** were obtained by recrystallization from CH_2Cl_2-ether. The X-ray analysis proved the (L_{Ment},S_C,R_{Ru})-configuration (Fig. 3-5). There is a strong resemblance between the structures of (L_{Ment},S_C,R_{Ru})-**23** and (L_{Ment},S_C,R_{Ru})-**25**. As shown in Fig. 3-5, the phenyl group of phenylacetonitrile bends towards the ruthenium center minimizing space filling.

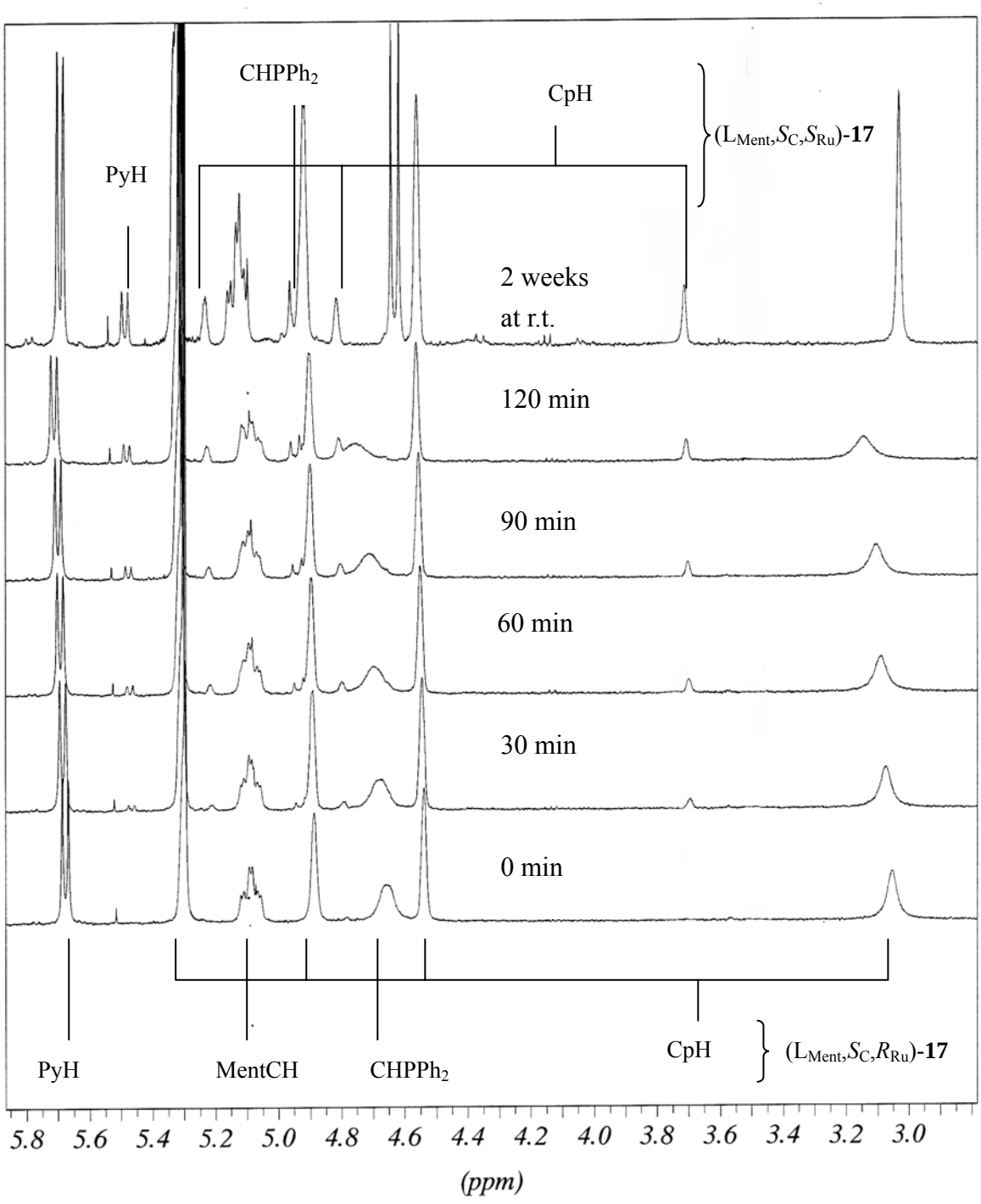

Figure 3-4. Time resolved ^{1}H NMR spectra of the isomerization of (L_{Ment},S_C,R_{Ru})-**17** to (L_{Ment},S_C,S_{Ru})-**17** at 60 °C in $CDCl_3$.

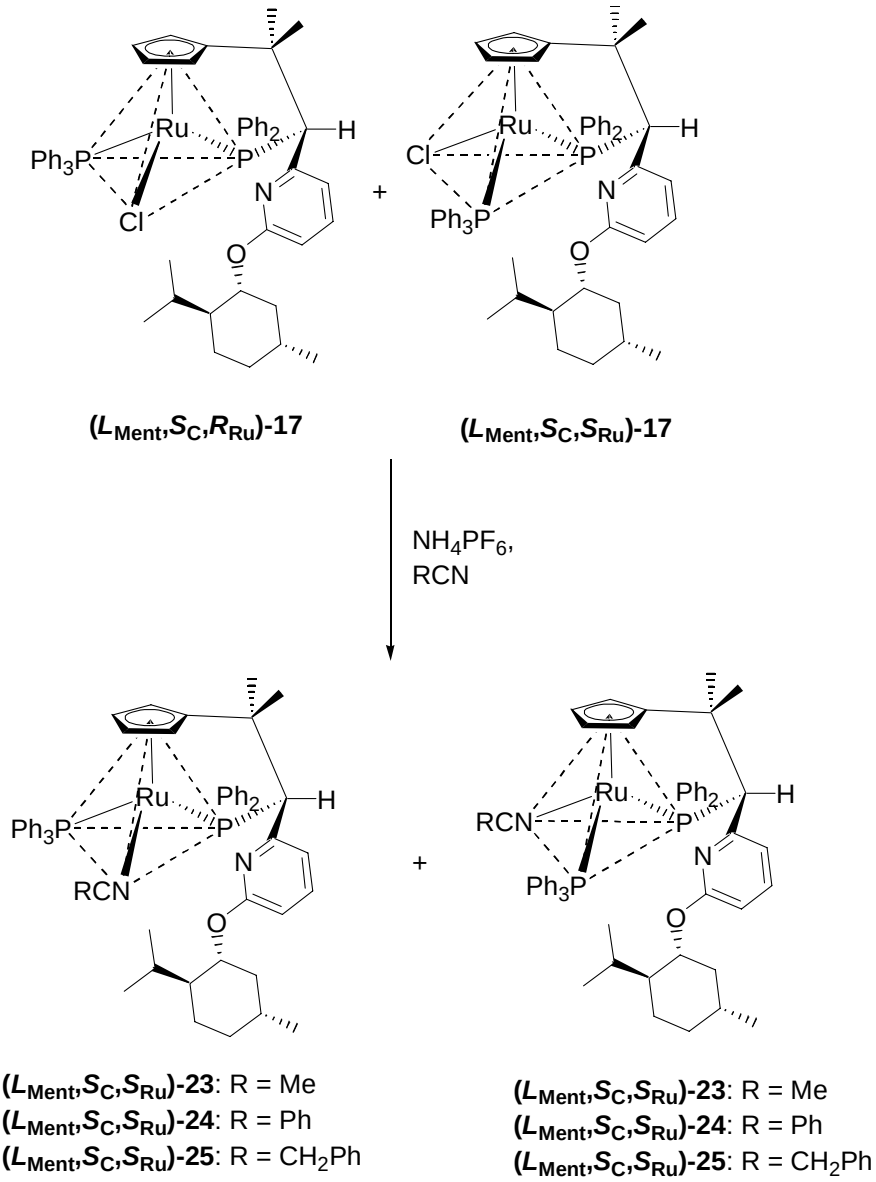

(*L*$_{Ment}$,*S*$_C$,*R*$_{Ru}$)-**17** (*L*$_{Ment}$,*S*$_C$,*S*$_{Ru}$)-**17**

(*L*$_{Ment}$,*S*$_C$,*S*$_{Ru}$)-**23**: R = Me
(*L*$_{Ment}$,*S*$_C$,*S*$_{Ru}$)-**24**: R = Ph
(*L*$_{Ment}$,*S*$_C$,*S*$_{Ru}$)-**25**: R = CH_2Ph

(*L*$_{Ment}$,*S*$_C$,*S*$_{Ru}$)-**23**: R = Me
(*L*$_{Ment}$,*S*$_C$,*S*$_{Ru}$)-**24**: R = Ph
(*L*$_{Ment}$,*S*$_C$,*S*$_{Ru}$)-**25**: R = CH_2Ph

Scheme 3-3.

Using amines such as piperidine and morpholine as monodentate ligands we expected a stereospecific substitution of the chloride ligand in (L$_{Ment}$,*S*$_C$,*R*$_{Ru}$)-**17** due to the formation of a hydrogen bond between the incoming amines and the nitrogen of the dangling pyridine. However, both reactions of (L$_{Ment}$,*S*$_C$,*R*$_{Ru}$)-**17** with piperidine and morpholine, respectively, and NH_4PF_6 gave a mixture of diastereomers of the same compound (54% yield for piperidine; 63% for morpholine). The IR spectra showed N-H bands at 3356 and 3282 cm^{-1}.[12] In the ESI-MS spectrum in dichloromethane a cation of *m/z* 917 was observed which corresponded to $[Cp(PN_{Ment})Ru(PPh_3)NH_3]^+$. This suggests that the product was (L$_{Ment}$,*S*$_C$,*R*$_{Ru}$)- and (L$_{Ment}$,*S*$_C$,*S*$_{Ru}$)-**26** with ammonia coordinated to the ruthenium center corroborated by the data of

the elemental analysis (Scheme 3-4). It has been reported that an ammine-ruthenium(II) complex $[CpRu(PPh_3)_2NH_3]PF_6$ was prepared by the reaction of $[CpRu(PPh_3)_2Cl]$ with NH_4PF_6 in the presence of thallium(I) carbonate in methanol.[12] In this reaction, the thallium(I) cation scavenged the chloride anion and the carbonate ion removed a proton from the ammonium ion. The ammonia formed coordinated to the metal center. Similarly, in our case the amines piperidine and morpholine abstracted a proton from the ammonium ion of the additive NH_4PF_6 and the resulting ammonia replaced the chloride ligand in (L_{Ment},S_C,R_{Ru})- and (L_{Ment},S_C,S_{Ru})-**17** to give (L_{Ment},S_C,R_{Ru})- and (L_{Ment},S_C,S_{Ru})-**26**. The ratio of the diastereomers of **26** was determined to be 57 : 43 by $^{31}P\{^1H\}$ NMR analysis (6% de).

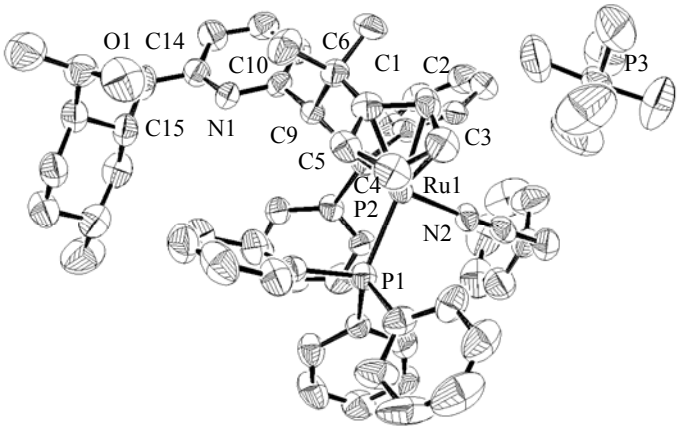

Figure 3-5. Molecular structure of (L_{Ment},S_C,R_{Ru})-**25**. Hydrogen atoms are omitted for clarity. Selected bond lengths [Å], angles and torsion angles [°]: Ru1-N2 2.018(5), Ru1-P1 2.305(2), Ru1-P2 2.330(2), Ru1-C1 2.230(7), Ru1-C2 2.270(6), Ru1-C3 2.233(5), Ru1-C4 2.191(5), Ru1-C5 2.180(6); N2-Ru1-P1 93.7(2), N2-Ru1-P2 91.5(1), P1-Ru1-P2 102.00 (6), Ru1-P2-C9 102.02(2); N2-Ru1-P2-C(9) -159.4(2), P1-Ru1-P2-C9 106.5(2), Ru1-P2-C9-C6 42.1(4), Ru1-P2-C9-C10 179.2(4).

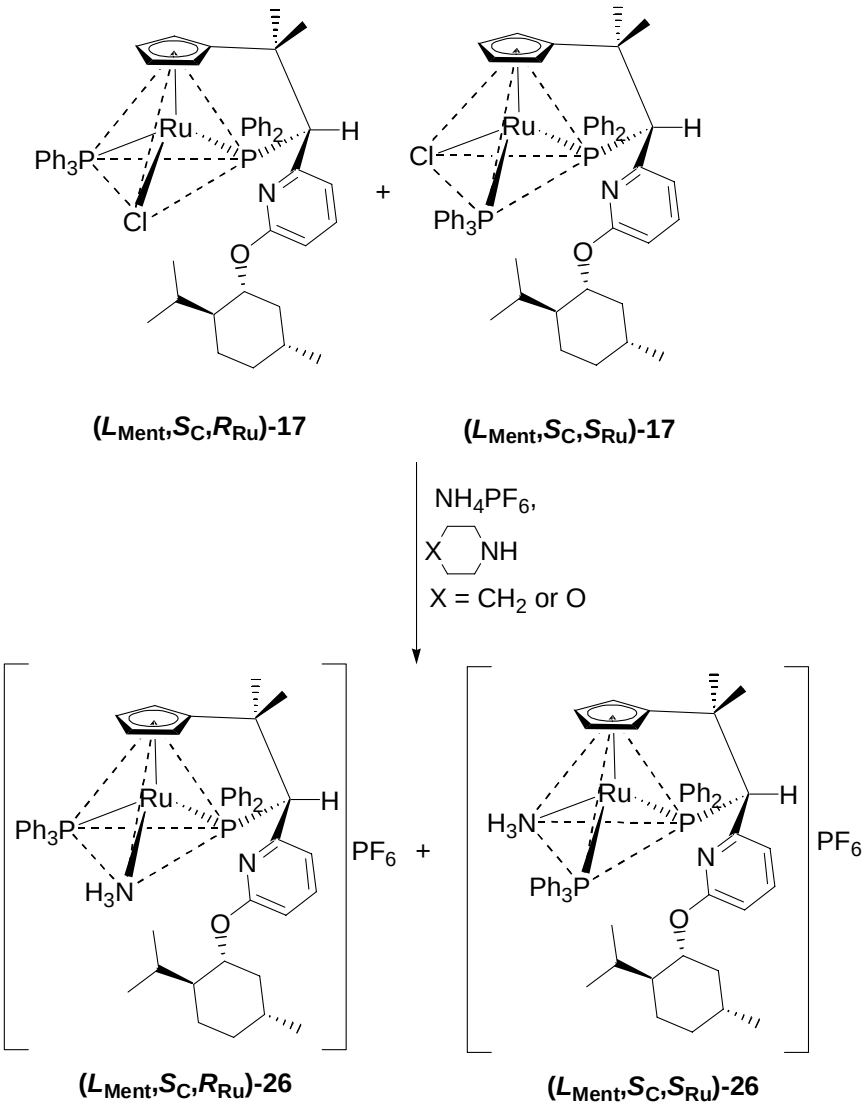

(L_{Ment},S_C,R_{Ru})-17 **(L_{Ment},S_C,S_{Ru})-17**

(L_{Ment},S_C,R_{Ru})-26 **(L_{Ment},S_C,S_{Ru})-26**

Scheme 3-4.

3.4 Experimental

3.4.1 General

Synthetic conditions, solvents, spectra, and analyses were obtained as previously described.

3.4.2 Chemicals

$RuCl_3 \cdot 3H_2O$ and $(Ph_3P)_3RuCl_2$ were commercially available. 2-(2-Cyclopentadienyl-1-diphenylphosphanyl-2-methylprop-1-yl)-6-[(1*R*,2*S*,5*R*)-menthoxy]pyridine **1** was obtained as previously descrived.[6)]

(R_{Ru})/(S_{Ru})-Chloro[1-[(2*S*)-2-(diphenylphosphanyl-κP)-1,1-dimethyl-2-[6-[[(1*R*,2*S*,5*R*)-menthoxy-2-pyridinyl]ethyl]-η^5-cyclopentadienyl](triphenylphosphine)ruthenium(II) (L_{Ment},S_C,R_{Ru})-17 and (L_{Ment},S_C,S_{Ru})-17: To a suspension of $(Ph_3P)_3RuCl_2$ (1.22 g, 1.27 mmol) in absolute ethanol (70 mL) was added a solution of (L_{Ment},S_C)-**1** (754 mg, 1.32 mmol) in CH_2Cl_2 (10 mL) at room temperature. The mixture was refluxed for 3 h and then cooled to room temperature. After evaporation of the solvent, the residue was chromatographed on silica gel using 25% EtOAc-petroleum ether (40/60) as an eluent to give a crude diastereomer mixture of (L_{Ment},S_C,R_{Ru})- and (L_{Ment},S_C,S_{Ru})-**17**. Crystallization from CH_2Cl_2-pentane afforded (L_{Ment},S_C,R_{Ru})- and (L_{Ment},S_C,S_{Ru})-**17** in 54% yield (651 mg) as orange crystals. Diastereomerically pure (L_{Ment},S_C,R_{Ru})-**17** was obtained by slow recrystallization from CH_2Cl_2-pentane or ethanol-pentane at room temperature.

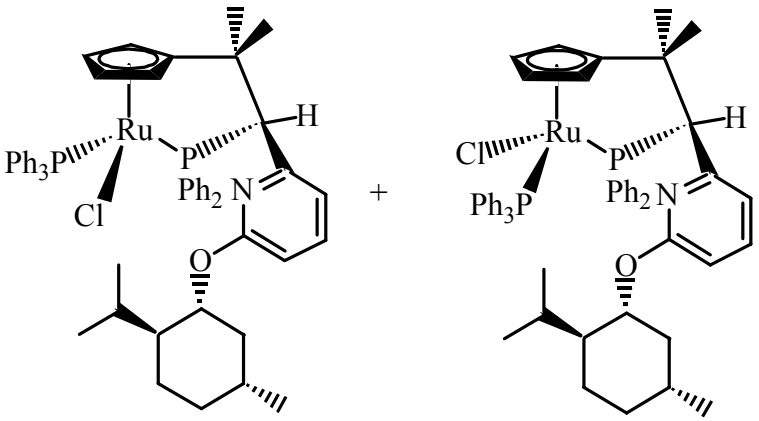

(L_{Ment},S_C,R_{Ru})-17 (L_{Ment},S_C,S_{Ru})-17

Mp.: 158-159 °C.

^{1}H NMR (400 MHz, CD_2Cl_2, 300 K, signals of the (L_{Ment},S_C,S_{Ru})-isomer given in brackets if distinguishable): δ = 7.83 (t, ^3J = 8.5 Hz, 2H, Ph), [7.41 (t, ^3J= 7.2 Hz, 2H, Ph)], 7.60 – 6.80 (m, 21H, Ph), [7.72 – 6.80 (m, 21H, Ph)], 6.88 (t, ^3J = 7.6 Hz, 1H, Py-H^4), 6.64 (t, ^3J = 7.6 Hz, 2H, Ph), [6.79 (t, ^3J = 7.4 Hz, 1H, Py-H^4)], 6.43 (d, ^3J = 7.6 Hz, 1H, Py-H$^{3/5}$), [6.41 (d, ^3J = 7.5 Hz, 1H, Py-H$^{3/5}$)], 5.66 (d, ^3J = 7.6 Hz, 1H, Py-H$^{3/5}$), [5.45 (d, ^3J = 7.5 Hz, 1H, Py-H$^{3/5}$)], 5.26 (s, 1H, Cp-H), [5.19 (s, 1H, Cp-H)], 5.10 (dt, ^3J = 4.3 Hz, ^3J = 10.7 Hz, 1H, OCH), [4.96 (dt, ^3J = 4.3 Hz, ^3J = 10.7 Hz, 1H, OCH)], 4.86 (s, 1H, Cp-H), [5.09 (s, 1H, Cp-H)], 4.59 (d, $^2J_{P\text{-}H}$ = 10.2 Hz, 1H, PPh_2CHPy), [4.92 (d, $^2J_{P\text{-}H}$ = 11.0 Hz, 1H, PPh_2CHPy)], 4.58 (s, 1H, Cp-H), 3.06 (s, 1H, Cp-H), [3.77 (s, 1H, Cp-H)], 2.35 (br d, J = 11.0 Hz, 1H, Ment), 2.07 – 1.98 (m, 1H, Ment), 1.87 – 1.50 (m, 6H, Ment), 1.28 (s, 3H, CH_3) [1.18 (s, 3H, CH_3)], 1.17 – 1.10 (m, 1H, Ment), 1.07 (d, ^3J = 6.7 Hz, 3H, CH_3), [0.93 (d, 3H, ^3J = 6.5 Hz, 3H, CH_3)], 1.01 (s, 3H, CH_3), [1.07 (s, 3H, CH_3)], 0.90 (d, ^3J = 7.0 Hz, 3H, CH_3), [0.99 (d, ^3J = 7.0 Hz, 3H, CH_3)], 0.73 (d, ^3J = 7.0 Hz, 3H, CH_3), [0.72 (d, ^3J = 7.0 Hz, 3H, CH_3)].

^{31}P{^{1}H} NMR (162 MHz, $CDCl_3$): (L_{Ment},S_C,R_{Ru})-**17**: δ = 42.8 (d, $^2J_{P\text{-}P}$ = 35.1 Hz, 1P), 62.8 (d, $^2J_{P\text{-}P}$ = 35.1 Hz, 1P); (L_{Ment},R_C,S_{Ru})-**17**: δ = 43.6 (d, $^2J_{P\text{-}P}$ = 35.1 Hz, 1P), 75.0 (d, $^2J_{P\text{-}P}$ = 35.1 Hz, 1P).

MS(ESI, CH_2Cl_2): *m/z* (%) = 935

Elemental analysis: $C_{54}H_{58}ClNOP_2Ru\cdot(CH_2Cl_2)_{1/2}$ (978.0):

Calcd. C 66.93, H 6.08, N 1.43.

Found C 66.60, H 6.34, N 1.31.

(R_{Ru})/(S_{Ru})-Acetonitrile[1-[(2*S*)-2-(diphenylphosphanyl-κP)-1,1-dimethyl-2-[6-[(1*R*,2*S*,5*R*)-menthoxy-2-pyridinyl]ethyl]-η^5-cyclopentadienyl](triphenylphosphine)-ruthenium(II) hexafluorophosphate (L_{Ment},S_C,R_{Ru})-23 and (L_{Ment},S_C,S_{Ru})-23: To a solution of (L_{Ment},S_C,R_{Ru})- and (L_{Ment},S_C,S_{Ru})-17 (156 mg, 0.167 mmol, ratio 85:15) in a mixture of acetonitrile (5 mL) and $CHCl_3$ (15 mL) was added NH_4PF_6 (67 mg, 0.41 mmol). The mixture was stirred for 18 h at room temperature and then evaporated in vacuo. The residue was washed with $CHCl_3$ and the filtrate was evaporated to give (L_{Ment},S_C,R_{Ru})- and (L_{Ment},S_C,S_{Ru})-23 in 91% yield (158 mg) as light yellow crystals.

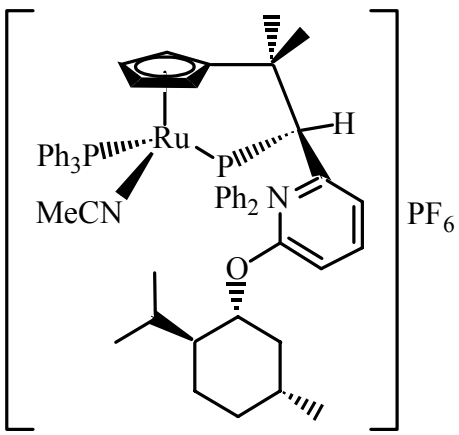

(L_{Ment},S_C,R_{Ru})-23

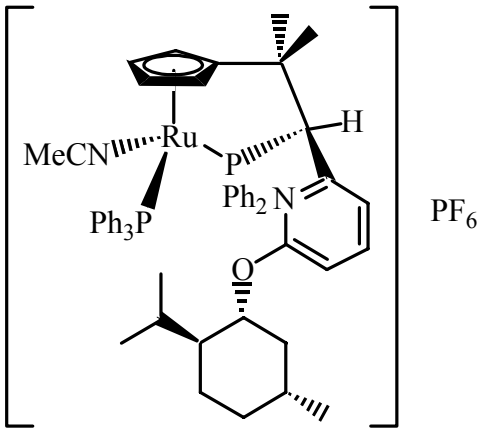

(L_{Ment},S_C,S_{Ru})-23

Mp.: 159-163 °C.

IR (KBr): ν = 2245 (CN) cm^{-1}.

^{1}H NMR (400 MHz, $CDCl_3$, 300 K, signals of the (L_{Ment},S_C,S_{Ru})-isomer given in brackets if distinguishable): δ = 7.90 – 6.90 (m, 24H, Ph, Py-H^4), 6.71 (t, ^3J = 7.6 Hz, 2H, Ph), [6.82 (t, ^3J = 7.1 Hz, 2H, Ph)], 6.44 (d, ^3J = 8.3 Hz, 1H, Py-H$^{3/5}$), [6.45 (d, ^3J = 8.1 Hz, 1H, Py-H$^{3/5}$)], 5.67 (s, 1H, Cp-H), [5.75 (s, 1H, Cp-H)], 5.44 (d, ^3J = 7.6 Hz, 1H, Py-H$^{3/5}$), [5.90 (br s, 1H, Py-H$^{3/5}$)], 5.21 (d, $^4J_{P\text{-}H}$ = 1.4 Hz, 1H, Cp-H), [5.53 (s, 1H, Cp-H)], 4.92 (m, 1H, OCH), 4.76 (s, 1H, Cp-H), [4.62 (s, 1H, Cp-H)], 4.44 (d, $^2J_{P\text{-}H}$ = 11.2 Hz, 1H, PCHPy), [4.91 (d, $^2J_{P\text{-}H}$ = 10.8 Hz, 1H, PCHPy)], 4.01 (s, 1H, Cp-H), [4.10 (s, 1H, Cp-H)], 2.16 (br d, ^3J = 11.4 Hz, 1H, Ment-H), 2.07 – 2.01 (m, 1H, Ment-H), 2.00 (s, 3H, CH_3CN), 1.83 – 1.50 (m, 4H, Ment-H), 1.52 (s, 3H, CH_3), [1.36 (s, 3H, CH_3)], 1.30 – 0.95 (m, 3H, Ment-H), 1.15 (s, 3H, CH_3), [1.23 (s, 3H, CH_3)], 1.02 (d, ^3J = 6.6 Hz, 3H, CH_3), [1.16 (d, ^3J = 7.0 Hz, 3H, CH_3)], 0.91 (d, ^3J = 7.0 Hz, 3H, CH_3), [0.87 (d, ^3J = 7.0 Hz, 3H, CH_3)], 0.75 (d, ^3J = 7.0 Hz, 3H, CH_3), [0.65 (d, ^3J = 6.9 Hz, 3H, CH_3)].

^{13}C{^{1}H} NMR (100 MHz, $CDCl_3$, 300 K, signals of the (L_{Ment},S_C,S_{Ru})-isomer given in brackets if distinguishable): δ = 162.32 (s, Py-C^2), [162.36 (s, Py-C^2)], 152.84 (d, $J_{C\text{-}P}$ = 8.2 Hz, P-Ar-C), [153.20, br d, $J_{C\text{-}P}$ = 10.0 Hz, P-Ar-C], 137.90 (s, Py-CH), [137.90 (s, Py-CH)], 135.36 (d, $J_{C\text{-}P}$ = 11.4 Hz, P-Ar-CH), [136.68 (d, $J_{C\text{-}P}$ = 11.4 Hz, P-Ar-CH)], 135.50 (d, $J_{C\text{-}P}$ = 38.1 Hz, P-Ar-C), 133.13 (d, $J_{C\text{-}P}$ = 10.7 Hz, P-Ar-CH), 132.60 (d, $J_{C\text{-}P}$ = 7.6 Hz, P-Ar-CH), [132.50 (d, $J_{C\text{-}P}$ = 9.9 Hz, P-Ar-CH)], 132.04 (d, $J_{C\text{-}P}$ = 9.2 Hz, P-Ar-CH), 130.52 (s, P-Ar-CH), [131.06 (s, P-Ar-CH)], 130.08 (d, $J_{C\text{-}P}$ = 38.9 Hz, P-Ar-C), [129.71 (d, $J_{C\text{-}P}$ = 28.9 Hz, P-Ar-C)], 129.22 (d, $J_{C\text{-}P}$ = 7.6 Hz, P-Ar-CH), 128.41 (d, $J_{C\text{-}P}$ = 9.9 Hz, P-Ar-CH), [128.57 (d, $J_{C\text{-}P}$ = 9.2 Hz, P-Ar-CH), 128.68 (d, $J_{C\text{-}P}$ = 9.1 Hz, P-Ar-CH), [128.00 (d, $J_{C\text{-}P}$ = 9.2 Hz, P-Ar-CH), 127.37 (d, $J_{C\text{-}P}$ = 9.9 Hz, P-Ar-CH), [126.90 (d, $J_{C\text{-}P}$ = 9.9 Hz, P-Ar-CH)], 126.34 (s, CN), [128.10 (s, CN)] 124.48 (s, Py-C), [122.05 (s, Py-C), 118.60 (s, Py-CH), [119.14 (s, Py-CH)], 110.01 (s, Py-CH), [110.10 (s,

Py-CH)], 90.30 (s, Cp-CH), [88.32 (d, $J_{C\text{-}P}$ = 5.1 Hz, Cp-CH)], 81.70 (d, $J_{C\text{-}P}$ = 5.1 Hz, Cp-CH), [83.85 (d, $J_{C\text{-}P}$ = 5.1 Hz, Cp-CH)], 78.53 (d, $J_{C\text{-}P}$ = 8.7 Hz, Cp-CH), [70.25 (d, $J_{C\text{-}P}$ = 9.2 Hz, Cp-CH)], 75.95 (d, $J_{C\text{-}P}$ = 19.7 Hz, P-CH), [73.61 (d, $J_{C\text{-}P}$ = 21.3 Hz, P-CH)], 74.73 (s, Cp-CH), [74.16 (br s, Cp-CH)], 61.50 (s, Cp-C), [65.87 (br s, Cp-CH)], 47.50 (s, Ment-CH), [47.50 (s, Ment-CH)], 40.90 (s, Ment-CH_2), [40.73 (s, Ment-CH_2)], 38.40 (d, $^2J_{C\text{-}P}$ = 8.0 Hz, Cp*C*Me$_2$), [38.22 (d, $^2J_{C\text{-}P}$ = 6.7 Hz, Cp*C*Me$_2$)], 34.51 (s, Ment-CH_2), [34.44 (s, Ment-CH_2), 31.63 (s, Ment-CH), [31.20 (s, Ment-CH)], 29.28 (d, $^3J_{C\text{-}P}$ = 19.1 Hz, CpC*Me*$_2$), [29.48 (d, $^3J_{C\text{-}P}$ = 19.4 Hz, CpC*Me*$_2$)], 26.31 (s, Ment-CH), [26.40 (s, Ment-CH)], 24.01 (s, Ment-CH_2), [23.77 (s, Ment-CH_2)], 23.20 (s, Ment-CH), [21.90 (s, Ment-CH)], 22.29 (s, Ment-Me), [22.18 (s, Ment-Me)], 20.70 (s, Ment-Me), [20.91 (s, Ment-Me)], 16.95 (s, Ment-Me), [17.13 (s, Ment-Me)], 2.55 (s, *C*H$_3$CN), [3.96 (s, *C*H$_3$CN)].

$^{31}P\{^1H\}$ NMR (162 MHz, $CDCl_3$): (L_{Ment},S_C,R_{Ru})-**23**: δ = 48.2 (d, $^2J_{P\text{-}P}$ = 30.9 Hz, 1P), 70.5 (d, $^2J_{P\text{-}P}$ = 30.9 Hz, 1P), -143.5 (septet, $^1J_{P\text{-}F}$ = 712.3 Hz, 1P); (L_{Ment},R_C,S_{Ru})-**23**: δ = 48.2 [overlapping with (L_{Ment},S_C,R_{Ru})-**23** signal], 77.4 (br d, $^2J_{P\text{-}P}$ = 24.4 Hz, 1P), -143.5 (septet, $^1J_{P\text{-}F}$ = 712.3 Hz, 1P).

ESI-MS (CH_2Cl_2, rel. int.): *m/z* = 941 (M^+, 18), 900 (M – MeCN, 100).

Elemental analysis: $C_{56}H_{61}F_6N_2OP_3Ru$ (1086.1)

Calcd. C 61.93, H 5.66, N 2.58.

Found C 61.85, H 5.85, N 2.58.

(R_{Ru})/(S_{Ru})-Benzonitrile[1-[(2*S*)-2-(diphenylphosphanyl-κP)-1,1-dimethyl-2-[6-[[(1*R*,2*S*,5*R*)-menthoxy-2-pyridinyl]ethyl]-η^5-cyclopentadienyl](triphenylphosphine)-ruthenium(II) hexafluorophosphate (L_{Ment},S_C,R_{Ru})-24 and (L_{Ment},S_C,S_{Ru})-24: To a solution of (L_{Ment},S_C,R_{Ru})- and (L_{Ment},S_C,S_{Ru})-**17** (150 mg, 0.153 mmol, ratio 85:15) in a mixture of benzonitrile (3 mL) and $CHCl_3$ (15 mL) was added NH_4PF_6 (60 mg, 0.37 mmol). The mixture was stirred for 20 h at room temperature and then evaporated in vacuo. The residue was washed with $CHCl_3$ and the filtrate was evaporated to give (L_{Ment},S_C,R_{Ru})- and (L_{Ment},S_C,S_{Ru})-**24** in 49% yield (75 mg) as light yellow crystals.

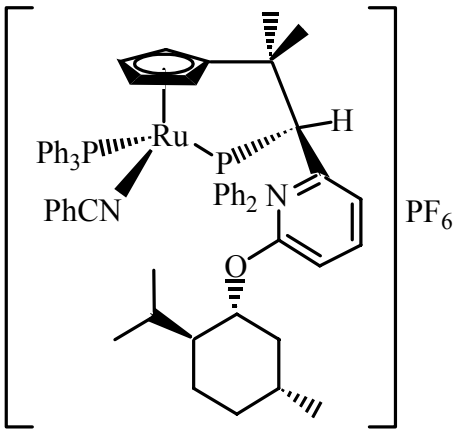

(L_{Ment},S_C,R_{Ru})-24

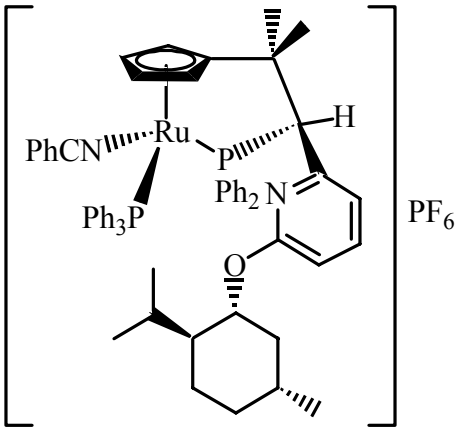

(L_{Ment},S_C,S_{Ru})-24

Mp.: 156 °C.

IR (KBr): ν = 2229 (CN) cm^{-1}.

^{1}H NMR (400 MHz, $CDCl_3$, 273 K, signals of the (L_{Ment},S_C,S_{Ru})-isomer given in brackets if distinguishable): δ = 7.69 – 6.90 (m, 28H, Ph, Py-H^4), 6.71 (t, ^3J = 6.7 Hz, 2H, Ph), [6.81 (t, ^3J = 7.0 Hz, 2H, Ph)], 6.46 (d, ^3J = 8.4 Hz, 1H, Py-H$^{3/5}$), [6.52 (d, ^3J = 7.3 Hz, 1H, Py-H$^{3/5}$)], 5.80 (s, 1H, Cp-H), [5.80 (s, 1H, Cp-H)], 5.90 (d, ^3J = 7.4 Hz, 1H, Py-H$^{3/5}$), [6.08 (br s, 1H, Py-H$^{3/5}$)], 5.30 (s, 1H, Cp-H), [5.30 (s, 1H, Cp-H)], 4.89 (dt, ^3J = 4.2 Hz, ^3J = 11.0 Hz, 1H, OCH), 4.85 (s, 1H, Cp-H), [4.72 (s, 1H, Cp-H)], 4.58 (d, $^2J_{P\text{-}H}$ = 11.1 Hz, 1H, PyCHPPh$_2$), [4.98 (d, $^2J_{P\text{-}H}$ = 11.5 Hz, 1H, PyCHPPh$_2$)], 4.14 (s, 1H, Cp-H), [4.14 (s, 1H, Cp-H)], 2.20 – 0.70 (m, 9H, Ment-H), 1.15 (s, 3H, CH_3), [1.29 (s, 3H, CH_3)], 1.18 (s, 3H, CH_3), [1.03 (s, 3H, CH_3)], 1.02 (d, ^3J = 6.4 Hz, 3H, CH_3), 0.91 (d, ^3J = 6.9 Hz, 3H, CH_3), [0.88 (d, ^3J = 7.1 Hz, 3H, CH_3)], 0.74 (d, ^3J = 6.8 Hz, 3H, CH_3), [0.62 (d, ^3J = 7.1 Hz, 3H, CH_3)].

^{13}C{^{1}H} NMR (100 MHz, $CDCl_3$, 300 K, signals of the (L_{Ment},S_C,S_{Ru})-isomer given in brackets if distinguishable): δ = 162.31 (s, Py-C), [162.69 (s, Py-C)], 152.67 (d, $J_{C\text{-}P}$ = 7.6 Hz, P-Ar-C), 137.91 (s, Py-CH), [138.06 (s, Py-CH)], 136.73 – 123.36 (m, Ar-C, Ar-CH, Py-CH, Py-C, CN), 119.29 (s, Py-CH), [118.78 (s, Py-CH)], 110.06 (s, Py-CH), 91.30 (d, $J_{C\text{-}P}$ = 3.1 Hz,, Cp-CH), [88.76 (d, $J_{C\text{-}P}$ = 6.1 Hz, Cp-CH)], 81.35 (d, $J_{C\text{-}P}$ = 2.9 Hz, Cp-CH), [84.03 (d, $J_{C\text{-}P}$ = 3.1 Hz, Cp-CH)], 79.28 (d, $J_{C\text{-}P}$ = 5.1 Hz, Cp-CH), [70.99 (d, $J_{C\text{-}P}$ = 5.1 Hz, Cp-CH)], 75.40 (d, $J_{C\text{-}P}$ = 19.8 Hz, P-CH), [73.66 (d, $J_{C\text{-}P}$ = 25.2 Hz, P-CH)], 74.65 (s, Cp-CH), [74.33 (s, Cp-CH)], 62.77 (s, Cp-C), [67.04 (br s, Cp-CH)], 47.52 (s, Ment-CH), [47.47 (s, Ment-CH)], 40.90 (s, Ment-CH_2), [40.65 (s, Ment-CH_2)], 38.29 (d, $^2J_{C\text{-}P}$ = 6.9 Hz, Cp*C*Me$_2$), [38.44 (d, $^2J_{C\text{-}P}$ = 7.6 Hz, Cp*C*Me$_2$)], 34.53 (s, Ment-CH_2), [34.44 (s, Ment-CH_2), 31.64 (s, Ment-CH), [31.17 (s, Ment-CH)], 29.32 (d, $^3J_{C\text{-}P}$ = 19.1 Hz, CpC*Me*$_2$), 26.39 (s, Ment-CH), [26.29 (s, Ment-CH)], 23.98 (s, Ment-CH_2), [23.82 (s, Ment-CH_2)], 23.06 (s, Ment-CH), [21.92 (s, Ment-CH)], 22.32 (s,

Ment-Me), [22.13 (s, Ment -Me)], 20.73 (s, Ment-Me), [21.00 (s, Ment-Me)], 16.96 (s, Ment-Me), [17.26 (s, Ment-Me)].

$^{31}P\{^{1}H\}$ NMR (162 MHz, $CDCl_3$, 273 K): (L_{Ment},S_C,R_{Ru})-**24**: δ = 69.9 (br s, 1P), 48.3 (d, $^{2}J_{P\text{-}P}$ = 31.7 Hz, 1P), -142.9 (septet, $^{1}J_{P\text{-}F}$ = 717.4 Hz, 1P); (L_{Ment},R_C,S_{Ru})-**24**: δ = 78.1 (br s, 1P), 49.5 (br s, 1P), -142.9 (septet, $^{1}J_{P\text{-}F}$ = 717.4 Hz, 1P).

ESI-MS (CH_2Cl_2, rel. int.): *m/z* = 1003 (M^+, 4), 900 (M – PhCN, 100).

Elemental analysis: $C_{61}H_{63}F_6N_2OP_3Ru$ (1148.2):

Calcd.	C 63.81,	H 5.53,	N 2.44.
Found	C 63.66,	H 5.98,	N 2.62.

(R_{Ru})/(S_{Ru})-[1-[(2*S*)-2-(Diphenylphosphanyl-κP)-1,1-dimethyl-2-[6-[[(1*R*,2*S*,5*R*)-menthoxy-2-pyridinyl]ethyl]-η^5-cyclopentadienyl](phenylacetonitrile)-(triphenylphosphine)ruthenium(II) hexafluorophosphate (L_{Ment},S_C,R_{Ru})-25 and (L_{Ment},S_C,S_{Ru})-25: To a solution of (L_{Ment},S_C,R_{Ru})- and (L_{Ment},S_C,S_{Ru})-**17** (120 mg, 0.123 mmol, ratio 85:15) in a mixture of phenylacetonitrile (3 mL) and $CHCl_3$ (15 mL) was added NH_4PF_6 (50 mg, 0.31 mmol). The mixture was stirred for 20 h at room temperature and then evaporated in vacuo. The residue was washed with $CHCl_3$ and the filtrate was evaporated to give (L_{Ment},S_C,R_{Ru})- and (L_{Ment},S_C,S_{Ru})-**25** in 71% yield (100 mg) as light yellow crystals.

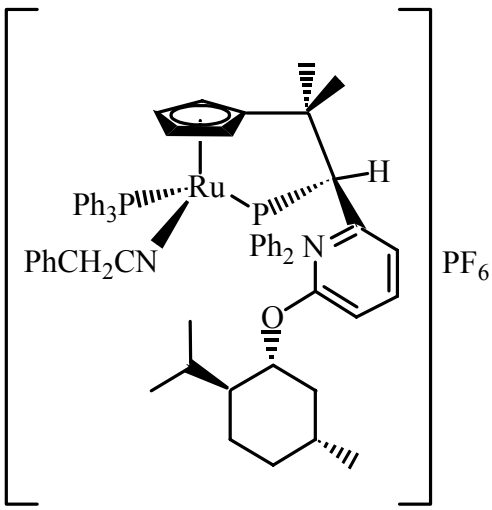

(L_{Ment},S_C,R_{Ru})-25

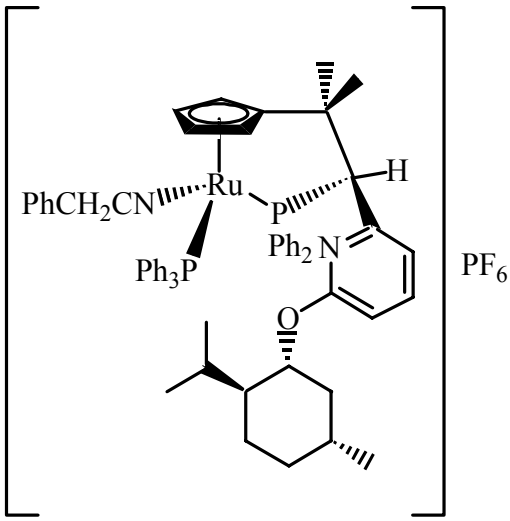

(L_{Ment},S_C,S_{Ru})-25

Mp.: 141 °C.

IR (KBr): ν = 2265 (CN) cm^{-1}.

^{1}H NMR (400 MHz, $CDCl_3$, 300 K, signals of the (L_{Ment},S_C,S_{Ru})-isomer given in brackets if distinguishable): δ = 7.80 – 6.85 (m, 29H, Ph, Py-H^4), 6.75 (d, ^3J = 7.6 Hz, 2H, $NCCH_2Ph$-$H^{2/6}$), 6.45 (d, ^3J = 7.6 Hz, 1H, Py-$H^{3/5}$), [6.28 (d, ^3J = 7.6 Hz, 1H, Py-$H^{3/5}$)], 5.82 (s, 1H, Cp-H), [5.82 (s, 1H, Cp-H)], 5.54 (d, ^3J = 7.3 Hz, 1H, Py-H$^{3/5}$), [5.54 (br s, 1H, Py-H$^{3/5}$)], 5.38 (s, 1H, Cp-H), [5.67 (s, 1H, Cp-H)], 4.96 (dt, ^3J = 4.2 Hz, ^3J = 10.8 Hz, 1H, OCH), 4.66 (br s, 1H, Cp-H), [4.66 (br s, 1H, Cp-H)], 4.54 (d, $^2J_{P\text{-}H}$ = 10.8 Hz, 1H, $PyCHPPh_2$), [4.92 (d, $^2J_{P\text{-}H}$ = 11.5 Hz, 1H, $PyCHPPh_2$)], 3.94 (d, ^2J = 18.6 Hz, 1H, CHCN), [3.56 (d, ^2J = 18.6 Hz, 1H, CHCN)], 3.88 (d, ^2J = 18.6 Hz, 1H, CHCN), [2.97 (d, ^2J = 18.6 Hz, 1H, CHCN)], 3.68 (s, 1H, Cp-H), [3.76 (s, 1H, Cp-H)], 2.20 – 0.70 (m, 9H, Ment-H), 1.39 (s, 3H, CH_3), [1.21 (s, 3H, CH_3)], 1.09 (s, 3H, CH_3), [1.05 (s, 3H, CH_3)], 1.05 (d, ^3J = 6.6 Hz, 3H, CH_3), 0.90 (d, ^3J = 7.6 Hz, 3H, CH_3), [0.86 (d, ^3J = 7.1 Hz, 6H, CH_3)], 0.73 (d, ^3J = 6.8 Hz, 3H, CH_3), [0.62 (d, ^3J = 7.1 Hz, 3H, CH_3)].

^{13}C{^{1}H} NMR (100 MHz, $CDCl_3$, 300 K, signals of the (L_{Ment},S_C,S_{Ru})-isomer given in brackets if distinguishable): δ = 162.28 (s, Py-C), [162.35 (s, Py-C)], 152.69 (d, $J_{C\text{-}P}$ = 7.9 Hz, P-Ar-C), 137.75 (s, Py-CH), [138.00 (s, Py-CH)], 138.63-123.13 (m, Ar-C, Ar-CH, Py-CH, Py-C, CN), 119.28 (s, Py-CH), [118.57 (s, Py-CH)], 109.94 (s, Py-CH), [110.04 (s, Py-CH)], 90.46 (d, $J_{C\text{-}P}$ = 3.8 Hz,, Cp-CH), [89.22 (br s, Cp-CH)], 82.85 (d, $J_{C\text{-}P}$ = 2.3 Hz, Cp-CH), 79.93 (d, $J_{C\text{-}P}$ = 7.6 Hz, Cp-CH), 75.44 (d, $J_{C\text{-}P}$ = 19.0 Hz, P-CH), [73.66 (d, $J_{C\text{-}P}$ = 25.2 Hz, P-CH)], 74.47 (s, Cp-CH), [74.31 (s, Cp-CH)], 62.33 (s, Cp-C), [66.75 (br s, Cp-CH)], 47.52 (s, Ment-CH), [47.47 (s, Ment-CH)], 40.96 (s, Ment-CH_2), [40.66 (s, Ment-CH_2)], 38.12 (d, $^2J_{C\text{-}P}$ = 6.9 Hz, Cp*C*Me_2), [38.46 (d, $^2J_{C\text{-}P}$ = 7.6 Hz, Cp*C*Me_2)], 34.53 (s, Ment-CH_2), [34.46 (s, Ment-CH_2), 31.74 (s, Ment-CH), [31.17 (s, Ment-CH)], 29.66 (d, $^3J_{C\text{-}P}$ = 19.8 Hz, CpC*Me*$_2$), 25.63 (s, Ph*C*H_2), [23.92 (s, Ph*C*H_2)], 26.36 (s, Ment-CH), [22.15 (s, Ment-CH)], 23.98 (s, Ment-CH_2), [23.82 (s, Ment-CH_2)], 22.90 (s, Ment-CH), [21.92 (s, Ment-CH)], 22.37 (s, Ment-Me), [22.84 (s, Ment-Me)], 20.69 (s, Ment-Me), [20.96 (s, Ment-Me)], 16.83 (s, Ment-Me), [17.22 (s, Ment-Me)].

^{31}P{^{1}H} NMR (162 MHz, $CDCl_3$, 300 K): (L_{Ment},S_C,R_{Ru})-**25**: δ = 70.0 (br d, $^2J_{P\text{-}P}$ = 29.7 Hz, 1P), 48.4 (d, $^2J_{P\text{-}P}$ = 29.7 Hz, 1P), -142.8 (septet, $^1J_{P\text{-}F}$ = 718.5 Hz, 1P); diastereomer (L_{Ment},R_C,S_{Ru})-**25**: δ = 78.0 (br d, $^2J_{P\text{-}P}$ = 30.0 Hz, 1P), 49.4 (br d, $^2J_{P\text{-}P}$ = 30.0 Hz, 1P), -142.8 (septet, $^1J_{P\text{-}F}$ = 718.5 Hz, 1P).

ESI-MS (CH_2Cl_2, rel. int.): *m/z* = 1017 (M^+, 5), 900 (M – $PhCH_2CN$, 100).

Elemental analysis: $C_{62}H_{65}F_6N_2OP_3Ru$ (1162.2):

Calcd.	C 64.08,	H 5.64,	N 2.41.
Found	C 63.71,	H 6.00,	N 2.47.

(R_{Ru})/(S_{Ru})-Ammine[1-[(2*S*)-2-(diphenylphosphanyl-κP)-1,1-dimethyl-2-[6-[(1*R*,2*S*,5*R*)-menthoxy-2-pyridinyl]ethyl]-η^5-cyclopentadienyl](triphenylphosphine)ruthenium(II) hexafluorophosphate (L_{Ment},S_C,R_{Ru})-26 and (L_{Ment},S_C,S_{Ru})-26: A mixture (85:15) of (L_{Ment},S_C,R_{Ru})-**17** and (L_{Ment},S_C,S_{Ru})-**17** (150 mg, 0.153 mmol) was dissolved in CH_2Cl_2. To the solution was added NH_4PF_6 (330 mg, 1.01 mmol) and then stirred for 30 min at room temperature. To the suspension was added amine, piperidine and morpholine, respectively (1.00 mmol). The mixture was stirred for 24 h and filtrated. The mother liqure was evaporated in vacuo. The residue was chromatographed on silica gel using EtOAc-ether (1:1, v/v) as an eluent to give (L_{Ment},S_C,R_{Ru})-**26** and (L_{Ment},S_C,S_{Ru})-**26** (57 : 43 ratio; 54% from piperidine; 63% from morpholine).

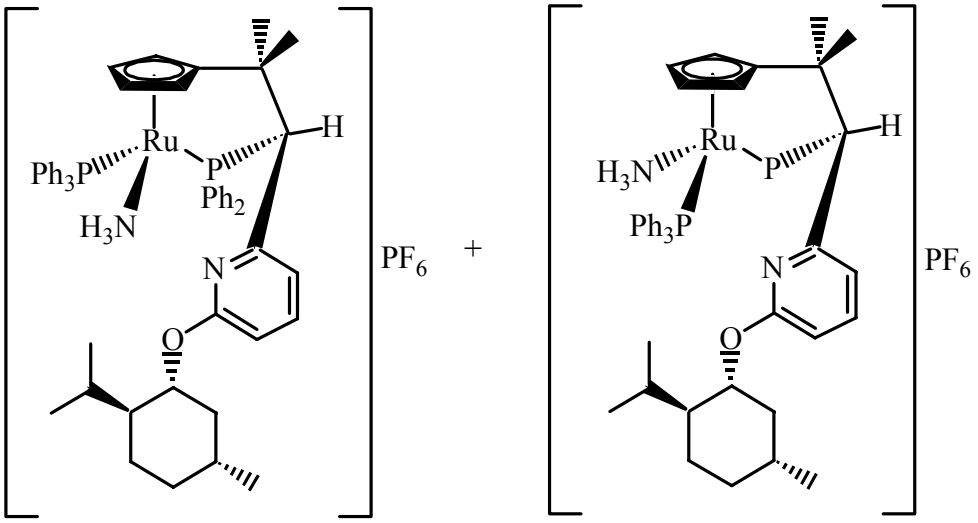

(L_{Ment},S_C,R_{Ru})-26 **(L_{Ment},S_C,S_{Ru})-26**

Mp.: 153 °C.

IR (KBr): ν = 3356, 3283 (NH) cm^{-1}.

^{1}H NMR (400 MHz, $CDCl_3$, 273 K, signals of the (L_{Ment},S_C,R_{Ru})-isomer given in brackets if distinguishable): δ = 7.91 – 6.60 (m, 26H, Ph, Py-H^4), 6.45 (d, ^3J = 7.9 Hz, 1H, Py-H$^{3/5}$), [6.43 (d, ^3J = 7.9 Hz, 1H, Py-H$^{3/5}$)], 5.82 (br s, 1H, Py-H$^{3/5}$), 5.62 (s, 1H, Cp-H), [5.39 (s, 1H, Cp-H)], 5.34 (s, 1H, Cp-H), [5.21 (s, 1H, Cp-H)], 4.97 (d, $^2J_{P\text{-}H}$ = 11.0 Hz, 1H, PCHPy), [4.23 (d, $^2J_{P\text{-}H}$ = 13.4 Hz, 1H, PCHPy)], 4.76 (s, 1H, Cp-H), [5.06 (s, 1H, Cp-H)], 4.71 (m, 1H, OCH), [4.88 (dt, ^3J = 4.3 Hz, ^3J = 10.4 Hz, 1H, OCH)], 4.06 (s, 1H, Cp-H), [4.32 (s, 1H, Cp-H)], 2.34 – 0.80 (m, 12H, Ment-H, NH_3), 1.25 (s, 3H, CH_3), [1.20 (s, 3H, CH_3)], 1.10 (s, 3H, CH_3), [1.10 (s, 3H, CH_3)], 0.90 (d, ^3J = 6.7 Hz, 3H, CH_3), [0.99 (d, ^3J = 6.7 Hz, 3H, CH_3)], 0.86 (d, ^3J = 7.3 Hz, 3H,

CH_3), [0.91 (d, ^3J = 7.0 Hz, 3H, CH_3)], 0.65 (d, ^3J = 7.3 Hz, 3H, CH_3), [0.74 (d, ^3J = 6.7 Hz, 3H, CH_3)].

$^{13}C\{^1H\}$ NMR (100 MHz, $CDCl_3$, 300 K, signals of the (L_{Ment},S_C,S_{Ru})-isomer given in brackets if distinguishable): δ = 162.38 (s, Py-C^2), [162.49 (s, Py-C^2)], 153.18 (d, $J_{C\text{-}P}$ = 9.2 Hz, P-Ar-C), [153.28, d, $J_{C\text{-}P}$ = 7.6 Hz, P-Ar-C], 137.78 (s, Py-CH), [137.78 (s, Py-CH)], 136.75-122.41 (m, P-Ar-C, P-Ar-CH, Py-C, Py-CH), 118.47 (s, Py-CH), [118.82 (s, Py-CH)], 110.04 (s, Py-CH), [110.10 (s, Py-CH)], 87.79 (d, $J_{C\text{-}P}$ = 5.3 Hz, Cp-CH), 82.31 (d, $J_{C\text{-}P}$ = 6.1 Hz, Cp-CH), 74.07 (s, Cp-CH), [75.16 (s, Cp-CH)], 73.40 (d, $J_{C\text{-}P}$ = 21.3 Hz, P-CH), 68.33 (d, $J_{C\text{-}P}$ = 10.7 Hz, Cp-CH), 58.95 (s, Cp-C), [64.46 (br s, Cp-CH)], 47.55 (s, Ment-CH), 40.92 (s, Ment-CH_2), [40.76 (s, Ment-CH_2)], 37.96 (d, $^2J_{C\text{-}P}$ = 6.1 Hz, Cp*C*Me_2), [38.43 (d, $^2J_{C\text{-}P}$ = 8.4 Hz, Cp*C*Me_2)], 34.53(s, Ment-CH_2), [34.47 (s, Ment-CH_2), 31.63 (s, Ment-CH), [31.18 (s, Ment-CH)], 28.99 (d, $^3J_{C\text{-}P}$ = 18.3 Hz, CpC*Me*$_2$), [29.62 (d, $^3J_{C\text{-}P}$ = 19.1 Hz, CpC*Me*$_2$)], 26.47 (s, Ment-CH), [26.35 (s, Ment-CH)], 24.01 (s, Ment-CH_2), [23.77 (s, Ment-CH_2)], 23.20 (s, Ment-CH), [21.90 (s, Ment-CH)], 22.24 (s, Ment-Me), [23.73 (s, Ment-Me)], 20.67 (s, Ment-Me), [20.89 (s, Ment-Me)], 17.02 (s, Ment-Me), [17.11 (s, Ment-Me)].

$^{31}P\{^1H\}$ NMR (162 MHz, $CDCl_3$, 273K): (L_{Ment},S_C,R_{Ru})-**26**: δ = 76.5 (d, $^2J_{P\text{-}P}$ = 30.1 Hz, 1P), 51.5 (d, $^2J_{P\text{-}P}$ = 30.1 Hz, 1P), -143.2 (septet, $^1J_{P\text{-}F}$ = 713.6 Hz, 1P); (L_{Ment},R_C,S_{Ru})-**26**: δ = 79.1 (br s, 1P), 52.4 (br s, 1P), -143.2 (septet, $^1J_{P\text{-}F}$ = 713.6 Hz, 1P).

ESI-MS (CH_2Cl_2, rel. int.): *m/z* = 917 (M^+, 5), 900 (M – NH_3, 100).

Elemental analysis: $C_{54}H_{61}F_6N_2OP_3Ru$ (1062.1):

Calcd. C 61.07, H 5.79, N 2.64.

Found C 61.19, H 5.61, N 2.66.

3.5 References

1. Brunner, H. *Eur. J. Inorg. Chem.* **2001**, 905.
2. Consiglio, G.; Morandini, F. *Chem. Rev.* **1987**, *87*, 761.
3. Brunner, H. *Angew. Chem., Int. Ed.* **1999**, *38*, 1194.
4. Brunner, H. *Adv. Orgamet. Chem.* **1980**, *18*, 151.
5. Brunner, H.; Köllnberger, A.; Mehmood, A.; Tsuno, T.; Zabel, M. *Organometallics* **2004**, 23, 4006.

6. Brunner, H.; Köllnberger, A.; Mehmood, A.; Tsuno, T.; Zabel, M. *J. Organomet. Chem.* **2004**, *689*, 4244.
7. Brunner, H.; Valério, C.; Zabel, M. *New J. Chem.* **2000**, *24,* 275.
8. Morandini, F.; Consiglio, G.; Straub, B.; Ciani, G.; Sironi, A. *J. Chem. Soc., Dalton Trans.* **1983**, 2293.
9. Consiglio, G.; Morandini, F.; Bangerter, F. *Inorg. Chem*. **1982**, *21*, 455.
10. Morandini, F.; Consiglio, G.; Lucchini, V. *Organometallics* **1985**, *4,* 1202.
11. Morandini, F.; Consiglio, G.; Ciani, G.; Sironi, A. *Inorg. Chim. Acta* **1984**, *82*, L27.
12. Conroy-Lewis, F. M.; Simpson, S. J. *J. Organomet. Chem.* **1990**, *396*, 83.

4 Pyramidal Stability of Chiral-at-Metal Half-Sandwich 16-Electron Fragments [CpRu(P-P')]$^+$

4.1 Abstract

The chiral-at-metal diastereomers ($R_{Ru,}R_C$)- and ($S_{Ru,}R_C$)-[CpRu(P-P')Hal], P-P' = (*R*)-Prophos and (*R*,*R*)-Norphos, Hal = Cl, Br, and I, were synthesized, separated, and characterized by X-ray crystallography. In particular, the compounds ($R_{Ru,}R_C$)- and ($S_{Ru,}R_C$)-[CpRu(Prophos)Cl] were investigated which had been the starting material in the preparation of many new compounds with retention of the Ru-configuration. Erroneously, in the 1980's these compounds had been considered to be configurationally stable at the metal atom. Halide exchange reactions and epimerization studies were carried out in methanol/chloroform mixtures. The rate determining step in these reactions was the dissociation of the Ru-Hal bond in ($R_{Ru,}R_C$)- and ($S_{Ru,}R_C$)-[CpRu(P-P')Hal] forming the 16-electron intermediates ($R_{Ru,}R_C$)- and ($S_{Ru,}R_C$)-[CpRu(P-P')]$^+$ which maintain their pyramidal structures. The Hal exchange reactions proceeded at 0 - 20 ^oC in first-order kinetics with half-lives of minutes/hours and occurred with predominant retention of the metal configuration accompanied by partial epimerization at the metal atom. Interestingly, the thermodynamically less stable ($R_{Ru,}R_C$)-diastereomer of [CpRu(Prophos)Cl] reacted about ten times faster then the thermodynamically more stable ($S_{Ru,}R_C$)-diastereomer. The change of the metal configuration in the epimerization of ($R_{Ru,}R_C$)- and ($S_{Ru,}R_C$)-[CpRu(P-P')Hal] took place in methanol containing solvents about 50 ^oC in first-order reactions with half-lives of minutes/hours. In $CDCl_3/CD_3OD$ mixtures the equilibrium composition ($R_{Ru,}R_C$)-/($S_{Ru,}R_C$)-[CpRu(Prophos)Cl] was 15:85. The rates of Hal exchange and epimerization increased by a factor of about 10 in going from $CDCl_3/CD_3OD$ 9:1 to 1:1 due to better solvation of the ions formed in the rate-determining step. Hal exchange reactions and epimerization studies indicated a high pyramidal stability of the 16-electron fragments ($R_{Ru,}R_C$)- and ($S_{Ru,}R_C$)-[CpRu(P-P')]$^+$ towards inversion. This is surprising because calculations had shown that 16-electron fragments $[CpM(PH_3)_2]^+$ with P-M-P angles around 100 ^{o} should have planar structures. Obviously, pyramidality of the fragments [CpRu(P-P')]$^+$ is enforced by the small P-Ru-P angles of 82 - 83 ^{o} observed in the X-ray analyses of the chelate compounds ($R_{Ru,}R_C$)- and ($S_{Ru,}R_C$)-[CpRu(P-

P')Hal]. These small angles resist planarization of the intermediates ($R_{Ru,}R_C$)- and ($S_{Ru,}R_C$)-[CpRu(P-P')]$^+$ and thus inversion of the metal configuration. The results are in accord with a basilica-type energy profile which has a relatively high barrier between the pyramidal intermediates ($R_{Ru,}R_C$)- and ($S_{Ru,}R_C$)-[CpRu(P-P')]$^+$ (Schemes 4-3 and 4-4).

4.2 Introduction

Dissociation of a ligand from an18-electron complex leaves an unsaturated 16-electron species, which may be a stable compound or an intermediate ready for subsequent addition reactions. Does the 16-electron species maintain its structure with a vacant site dissociated or does it rearrange simultaneously or subsequently to its formation? Are the 16-electron species [(η-C_nH_n)ML_2], obtained on dissociation of X from three-legged piano stool complexes [(η-C_nH_n)ML_2X], planar or pyramidal? The alternative is relevant in particular for chiral-at-metal compounds of the type [(η-C_nH_n)MLL'X],[1-3] because an intermediate [(η-C_nH_n)MLL'] would retain chirality as long as it is pyramidal, whereas it would lose chirality when it is planar. Chiral-at-metal compounds are especially suitable to investigate such problems. In the present paper we describe our studies concerning [CpRu(P-P')Hal] compounds and compare the new results with the [CpMn(NO)(PPh_3)X] system for which pyramidal intermediates have been established.

The parent [CpRu(P-P')Hal] type compound is [CpRu(PPh_3)$_2$Cl] the structure of which is known.[4] Chiral analogs are the diastereomers ($R_{Ru,}R_C$)- and ($S_{Ru,}R_C$)-[CpRu(Prophos)Cl] **27a'** and **27a**, (*R*)-Prophos = (*R*)-1,2-bisdiphenylphosphanylpropane, which have been separated[5,6] and used as starting materials for the preparation of optically active organometallic [CpRu(Prophos)X] compounds with retention of configuration.[2] These reactions have been carried out in methanol at room temperature and in boiling methanol, which, as we will show in this paper, is crucial, because **27a'** and **27a** (Scheme 4-1) epimerize in methanol containing solutions (see below). Likewise, the diastereomers of ($R_{Ru,}R_C$)- and ($S_{Ru,}R_C$)-[CpRu(Norphos)Cl] **28a'** and **28a** as well as ($S_{Ru,}R_C$)- and ($R_{Ru,}R_C$)-[CpRu(Norphos)I] **28c'** and **28c** (Scheme 4-1) have been separated.[7] The configurational lability at the Ru center has been noticed but detailed investigations have not been carried out.

P-P'

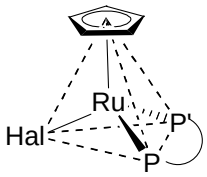

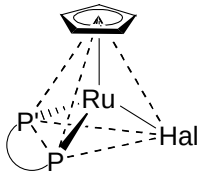

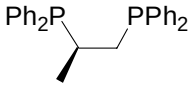

(*R*)-Prophos

Hal	Cl	Br	I
No.	**27a**	**27b**	**27c**
Conf.	($S_{Ru}R_C$)	(R_{Ru},R_C)	(R_{Ru},R_C)

Hal	Cl	Br	I
No.	**27a'**	**27b'**	**27c'**
Conf.	($R_{Ru}R_C$)	(S_{Ru},R_C)	(S_{Ru},R_C)

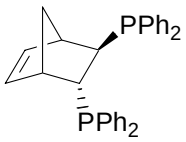

(*R*,*R*)-Norphos

Hal	Cl	Br	I
No.	**28a**	**28b**	**28c**
Conf.	($S_{Ru}R_C$)	(R_{Ru},R_C)	(R_{Ru},R_C)

Hal	Cl	Br	I
No.	**28a'**	**28b'**	**28c'**
Conf.	($R_{Ru}R_C$)	(S_{Ru},R_C)	(S_{Ru},R_C)

Scheme 4-1. The diastereomers **27a-c** and **27a'-c'** of [CpRu(Prophos)Hal] and **28a-c** and **28a**'-**c**' of [CpRu(Norphos)Hal] with their respective configurations. The priority sequence of the ligands for [CpRu(Prophos)Cl] is Cp > Cl > PCHMe > PCH_2, whereas for the corresponding bromo and iodo compounds it is Br(I) > Cp > PCHMe > PCH_2 which leads to different configurational symbols for the same relative configurations. The priority sequences for the Norphos derivatives are Cp > Cl > P_{endo} > P_{exo} and Br(I) > Cp > P_{endo} > P_{exo} (subrule 3 of the CIP system[8]). The two configurational symbols of (*R*,*R*)-Norphos were reduced to one (*R*) in formulas such as ($R_{Ru,}R_C$) and ($S_{Ru,}R_C$).

4.3 Scheme 4-2 with Fast and Scheme 4-3 with Slow Pyramidal Inversion

The chiral-at-metal half-sandwich compounds [CpMn(NO)(PPh_3)COOR'] (R' = CH_3, L-$C_{10}H_{19}$)[9-12] and [CpMn(NO)(PPh_3)C(O)R'] (R' = CH_3, C_6H_5 and *p*-C_6H_4R")[13-17] are configurationally stable in the solid state. In solution, however, they are configurationally labile. They change the metal configuration in first-order reactions approaching the racemization or in case of L-menthyl the epimerization equilibria. In non-polar solvents the half lives $\tau_{1/2}$ are in the range of minutes to hours at ambient temperatures.[9,10,13-15] The concentration and solvent dependence of the racemization and epimerization have been investigated including Hammett correlations and the influence of added triphenylphosphine.[10,12-15] These studies as well as exchange reactions with deuterated triphenylphosphine[12] and substitution reactions with other phosphines, which occurred with

partial retention of configuration,[13,16,17] are in accord with Scheme 4-2. Reviews summarizing these mechanistic studies are available.[1,18-20]

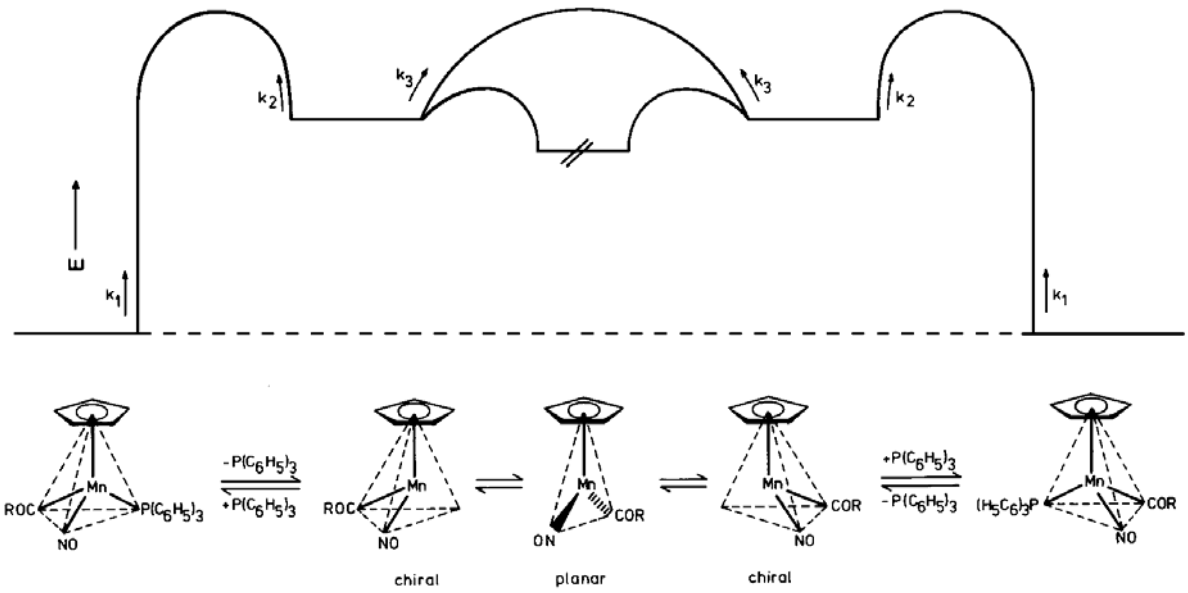

Scheme 4-2. Energy diagram for the racemization of the compounds [CpMn(NO)(PPh_3)C(O)R].

The rate-determining step in the racemization of (*R*)-[CpMn(NO)(PPh_3)C(O)R] in Scheme 4-2 is the cleavage of the manganese-triphenylphosphane bond giving free triphenylphosphane and a pyramidal intermediate (*R*)-[CpMn(NO)C(O)R] with an empty coordination site. Activation energies are in the order of 25-30 kcal/mol.[10,14,15] Activation entropies are strongly positive in agreement with an increase in the number of species. The unsaturated intermediate (*R*)-[CpMn(NO)C(O)R] is high in energy and cannot be detected by spectroscopy. It can react with the dissociated or with added triphenylphosphane, with deuterated triphenylphosphane or with other added ligands. All these reactions occur with retention of the metal configuration. However, the pyramidal intermediate (*R*)-[CpMn(NO)C(O)R] can also invert to its mirror image (*S*)-[CpMn(NO)C(O)R] from which the opposite configurational side is accessible. The barriers to the right (k_3) and to the left (k_2) from the pyramidal intermediate (*R*)-[CpMn(NO)C(O)R] are assumed to have about the same height. Due to the air-sensitivity and the instability (formation of paramagnetic impurities) detailed investigations of the competition ratio k_3/k_2 have not been possible in the CpMn system. Omitting the crossed out part, the energy profile of Scheme 4-2 resembles the cross-

section of a hall church in which the central nave and the side naves have the same height, dominantly build in the late gothic period in Europe.

A crucial point is the middle part of Scheme 4-2. Is the planar species [CpMn(NO)C(O)R] an intermediate or a transition state in the interconversion of the pyramids (*R*)- and (*S*)-[CpMn(NO)C(O)R]? There is a multitude of planar 16-electron half-sandwich compounds including species of the CpRu type (see below). Theoretical studies showed that fragments [(η-C_nH_n)M(CO)$_2$] are pyramidal, the planar species being transition states, whereas fragments [(η-C_nH_n)M(PH_3)$_2$] adopt planar configurations.[21,22] In fact, planar 16-electron complexes of the type [CpRu(PR_3)Hal] were described[23] and planarity was assigned to species such as [CpRu(P-P)]$^+$ on the basis of spectroscopy.[24] However, the problem has not been investigated with the help of chirality, which allows additional and unequivocal decisions, not accessible with other methods. Using stereochemistry we will show in the present paper that 16-electron species [CpRu(P-P')]$^+$ are pyramidal, the planar fragments being transition states as indicated in Scheme 4-3.

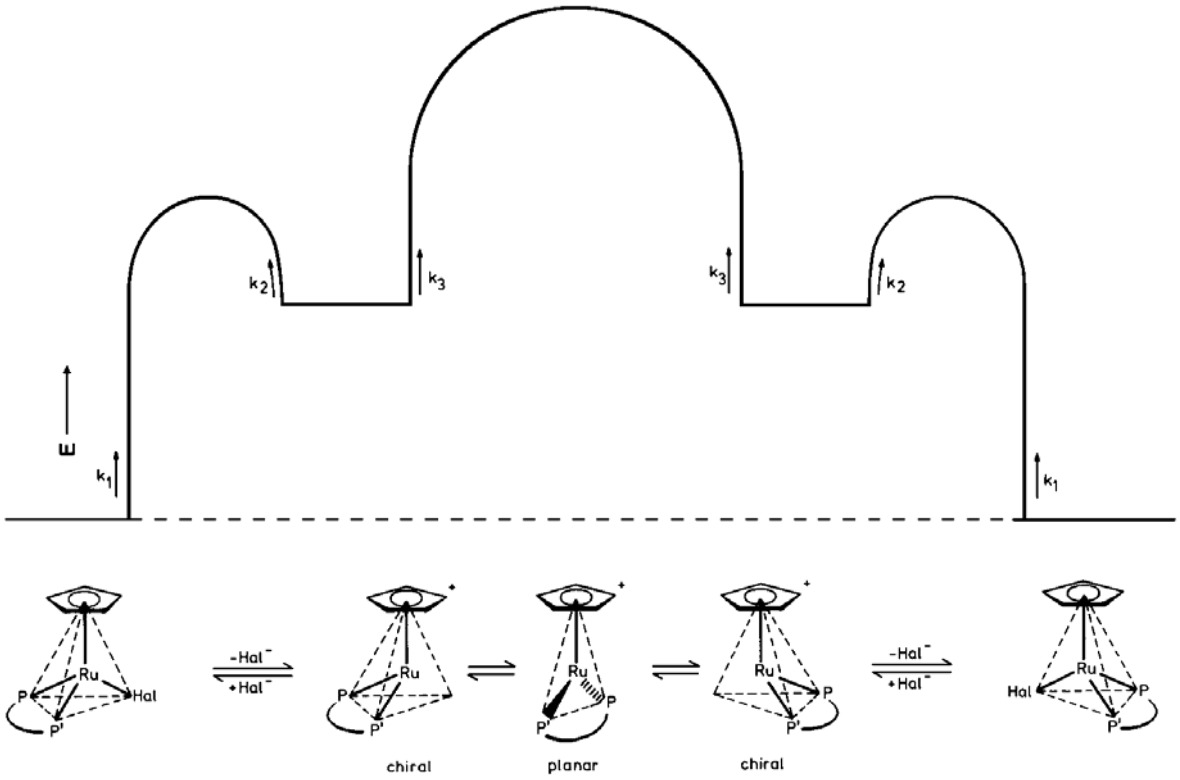

Scheme 4-3. Energy diagram for the racemization of the compounds [CpRu(P-P')Hal].

In addition, it will be demonstrated that the competition ratio k_3/k_2 for $[CpRu(P\text{-}P)]^+$ is much smaller than for [CpMn(NO)C(O)R] involving a significant retardation of the pyramidal inversion. The energy profile of Scheme 4-3 resembles the cross-section of a basilica in which the central part is much higher than the side parts, found in buildings and churches since the late Roman times all over the world.

The main difference between Schemes 4-2 and 4-3 is the competition ratio k_3/k_2 of the pyramidal intermediates $[CpRu(P\text{-}P')]^+$ for the pyramidal inversion involving the change of the metal configuration versus the back reaction with Hal^- (or other nucleophiles). For the Mn compounds in Scheme 4-2 the competition ratio k_3/k_2 is about 1. That means, that substitution reactions with added nucleophiles inevitably will be accompanied by extensive racemization. For the Ru compounds in Scheme 4-3, however, the competition ratio k_3/k_2 is much smaller than 1, as k_3 is much smaller than k_2. As a consequence the back reaction of the unsaturated pyramidal intermediates with Hal^- (or other nucleophiles) should be fast compared to the change of the metal configuration. Of course k_2 depends on the concentration of the nucleophile used. For high nucleophile concentrations, however, pseudo first-order conditions prevail.

Actually, we did not investigate the [CpRu(P-P')Hal] system with enantiomers R_{Ru}/S_{Ru} but with diastereomers $(R_{Ru,}R_C)/(S_{Ru,}R_C)$ (ligand P-P' = (*R*)-Prophos and (*R*,*R*)-Norphos, Hal = Cl, Br, I) in which the diastereomers $(R_{Ru,}R_C)$ and $(S_{Ru,}R_C)$ give rise to different signals in the NMR. Using diastereomers the energy profile becomes unsymmetrical, right and left halves being different (Scheme 4-4).

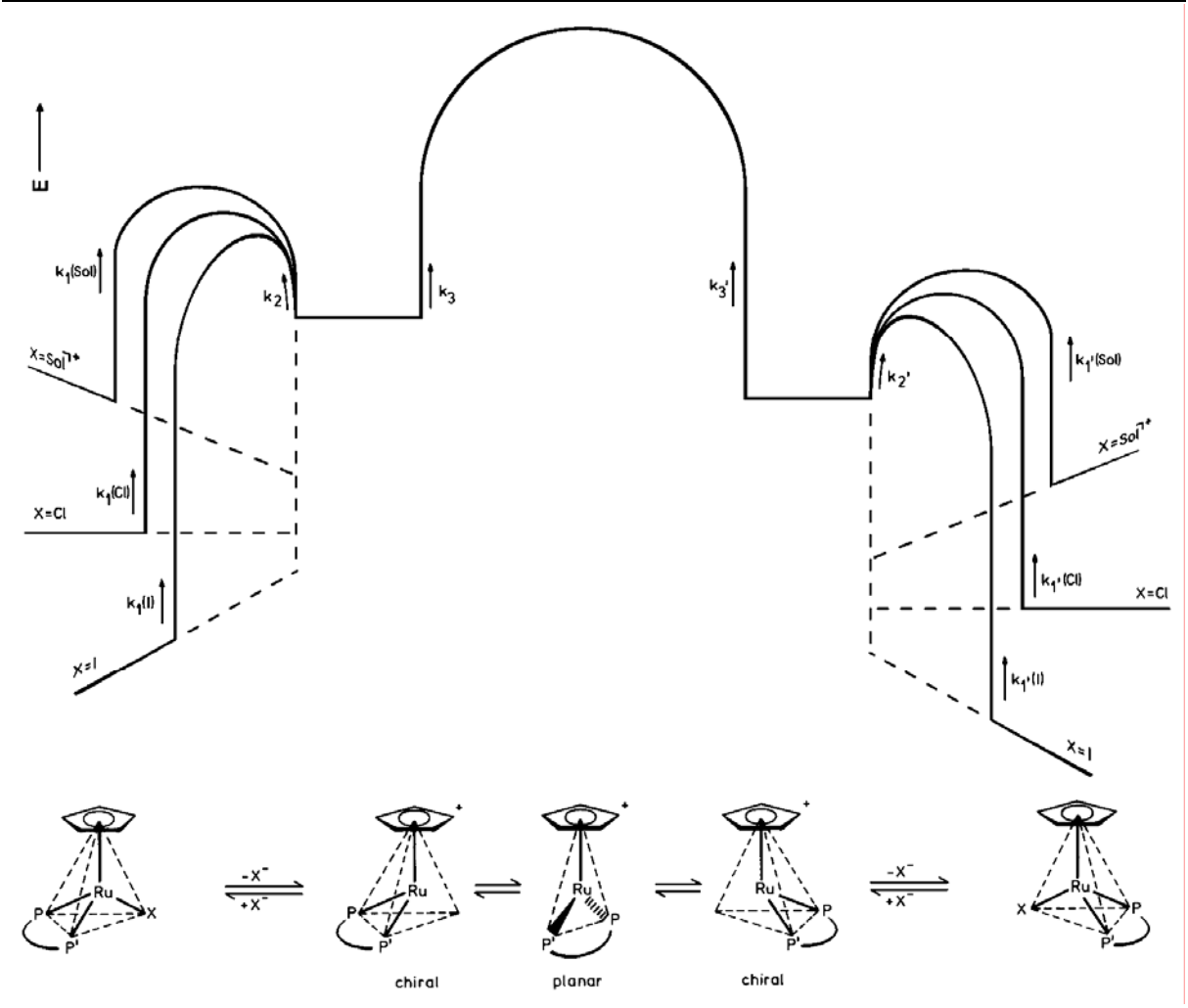

Scheme 4-4. Energy diagram for the epimerization of the compounds [CpRu(P-P')Hal].

4.4 Experimental

4.4.1 Materials and Measurements

The diastereomer mixtures ($R_{Ru,}R_C$)- and ($S_{Ru,}R_C$)-[CpRu(Prophos)Cl], ($R_{Ru,}R_C$)- and ($S_{Ru,}R_C$)- [CpRu(Norphos)Cl] and ($R_{Ru,}R_C$)- and ($S_{Ru,}R_C$)-[CpRu(Norphos)I] were prepared and separated as described in refs. 6 and 7. ^{1}H and ^{31}P{^{1}H} NMR spectra were measured using a Bruker Avance 400 spectrometer. TMS was used as an internal standard for ^{1}H NMR, while H_3PO_4 was used as an external standard for ^{31}P{^{1}H} NMR. ESI-MS spectra were obtained with a Thermoquest TSQ 7000 spectrometer. Only the most intense peak of a cluster is given.

(R_{Ru})-/(S_{Ru})-Bromo[η^5-cyclopentadienyl][[(1*R*)-1-methyl-1,2-ethanediyl]bis[diphenylphosphine-κP]]ruthenium(II), ($R_{Ru,}R_C$)- and ($S_{Ru,}R_C$)-[CpRu(Prophos)Br] (27b and 27b'): ($R_{Ru,}R_C$)- and ($S_{Ru,}R_C$)-[CpRu(Prophos)Cl] (80 mg, 0.12 mmol) was dissolved in 10 mL of methanol. NaBr (750 mg, 6.3 mmol) was added and the reaction mixture was heated to 50 ^{o}C for 20 h. Yield quantitative, orange solid.

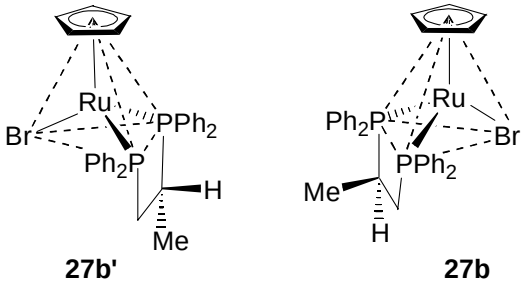

27b' **27b**

($R_{Ru,}R_C$)-[CpRu(Prophos)Br] (27b): ^{1}H NMR ($CDCl_3$): δ = 7.98-7.92 (m, 2H, ArH), 7.60-7.53 (m, 2H, ArH), 7.48-7.20 (m, 16H, ArH), 4.46 (s, 5H, CpH), 3.19-3.05 (m, 1H, CH), 2.78-2.60 (m, 1H CH), 1.96-1.86 (m, 1H, CH), 1.12 (dd, $^3J_{H-H}$ = 6.7 Hz, $^3J_{P-H}$ = 10.2 Hz, 3H, Me).

^{31}P{^{1}H} NMR ($CDCl_3$): δ = 84.42 (d, $^3J_{P-P}$ = 35.8 Hz, 1P), 59.51 (d, $^3J_{P-P}$ = 35.8 Hz, 1P).

EI MS: *m/z* = 660.1 [M^+]. $C_{32}H_{31}BrP_2Ru$ (658.0).

(S_{Ru},R_C)-[CpRu(Prophos)Br] (27b'): ^{1}H NMR ($CDCl_3$): δ = 7.89-7.95 (m, 2H, ArH), 7.47-7.21 (m, 18H, ArH), 4.37 (s, 5H, CpH), 3.02-2.59 (m, 3H, CH-CH_2), 1.01 (dd, $^3J_{H-H}$ = 7.1 Hz, $^3J_{P-H}$ = 12.8 Hz, 3H, Me).

$^{31}P\{^1H\}$ NMR ($CDCl_3$): δ = 81.98 (d, $^3J_{P-P}$ = 30.5 Hz, 1P), 73.72 (d, $^3J_{P-P}$ = 30.5 Hz, 1P).

(R_{Ru})-/(S_{Ru})-[η^5-cyclopentadienyl]iodo[[(1*R*)-1-methyl-1,2-ethanediyl]bis[diphenylphosphine-κP]]ruthenium(II), (R_{Ru},R_C)- and (S_{Ru},R_C)-[CpRu(Prophos)I] (27c and 27c'): Synthesis in analogy to the corresponding bromo complex. Yield quantitative, orange solid.

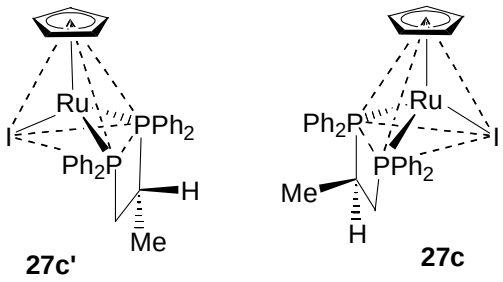

(R_{Ru},R_C)-[CpRu(Prophos)I] (27c): ^{1}H NMR ($CDCl_3$): δ = 8.02-7.97 (m, 2H, ArH), 7.61-7.57 (m, 2H, ArH), 7.49-7.24 (m, 16H, ArH), 4.61 (s, 5H, CpH), 3.46-3.34 (m, 1H, CH), 2.94-2.69 (m, 1H, CH), 2.03-1.93 (m, 1H, CH), 1.27 (dd, $^3J_{H-H}$ = 6.8 Hz, $^3J_{P-H}$ = 10.9 Hz, 3H, Me).

$^{31}P\{^1H\}$ NMR ($CDCl_3$): δ = 86.03 (d, $^3J_{P-P}$ = 33.6 Hz, 1P), 62.17 (d, $^3J_{P-P}$ = 33.6 Hz, 1P).

EI MS: *m/z* = 705.9 [M^+].

Elemental analysis: $C_{32}H_{31}IP_2Ru$ (705.0)

Calcd C 54.18, H 4.85.

Found: C 54.51, H 4.40.

(S_{Ru},R_C)-[CpRu(Prophos)I] (27c'): ^{1}H NMR ($CDCl_3$): δ = 8.07-8.02 (m, 2H, ArH), 7.94-787 (m, 2H, ArH), 7.52-7.22 (m, 14H, ArH), 7.15-7.09 (m, 2H, ArH), 4.56 (s, 5H, CpH), 3.13-2.90 (m, 1H, CH), 2.94-2.69 (m, 1H, CH), 2.03-1.93 (m, 1H, CH), 1.23 (dd, $^3J_{H-H}$ = 7.0 Hz, $^3J_{P-H}$ = 13.6 Hz, 3H, Me).

$^{31}P\{^1H\}$ NMR ($CDCl_3$): δ = 84.41 (d, $^3J_{P-P}$ = 28.4 Hz, 1P), 72.04 (d, $^3J_{P-P}$ = 28.4 Hz, 1P).

(R_{Ru})/(S_{Ru})-[1*R*-(2-endo,3-exo)]-[Bicyclo[2.2.1]hept-5-ene-2,3-diylbis[diphenylphosphine]-P,P']bromo(η^5-cyclopentadienyl)ruthenium(II), (R_{Ru},R_C)- and (S_{Ru},R_C)-

[CpRu(Norphos)Br] (28b and 28b'): Synthesis in analogy to the corresponding iodo complex in ref. 7. Yield quantitative, orange solid.

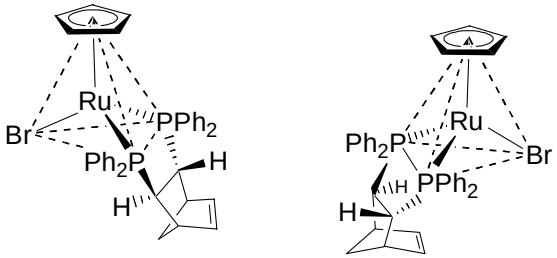

28b **28b'**

EI MS: *m/z* = 710.1 [M^+, 100%].

Elemental analysis: $C_{36}H_{33}BrP_2Ru$ (708.6)

Calcd C 61.04, H 4.66.

Found C 60.44, H 4.92.

For the halide exchange and the epimerization reactions highly enriched samples of (R_{Ru},R_C)- and (S_{Ru},R_C)-[CpRu(Prophos)Hal] **27** and (R_{Ru},R_C)- and (S_{Ru},R_C)-[CpRu(Norphos)Hal] **28** were used. Thus, the epimerization reactions in $CDCl_3$/CH_3OH 9:1 (v/v) started with samples of (R_{Ru},R_C)/(S_{Ru},R_C)-[CpRu(Prophos)Cl] **27a'/27a** = 97:3 and 3:97. Dissolution of the samples (for the Hal exchange reactions in the presence of [Bu_4N]Hal) sometimes was reluctant. It took about 10-15 min to make the first measurement in the NMR spectrometer adjusted to the respective temperature. During this time interval epimerization halide exchange and epimerization had already started for some samples. Therefore, the diastereomer ratios of the first measurement under controlled conditions were used as "starting ratios" in Tables, Figures, and calculations.

For all the kinetic measurements the integrals of the Cp or Me signals in the ^{1}H NMR spectra were used which proved to be more sensitive than the ^{31}P signals in the $^{31}P\{^1H\}$ NMR spectra.

For the X-ray structure determinations ($R_{Ru,}R_C$)-[CpRu(Prophos)Br] **27b** and ($R_{Ru,}R_C$)-[CpRu(Prophos)I] **27c** were crystallized from methanol. A sample of ($R_{Ru,}R_C$)- and ($S_{Ru,}R_C$)-[CpRu(Norphos)I] **28c** and **28c'** of composition 33:67 was crystallized from a 1:3 mixture of CH_2Cl_2/CH_3OH to give a crystalline fraction of ($R_{Ru,}R_C$)/($S_{Ru,}R_C$)-[CpRu(Norphos)I] **28c**/**28c'** 27:73 which contained crystals of both diastereomers.

4.5 Results

4.5.1 Configurations

The Prophos ligand was used in its (*R*)-configuration.[25] The configuration of the less soluble diastereomer of [CpRu(Prophos)Cl] having the low field Cp signal in the NMR had been determined as (S_{Ru},R_C).[6] It was the diastereomer which dominated the equilibrium.[6] The same relative configuration was assigned to the less soluble diastereomers (R_{Ru},R_C)-[CpRu(Prophos)Br] **27b** and (R_{Ru},R_C)-[CpRu(Prophos)I] **27c** which were the major diastereomers in the (R_{Ru},R_C)/(S_{Ru},R_C) equilibria having the low field Cp signals.

The Norphos ligand was used in its (*R*,*R*)-configuration.[26-28] The configuration of the major diastereomer of [CpRu(Norphos)I] in the equilibrium had been determined as (R_{Ru},R_C).[7] It had the low-field olefin NMR signals at 5.57 and 6.42 ppm. The same relative configuration was assigned to the major diastereomers (S_{Ru},R_C)-[CpRu(Norphos)Cl] **28a** and (R_{Ru},R_C)-CpRu(Norphos)Br] **28b** in the (R_{Ru},R_C)/(S_{Ru},R_C) equilibria having the same NMR properties in the olefin region.

4.5.2 Halide Exchange in [CpRu(Prophos)Cl] and [CpRu(Norphos)Cl]

Cl/I Exchange in [CpRu(Prophos)Cl] (27a' and 27a) in $CDCl_3/CH_3OH$ 9:1. The kinetics of the Cl/I exchange in **27a'** and **27a** was measured with an excess of $[Bu_4N]I$ in the solvent mixture $CDCl_3/CH_3OH$ (9:1, v/v) at 300 K. Figure 4-1 shows the reaction of a sample of **27a'**/**27a** = 85:15 with a 14-fold excess of $[Bu_4N]I$. The concentration of **27a'** decreased with time, whereas the concentrations of (S_{Ru},R_C)-[CpRu(Prophos)I] **27c'** and (R_{Ru},R_C)-[CpRu(Prophos)I] **27c** increased. Surprisingly, the concentration of **27a** did not change appreciably which means that the (S_{Ru},R_C)-diastereomer reacted much more slowly with $[Bu_4N]I$ than the (R_{Ru},R_C)-diastereomer. The first-order rate constant for the disappearance of **27a'** at 300 K was $k = 7.2 \times 10^{-3}$ min^{-1}.

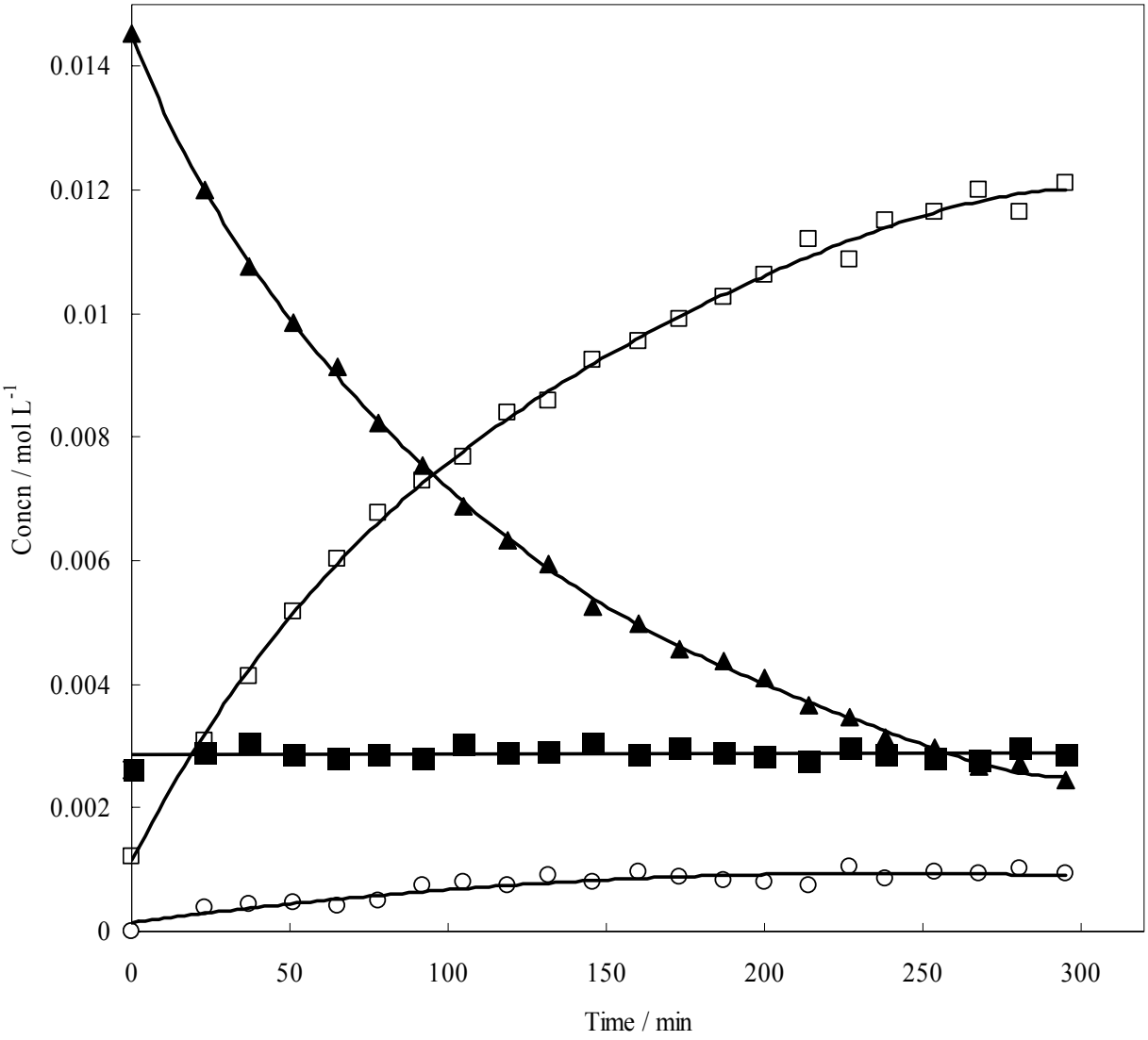

Figure 4-1. Cl/I exchange reaction in (R_{Ru},R_C)-/(S_{Ru},R_C)-[CpRu(Prophos)Cl] 85:15 (**27a'**/**27a**: ▲/■; 18.4 mmol L^{-1}) with [Bu_4N]I (0.25 mol L^{-1}) in $CDCl_3$/CH_3OH (9:1, v/v) at 300 K. The products are (S_{Ru},R_C)-[CpRu(Prophos)I] (**27c'**: □) and (R_{Ru},R_C)-[CpRu(Prophos)I] (**27c**: ○).

As the concentration of (S_{Ru},R_C)-[CpRu(Prophos)Cl] **27a** stayed almost constant, the two substitution products (S_{Ru},R_C)-[CpRu(Prophos)I] **27c'** and (R_{Ru},R_C)-[CpRu(Prophos)I] **27c** originated from the disappearing **27a'**. It mainly transformed to **27c'**. (R_{Ru},R_C)-[CpRu(Prophos)Cl] **27a'** and (S_{Ru},R_C)-[CpRu(Prophos)I] **27c'** have the same relative configuration, because the change of the configurational symbol is only due to a change in the ligand priority sequence. Thus, the Cl/I exchange in **27a'** occurred predominantly with retention of configuration at the metal atom. Definitely, however, a small amount of **27a'** was converted into **27c** with inversion of configuration (Scheme 4-5).

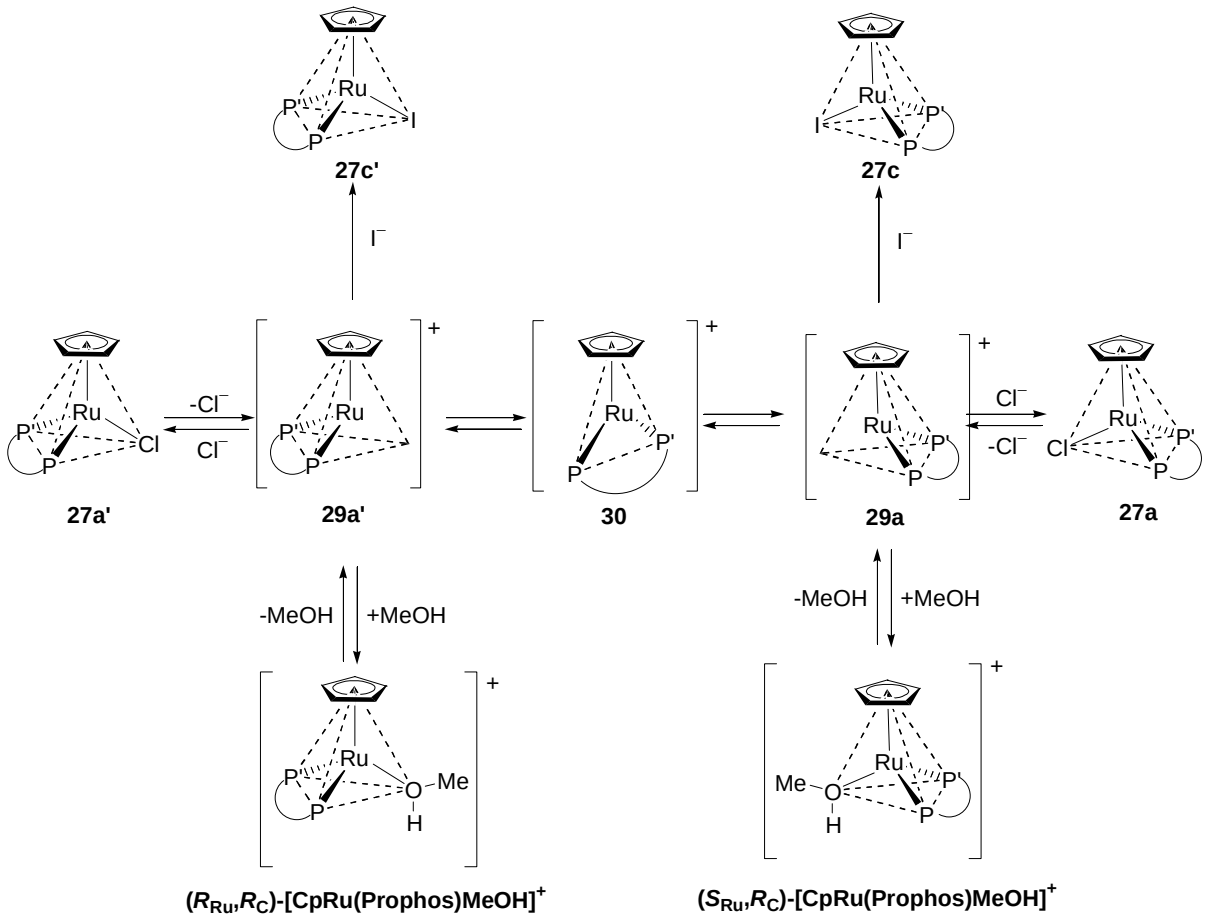

Scheme 4-5. The Cl/I exchange mechnaism of (R_{Ru},R_C)-/(S_{Ru},R_C)-[CpRu(Prophos)Cl] **27a'**/**27a** [P-P' = (*R*)-Prophos].

These experimental facts can be explained by assuming an energy profile as in Scheme 4-4. The Cl/I exchange in **27a'** starts on the left side with the cleavage of the Ru-Cl bond. This is the rate-determining step which requires a high activation energy. An unsaturated intermediate (R_{Ru},R_C)-[CpRu(Prophos)]$^+$ **29a**' with pyramidal geometry is formed which has kept its metal configuration. This intermediate can react in a fast reaction with iodide to give the substitution product **27c'** with retention of the metal configuration. It can also react with MeOH, present in the solvent mixture, to give the species (R_{Ru},R_C)-[CpRu(Prophos)MeOH]$^+$ as a temporary parking lot. However, the intermediate (R_{Ru},R_C)-[CpRu(Prophos)]$^+$ **29a'** which was not observed experimentally can also invert its configuration, crossing the middle of Scheme 4-4, to form its diastereomer (S_{Ru},R_C)-[CpRu(Prophos)]$^+$ **29a** which subsequently is quenched to **27c**. As the iodo complexes **27c** and **27c'** are more stable than the chloro starting material **27a'**, particularly in the presence of an excess of iodide, and the parking-lot species

(R_{Ru},R_C)-[CpRu(Prophos)MeOH]$^+$, the chloro complex will be quantitatively converted into the iodo products (Scheme 4-5).

The crucial point in the Cl/I exchange in **27a'** is the choice of the intermediate **29a'** to invert its configuration (k_3 path) or to react to the iodo complex **27c'** with retention of configuration (k_2 path). This choice is best treated with the competition ratio k_3/k_2. The competition ratio k_3/k_2 can be determined from the product ratio **27c**/**27c'** which is constant throughout the reaction. We neglected the first three measurements of Fig. 4-1, because the concentration of the new products was still too low and calculated the average of all the other measurement points. The competition ratio $k_3/k_2 = 0.08$ shows that the inversion of the intermediate (k_3 path) is slow compared to the reaction of the intermediate with excess iodide (k_2 path) indicating a basilica-type energy profile as in Schemes 4-3 and 4-4.

The rate constants of the Cl/I exchange in **27a'** with $[Bu_4N]I$ increased with rising temperature (Table 4-1, upper part). A large excess of $[Bu_4N]I$ was used in all these reactions to guarantee pseudo first-order conditions. In this temperature variation the competition ratio k_3/k_2 showed considerable scattering due to the inaccuracy of the determination of the concentration of **27c** which is only formed in small amounts.

In these measurements too a reluctance of **27a** to undergo Cl/I exchange was noticed. To measure the Cl/I exchange in the (S_{Ru},R_C)-diastereomer a sample of **27a**/**27a'** 97:3 was treated with an excess of $[Bu_4N]I$ in $CDCl_3/CH_3OH$ (9:1, v/v) at 300-323 K. Table 4-1 shows that the rate constants for the disappearance of **27a** in the Cl/I exchange are 10-15 times slower than for **27a'**. The reason is that **27a**, the right side species in Scheme 4-4, is the thermodynamically more stable diastereomer. It dominates the equilibrium **27a**/**27a'** 85:15 (see below) which means that it is more stable (and less reactive) than **27a'**. This reflects a higher activation energy for $k_{3'}$ compared to k_3 (see Scheme 4-4).

We did not determine the competition ratios $k_{3'}/k_{2'}$ for the Cl/I exchange in **27a**, because samples even highly enriched in **27a** contained some **27a'** which in a fast reaction gave (S_{Ru},R_C)- and (R_{Ru},R_C)-[CpRu(Prophos)I] **27c'** and **27c** (see above), before **27a** was slowly converted to (R_{Ru},R_C)- and (S_{Ru},R_C)-[CpRu(Prophos)I] **27c** and **27c'** from which the ratios $k_{3'}/k_{2'}$ would have to be calculated.

The activation parameters for the Cl/I exchange reactions in **27a'** and **27a** with $[Bu_4N]I$ are given in Table 4-1 (upper part). The reactions start with the cleavage of the Ru-Cl bond. Negative values were found for the entropy of activation, whereas for reactions of the Mn compounds described above, in which the initial step is the cleavage of the Mn-PPh_3 bond, activation entropies had been positive. Both reaction types are dissociations in which the number of particles increases. However, in the Mn system a neutral complex breaks up into two neutral fragments leading to a positive entropy of activation. Differently, in the Ru system a neutral complex forms two ions which are strongly solvated by the polar solvent methanol. This increases the order reflected by a negative entropy of activation.

Cl/Br Exchange in [CpRu(Prophos)Cl] (27a' and 27a) in $CDCl_3/CH_3OH$ 9:1. The kinetics of the Cl/Br exchange in **27a'** and **27a** was measured with an excess of $[Bu_4N]Br$ under similar conditions as the Cl/I exchange in the solvent mixture $CDCl_3/CH_3OH$ (9:1, v/v). As in the Cl/I exchange the concentration of **27a'** decreased with time, whereas the concentrations of (S_{Ru},R_C)-[CpRu(Prophos)Br] **27b'** and (R_{Ru},R_C)-[CpRu(Prophos)Br] **27b** increased. Similar to the Cl/I system, the concentration of **27a** did not change appreciably during the Cl/Br exchange reaction. The first-order rate constant for the disappearance of **27a'** in the Cl/Br exchange at 300 K was $k_1 = 6.2 \times 10^{-3}$ min^{-1} compared to $k_1 = 7.2 \times 10^{-3}$ min^{-1} in the Cl/I exchange. Thus, within the limits of error, the rate constants for the Cl/Br and the Cl/I exchange are the same. This also holds for the temperature dependence of the rate constants (Table 4-1, lower part). The reason for this is obvious from Scheme 4-4. For both processes, the Cl/Br and the Cl/I exchange, the rate determining step is the cleavage of the Ru-Cl bond in **27a'** in which the unsaturated intermediate (R_{Ru},R_C)-[CpRu(Prophos)]$^+$ **29a**' is formed. Quenching of the intermediate with excess bromide or excess iodide are fast reactions which do not affect the rate determining step. The competition ratios k_3/k_2 in the Cl/Br exchange reactions were similar to those of the Cl/I systems (Table 4-1, lower part).

Table 4-1. Kinetics of the disappearance of (R_{Ru},R_C)-[CpRu(Prophos)Cl] **27a'** and (S_{Ru},R_C)-[CpRu(Prophos)Cl] **27a** in the Cl/Hal exchange reactions with [Bu_4N]I (upper part) and [Bu_4N]Br (lower part) in $CDCl_3/CH_3OH$ (9:1, v/v) and activation parameters.

Reaction	Additive	Temp/K	k_1 or $k_{1'}$/min^{-1}	$\tau_{1/2}$/min^{-1}	k_3/k_2
		300	7.2×10^{-3}	96	0.08
(R_{Ru},R_C)-[CpRu(Prophos)Cl] →		308	1.5×10^{-2}	46	0.06
(S_{Ru},R_C)-[CpRu(Prophos)I]	[Bu_4N]I	313	2.7×10^{-2}	26	0.04
		323	5.4×10^{-2}	13	0.11
Activation energy E_a = 71 kJ mol^{-1}					
Frequency factor A = 2.0×10^{10} min^{-1}					
Activation enthalpy $\Delta H^{\ddagger}$ (300 K) = 69 kJ mol^{-1}					
Activation entropy $\Delta S^{\ddagger}$ (300 K) = -90 J mol^{-1} K^{-1}					
Gibbs free energy $\Delta G^{\ddagger}$ (300 K) = 96 kJ mol^{-1}					
		300	6.2×10^{-4}	1120	
(S_{Ru},R_C)-[CpRu(Prophos)Cl] →		308	1.3×10^{-3}	530	
(R_{Ru},R_C)-[CpRu(Prophos)I]	[Bu_4N]I	313	3.1×10^{-3}	220	
		323	7.7×10^{-3}	90	
Activation energy E_a = 91 kJ mol^{-1}					
Frequency factor A = 3.5×10^{12} min^{-1}					
Activation enthalpy $\Delta H^{\ddagger}$ (300 K) = 88 kJ mol^{-1}					
Activation entropy $\Delta S^{\ddagger}$ (300 K) = -47 J mol^{-1} K^{-1}					
Gibbs free energy $\Delta G^{\ddagger}$ (300 K) = 102 kJ mol^{-1}					
		300	6.2×10^{-3}	110	0.04
(R_{Ru},R_C)-[CpRu(Prophos)Cl] →		308	1.8×10^{-2}	38	0.05
(S_{Ru},R_C)-[CpRu(Prophos)Br]	[Bu_4N]Br	313	3.9×10^{-2}	18	0.05
		323	6.0×10^{-2}	12	0.04
Activation energy E_a = 81 kJ mol^{-1}					
Frequency factor A = 8.2×10^{11} min^{-1}					
Activation enthalpy $\Delta H^{\ddagger}$ (300 K) = 78 kJ mol^{-1}					
Activation entropy $\Delta S^{\ddagger}$ (300 K) = -59 J mol^{-1} K^{-1}					
Gibbs free energy $\Delta G^{\ddagger}$ (300 K) = 96 kJ mol^{-1}					
		300	7.8×10^{-4}	890	
(S_{Ru},R_C)-[CpRu(Prophos)Cl] →		308	1.7×10^{-3}	400	
(R_{Ru},R_C)-[CpRu(Prophos)Br]	[Bu_4N]Br	313	3.1×10^{-3}	220	
		323	9.0×10^{-3}	77	
Activation energy E_a = 86 kJ mol^{-1}					
Frequency factor A = 7.6×10^{11} min^{-1}					
Activation enthalpy $\Delta H^{\ddagger}$ (300 K) = 84 kJ mol^{-1}					
Activation entropy $\Delta S^{\ddagger}$ (300 K) = -60 J mol^{-1} K^{-1}					
Gibbs free energy $\Delta G^{\ddagger}$ (300 K) = 102 kJ mol^{-1}					

Table 4-2. Kinetics of the disappearance of (R_{Ru},R_C)-[CpRu(Prophos)Cl] **27a'** and (S_{Ru},R_C)-[CpRu(Prophos)Cl] **27a** in the Cl/Hal exchange reaction with [PyCH$_2$Ph]I (upper part) and [PyCH$_2$Ph]Br (lower part) in CDCl$_3$/CD$_3$OD (1:1, v/v) and activation parameters. For the Cl/Br substitution of (S_{Ru},R_C)-[CpRu(Prophos)Cl] many ^{1}H NMR spectra were measured in the presence of a small amount of Cp$_2$Co (see text).

Reaction	Additive	Temp/K	k_1 or $k_{1'}$/min^{-1}	$\tau_{1/2}$/min^{-1}	k_3/k_2
		283	8.1 x 10^{-3}	86	0.08
(R_{Ru},R_C)-[CpRu(Prophos)Cl] →		288	1.5 x 10^{-2}	45	0.15
(S_{Ru},R_C)-[CpRu(Prophos)I]	[PyCH$_2$Ph]I	293	3.1 x 10^{-2}	23	0.12
		300	6.3 x 10^{-2}	11	0.09
Activation energy E_a = 86 kJ mol^{-1}					
Frequency factor A = 6.0 x 10^{13} min^{-1}					
Activation enthalpy $\Delta H^‡$ (300 K) = 83 kJ mol^{-1}					
Activation entropy $\Delta S^‡$ (300 K) = -24 J mol^{-1} K^{-1}					
Gibbs free energy $\Delta G^‡$ (300 K) = 91 kJ mol^{-1}					
		300	8.8 x 10^{-3}	82	
(S_{Ru},R_C)-[CpRu(Prophos)Cl] →		308	1.5 x 10^{-2}	46	
(R_{Ru},R_C)-[CpRu(Prophos)I]	[PyCH$_2$Ph]I	313	3.3 x 10^{-2}	21	
		323	1.1 x 10^{-1}	6	
Activation energy E_a = 92 kJ mol^{-1}					
Frequency factor A = 7.0 x 10^{13} min^{-1}					
Activation enthalpy $\Delta H^‡$ (300 K) = 90 kJ mol^{-1}					
Activation entropy $\Delta S^‡$ (300 K) = -22 J mol^{-1} K^{-1}					
Gibbs free energy $\Delta G^‡$ (300 K) = 96 kJ mol^{-1}					
		283[a]	1.1 x 10^{-2}	61	0.09
(R_{Ru},R_C)-[CpRu(Prophos)Cl] →		288[a]	2.0 x 10^{-2}	35	n.d.
(S_{Ru},R_C)-[CpRu(Prophos)Br]	[PyCH$_2$Ph]Br	293[a]	3.0 x 10^{-2}	23	0.11
		293[b]	3.0 x 10^{-2}	23	
		300[a]	5.9 x 10^{-2}	12	0.13
Activation energy E_a = 89 kJ mol^{-1}					
Frequency factor A = 2.3 x 10^{14} min^{-1}					
Activation enthalpy $\Delta H^‡$ (300 K) = 86 kJ mol^{-1}					
Activation entropy $\Delta S^‡$ (300 K) = -12 J mol^{-1} K^{-1}					
Gibbs free energy $\Delta G^‡$ (300 K) = 90 kJ mol^{-1}					
		300[b]	6.6 x 10^{-3}	106	
(S_{Ru},R_C)-[CpRu(Prophos)Cl] →		305[b]	1.4 x 10^{-2}	48	
(R_{Ru},R_C)-[CpRu(Prophos)Br]	[PyCH$_2$Ph]Br	318[b]	4.9 x 10^{-2}	17	
		323[b]	9.0 x 10^{-2}	8	
Activation energy E_a = 88 kJ mol^{-1}					
Frequency factor A = 1.4 x 10^{13} min^{-1}					
Activation enthalpy $\Delta H^‡$ (300 K) = 85 kJ mol^{-1}					
Activation entropy $\Delta S^‡$ (300 K) = -36 J mol^{-1} K^{-1}					
Gibbs free energy $\Delta G^‡$ (300 K) = 96 kJ mol^{-1}					

a) In the absence of Cp$_2$Co. b) In the presence of Cp$_2$Co

Cl/I Exchange in [CpRu(Prophos)Cl] (27a' and 27a) in $CDCl_3/CD_3OD$ 1:1. The kinetics of the Cl/I exchange in **27a'** and **27a** was measured with an excess of benzylpyridinium iodide ([$PyCH_2Ph$]I) in the solvent mixture $CDCl_3/CD_3OD$ (1:1, v/v) at different temperatures. With respect to the I^- salt we changed to [$PyCH_2Ph$]I) because of overlap of the methyl signals of **27a'**/**27a** and Bu_4NI in the ^1H NMR spectrum and with respect to the methanol admixture we changed from CH_3OH to CD_3OD because of problems with the internal lock signals. Table 4-2 shows that the rates in $CDCl_3/CD_3OD$ 1:1 are much faster than the rates in $CDCl_3/CH_3OH$ 9:1. Suitable comparisons are possible for the measurements at 300 K in Tables 4-1 and 4-2. Going from $CDCl_3/CH_3OH$ 9:1 to 1:1 the rate of the Cl/I substitution increased by a factor of about 10 both for **27a'** and **27a**. Similar to $CDCl_3/CH_3OH$ 9:1 the Cl/I exchange in $CDCl_3/CD_3OD$ 1:1 was 7 times faster for **27a'** than for its more stable diastereomer **27a**.

Cl/Br Exchange in [CpRu(Prophos)Cl] (27a' and 27a) in $CDCl_3/CD_3OD$ 1:1. Contrary to the Cl/I exchange in $CDCl_3/CD_3OD$ 1:1, the Cl/Br exchange in the system (S_{Ru},R_C)- and (R_{Ru},R_C)-[CpRu(Prophos)Cl]/[$PyCH_2Ph$]Br in $CDCl_3/CD_3OD$ 1:1 suffered from extensive line broadening of the NMR spectra. The reason for this was that traces of air-oxygen introduced during sample preparation oxidized a small amount of [CpRu(Prophos)Cl] to the paramagnetic radical cation [CpRu(Prophos)Cl]$^{\bullet+}$ (see below) leading to the observed broadening and shifting of the NMR signals. Concomitantly with the line broadening, the quartets of the methyl signal of the Prophos ligand in the ^1H NMR spectra became doublets, because the coupling to phosphorus was lost. Addition of a small amount of the strongly reducing agent Cp_2Co or iodide ion removed the radical cation [CpRu(Prophos)Cl]$^+$ allowing for good ^1H NMR spectra (Figs. 4-2, 4-3, and 4-4) including a regain of the phosphorus coupling to the H atoms in the Prophos ligand.[29,30)] Measurements in the presence and absence of Cp_2Co gave the same rate constants (Table 4-2), although in the presence of Cp_2Co the signals of (S_{Ru},R_C)- and (R_{Ru},R_C)-[CpRu(Prophos)D] appeared in low intensity (see below).

As in $CDCl_3/CH_3OH$ (9:1) the rate constants within the limits of error were identical for the Cl/Br and the Cl/I exchange in $CDCl_3/CD_3OD$ (1:1) (Table 4-2) indicating the same rate-determining steps k_1 and $k_{1'}$ for both systems. The competition ratios were a little larger in $CDCl_3/CD_3OD$ (1:1) than in $CDCl_3/CH_3OH$ (9:1) indicating a slight adjustment of the central and peripheral heights of the basilica-type energy profile.

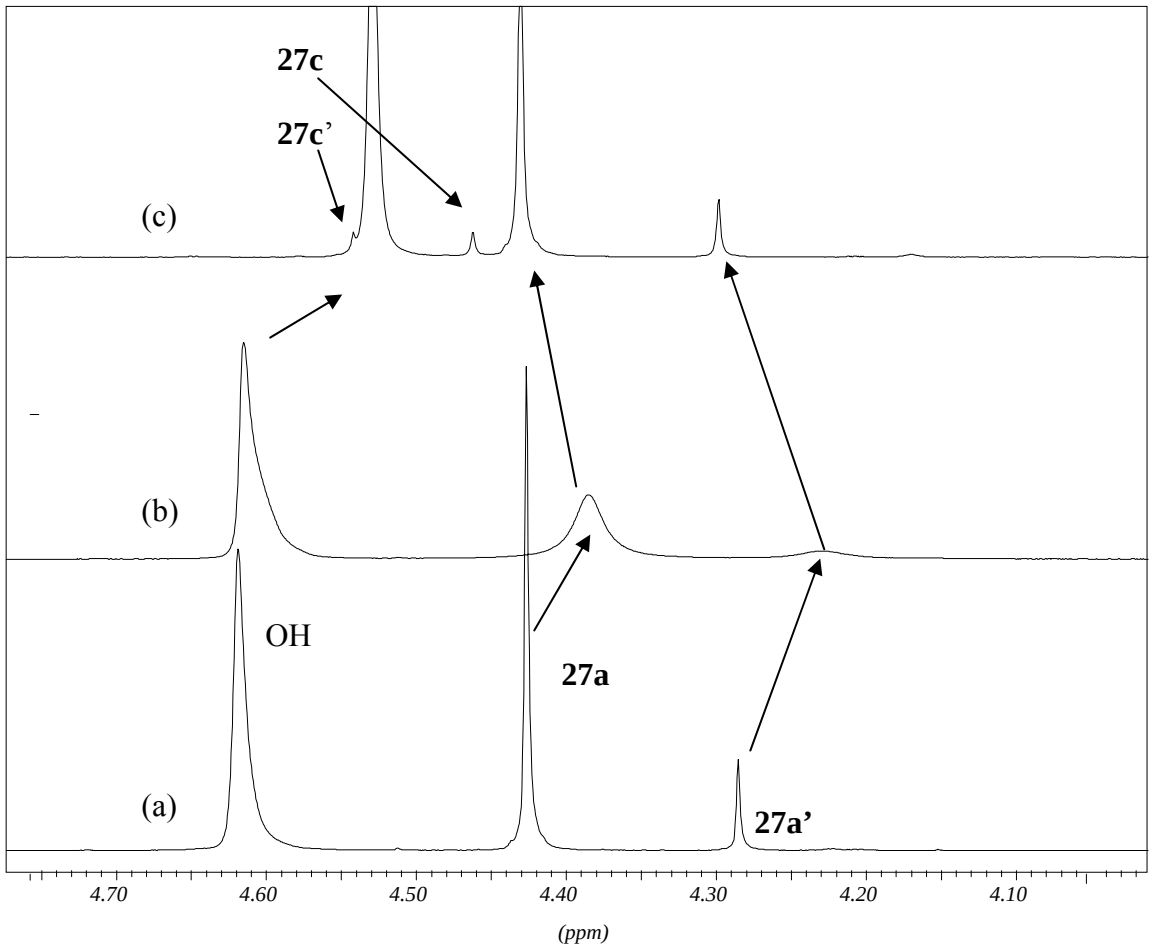

Figure 4-2. ^{1}H NMR spectra of (R_{Ru},R_C)/(S_{Ru},R_C)-[CpRu(Prophos)Cl] **27a'**/**27a** (7.0 mg, 81 : 19 ratio) in a rang of 4.8 – 4.0 ppm in CDCl3/CD3OD (0.40 mL, 1:1, *v/v*) at 300 K: (a) within 5 min after the preparation of the solution; (b) after 25 min; (c) after ca. 30 min added benzylpyridine iodide ($PyCH_2PhI$; 52 mg).

Cl/I and Cl/Br Exchange in [CpRu(Prophos)Cl] (27a' and 27a) in CD_3OD. The kinetics of the Cl/I and the Cl/Br exchange in **27a'** and **27a** was measured with an excess of [$PyCH_2Ph$]I and [$PyCH_2Ph$]Br in pure CD_3OD at different temperatures(Table 4-3). The results were very similar to those in the solvent mixture $CDCl_3$/CD_3OD 1:1. The rates in pure CD_3OD were only a little higher than the rates given in Table 4-2 for $CDCl_3$/CD_3OD 1:1 (up to a factor of 2). Thus, the rates of the Hal substitution reactions changed going from $CDCl_3$/CH_3OH 9:1 to $CDCl_3$/CD_3OD 1:1 by a factor of about 10. However, going from $CDCl_3$/CD_3OD 1:1 to pure CD_3OD they increased only marginally.

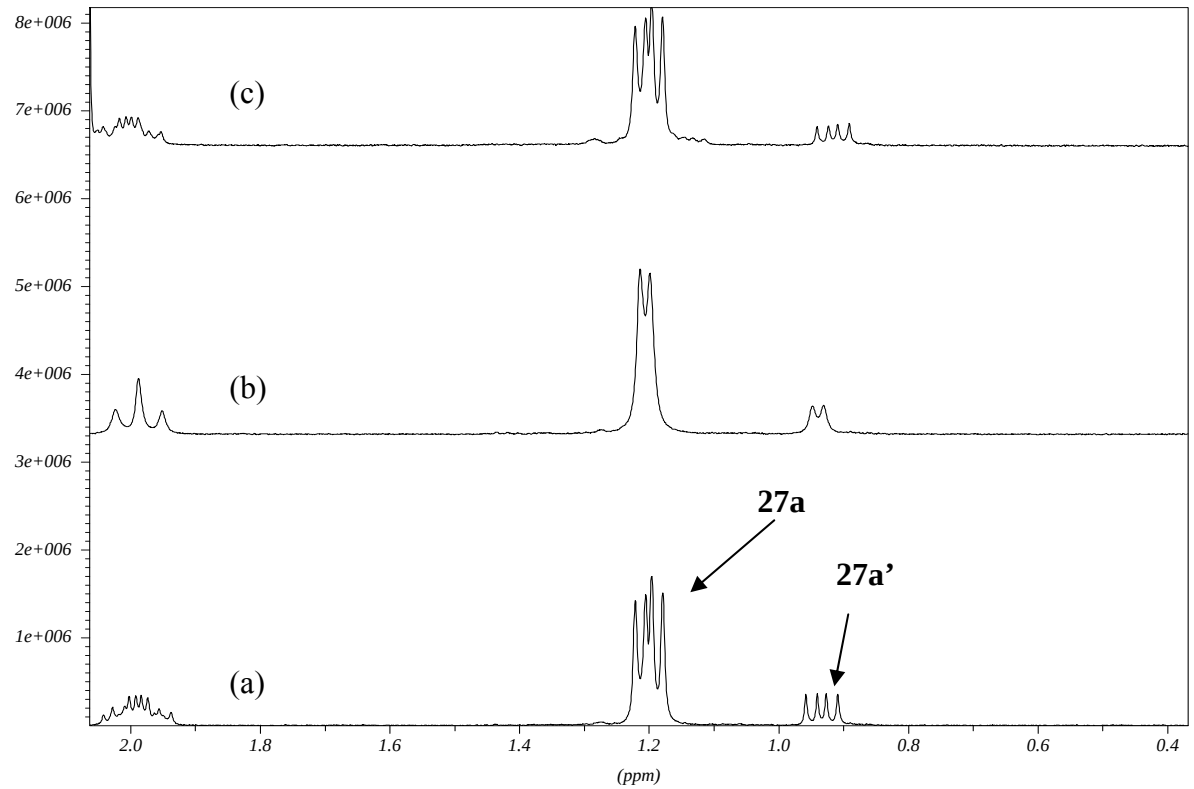

Figure 4-3. ^{1}H NMR spectra of (S_{Ru},R_C)/(R_{Ru},R_C)-[CpRu(Prophos)Cl] **27a**/**27a'** (7.0 mg, 81 : 19 ratio) in a rang of 2.1 – 0.4 ppm in $CDCl_3$/CD_3OD (0.40 mL, 1:1, *v/v*) at 300 K: (a) within 5 min after the preparation of the solution; (b) after 25 min; (c) after ca. 30 min added [$PyCH_2Ph$]I (52 mg).

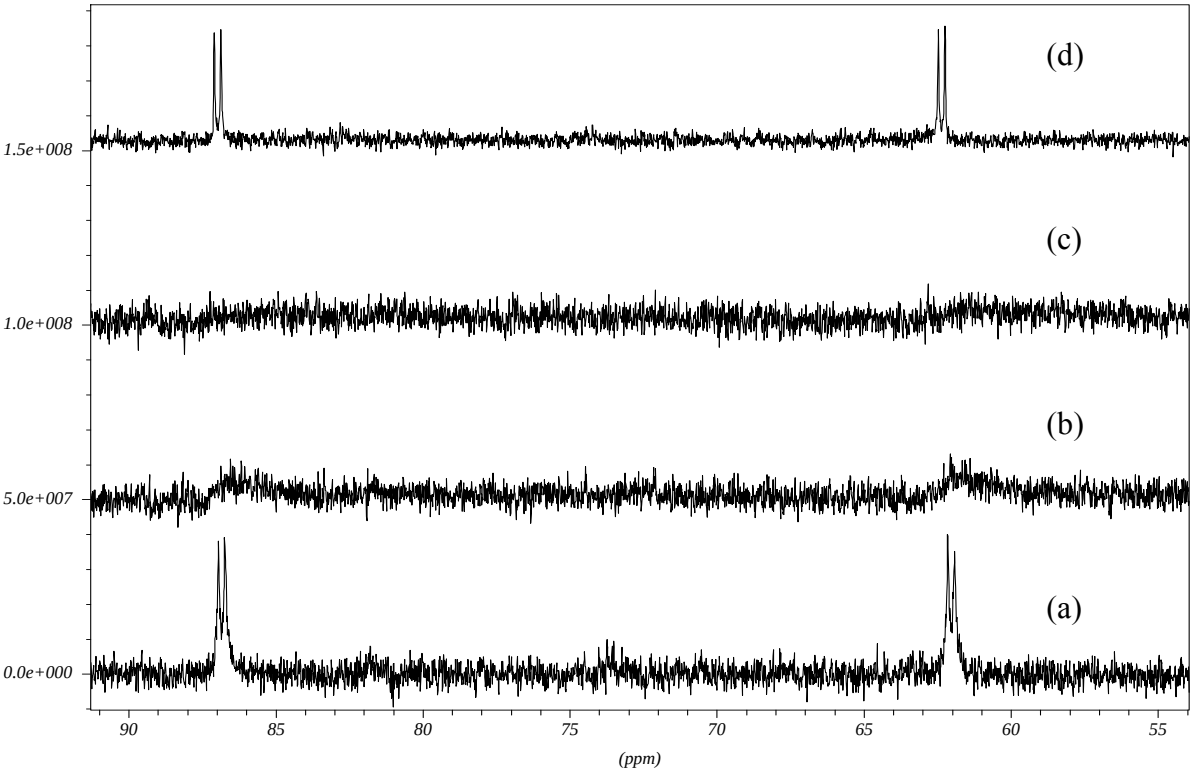

Figure 4-4. $^{31}P\{^1H\}$ NMR Spectra of (S_{Ru},R_C)-[CpRu(Prophos)Cl] **27a** (7.0 mg) in $CDCl_3$/CD_3OD (4.0 mL, 1:1, v/v): (a) measurement within 10 min; (b) after 20 min; (c) after 30 min; and (d) added [$PyCH_2Ph$]I (67 mg).

Table 4-3. Kinetics of the Cl/Br[a)] or Cl/I substitution reaction of enriched samples of (R_{Ru},R_C)/(S_{Ru},R_C)-[CpRu(Prophos)Cl] **27a'**/**27a** in CD_3OD and activation parameters. All measurements were performed using the Cp signals of the ^{1}H NMR spectra.

Reaction	Additive	Temp/K	k_1 or $k_{1'}$/min^{-1}	$\tau_{1/2}$/min^{-1}
		283	1.8 x 10^{-2}	39
(R_{Ru},R_C)-[CpRu(Prophos)Cl] →		288	3.1 x 10^{-2}	23
(S_{Ru},R_C)-[CpRu(Prophos)I]	[PyCH$_2$Ph]I	293	6.6 x 10^{-2}	11
		300	1.4 x 10^{-1}	5
Activation energy E_a = 87 kJ mol^{-1}				
Frequency factor A = 2.2 x 10^{14} min^{-1}				
Activation enthalpy $\Delta H^{\ddagger}$ (300 K) = 85 kJ mol^{-1}				
Activation entropy $\Delta S^{\ddagger}$ (300 K) = -13 J mol^{-1} K^{-1}				
Gibbs free energy $\Delta G^{\ddagger}$ (300 K) = 89 kJ mol^{-1}				
		293	8.8 x 10^{-3}	79
(S_{Ru},R_C)-[CpRu(Prophos)Cl] →		300	3.1 x 10^{-2}	22
(R_{Ru},R_C)-[CpRu(Prophos)I]	[PyCH$_2$Ph]I	308	6.2 x 10^{-2}	11
		313	1.5 x 10^{-1}	5
Activation energy E_a = 103 kJ mol^{-1}				
Frequency factor A = 2.1 x 10^{16} min^{-1}				
Activation enthalpy $\Delta H^{\ddagger}$ (300 K) = 100 kJ mol^{-1}				
Activation entropy $\Delta S^{\ddagger}$ (300 K) = 25 J mol^{-1} K^{-1}				
Gibbs free energy $\Delta G^{\ddagger}$ (300 K) = 93 kJ mol^{-1}				
		283	1.4 x 10^{-2}	50
(R_{Ru},R_C)-[CpRu(Prophos)Cl] →		288	2.8 x 10^{-2}	25
(S_{Ru},R_C)-[CpRu(Prophos)Br]	[PyCH$_2$Ph]Br	293	4.8 x 10^{-2}	15
		300	1.2 x 10^{-1}	6
Activation energy E_a = 88 kJ mol^{-1}				
Frequency factor A = 2.3 x 10^{14} min^{-1}				
Activation enthalpy $\Delta H^{\ddagger}$ (300 K) = 86 kJ mol^{-1}				
Activation entropy $\Delta S^{\ddagger}$ (300 K) = -12 J mol^{-1} K^{-1}				
Gibbs free energy $\Delta G^{\ddagger}$ (300 K) = 89 kJ mol^{-1}				
		293	4.7 x 10^{-3}	150
(S_{Ru},R_C)-[CpRu(Prophos)Cl] →		300	1.3 x 10^{-2}	53
(R_{Ru},R_C)-[CpRu(Prophos)Br]	[PyCH$_2$Ph]Br	308	3.8 x 10^{-2}	18
		313	8.1 x 10^{-2}	9
Activation energy E_a = 108 kJ mol^{-1}				
Frequency factor A = 7.6 x 10^{16} min^{-1}				
Activation enthalpy $\Delta H^{\ddagger}$ (300 K) = 105 kJ mol^{-1}				
Activation entropy $\Delta S^{\ddagger}$ (300 K) = 36 J mol^{-1} K^{-1}				
Gibbs free energy $\Delta G^{\ddagger}$ (300 K) = 95 kJ mol^{-1}				

a) In the presence of Cp_2Co.

4.5.3 Epimerization of [CpRu(Prophos)Cl] and [CpRu(Prophos)I]

Epimerization of [CpRu(Prophos)Cl] (27a and 27a') in $CDCl_3/CH_3OH$ 9:1. (S_{Ru},R_C)- and (R_{Ru},R_C)-[CpRu(Prophos)Cl] **27a** and **27a'**have extensively been used as starting materials for reactions occurring with retention of configuration in methanol at room temperature and in boiling methanol.[2] Thus, they were assumed to be configurationally stable in solution. However, our studies proved that **27a** and **27a'** did epimerize at the metal center in methanol containing solvents.

In $CDCl_3/CH_3OH$ 9:1 (v/v) a sample **27a**/**27a'** = 14.3:85.7 epimerized at 293 K to the equilibrium composition **27a**/**27a'** = 86.0:14.0 with $k_{ep} = 3.3 \times 10^{-4}$ (min^{-1}) corresponding to a half-life $\tau_{1/2}$ = 35 h for the approach to equilibrium (Table 4-3). Using the equilibrium constant K = 6.1 the rate constants $k_{\rightarrow}$ and $k_{\leftarrow}$ for the forward reaction (S_{Ru},R_C) → (R_{Ru},R_C) and the backward reaction (R_{Ru},R_C) → (S_{Ru},R_C) could be calculated. Table 4-4 shows the temperature dependence of the rate constants of the epimerization reaction. At 323 K the half-life for approach to equilibrium was down to 1.43/1.52 h. NMR measurements at higher temperatures would come too close to the boiling point of $CDCl_3$. As to be expected, samples enriched in the diastereomer **27a'** gave the same equilibrium ratios, rate constants, and half-lives as samples enriched in **27a** (Table 4-4).

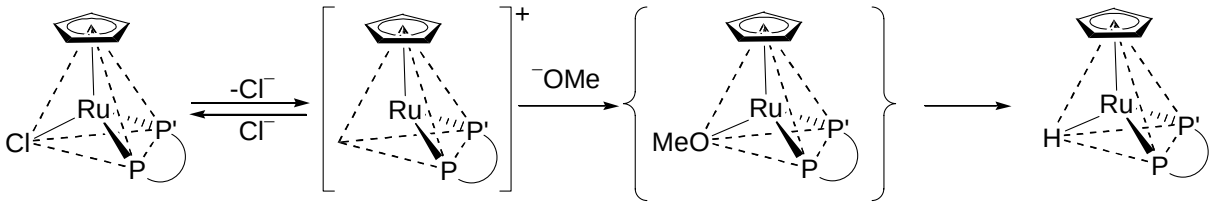

27a **29a** **31a** **32a**

Scheme 4-6. Reaction of **27a** with OMe^- (P-P' = Prophos).

In the investigation of the epimerization of [CpRu(Prophos)Cl] in methanol containing solvents we did not add Cp_2Co which had been successful in sharpening the NMR spectra of the Hal exchange reactions (see above). The reason was a side reaction which produced the by-products (R_{Ru},R_C)/(S_{Ru},R_C)-[CpRu(Prophos)H] (**32a**) and (R_{Ru},R_C)/(S_{Ru},R_C)-[CpRu(Prophos)D], respectively. Cp_2Co removes traces of air-oxygen according to the equation: 4 $Cp_2Co + O_2 \rightarrow 2\ [Cp_2Co]_2O$. In methanol the oxide ion gives OMe^- and OH^-. Obviously, at higher OMe^- concentrations the intermediates (R_{Ru},R_C)/(S_{Ru},R_C)-

[CpRu(Prophos)]$^+$ **29a'**/**29a** formed in the bond cleavage of **27a'**/**27a**, react with OMe^- to give the complexes (R_{Ru},R_C)/(S_{Ru},R_C)-[CpRu(Prophos)OMe] **31a** which transform to the hydrides (R_{Ru},R_C)/(S_{Ru},R_C)-[CpRu(Prophos)H] **32a** (Scheme 4-6). The diastereomers **32a** had been prepared and studied by Consiglio et al.[31)] In methanol containing solvents higher OMe^- concentrations arise from addition of either Cp_2Co/O_2 or NaOMe. In both cases in solutions of **27a'**/**27a** the NMR signals of (R_{Ru},R_C)/(S_{Ru},R_C)-[CpRu(Prophos)H] appear at room temperature within min and rise according to the kinetics of the cleavage of the Ru-Cl bonds.

Table 4-4. Kinetics[a)] of the epimerization of enriched samples of (R_{Ru},R_C)/(S_{Ru},R_C)-[CpRu(Prophos)Cl] **27a'**/**27a** in $CDCl_3/CH_3OH$ (9:1, v/v) and activation parameters.

Starting ratio (S_{Ru},R_C):(R_{Ru},R_C) Act. param.	Temp. /K	equilibrium ratio (S_{Ru},R_C):(R_{Ru},R_C)	K	k_{ep} /min^{-1}	$\tau_{1/2}$ /h	$k_{\rightarrow}$ /min^{-1}	$k_{\leftarrow}$ /min^{-1}
14.3:85.7	293	86.0:14.0	6.1	3.3×10^{-4}	35.0	2.8×10^{-4}	5.4×10^{-5}
5.8:94.2	300	85.0:15.0	5.7	5.0×10^{-4}	23.1	4.8×10^{-4}	8.8×10^{-5}
96.3: 3.7	300	84.0:16.0	5.3	3.8×10^{-4}	30.4	3.1×10^{-4}	7.2×10^{-5}
11.9:88.1	308	85.6:14.4	6.0	1.2×10^{-3}	9.63	1.0×10^{-3}	2.0×10^{-4}
27.2:62.8	313	84.4:15.6	5.4	2.4×10^{-3}	4.81	2.1×10^{-3}	3.2×10^{-4}
12.6:87.4	323	81.2:18.8	4.3	8.1×10^{-3}	1.43	6.2×10^{-3}	1.9×10^{-3}
95.0: 5.0	323	83.4:16.6	5.0	7.6×10^{-3}	1.52	6.1×10^{-3}	1.5×10^{-3}

Activation energy $E_{a\rightarrow}$ = 88 kJ mol^{-1}	$E_{a\leftarrow}$ = 95 kJ mol^{-1}
Frequency factor $A_{\rightarrow}$ = 9.7×10^{11} min^{-1}	$A_{\leftarrow}$ = 3.7×10^{12} min^{-1}
Activation enthalpy $\Delta H^{\ddagger}_{\rightarrow}$ (300 K) = 86 kJ mol^{-1}	$\Delta H^{\ddagger}_{\leftarrow}$ (300 K) = 93 kJ mol^{-1}
Activation entropy $\Delta S^{\ddagger}_{\rightarrow}$ (300 K) = -58 J mol^{-1} K^{-1}	$\Delta S^{\ddagger}_{\leftarrow}$ (300 K) = -47 J mol^{-1} K^{-1}
Gibbs free energy $\Delta G^{\ddagger}_{\rightarrow}$ (300 K) = 103 kJ mol^{-1}	$\Delta G^{\ddagger}_{\leftarrow}$ (300 K) = 107 kJ mol^{-1}

a) Measurements were performed using the Cp signals of the ^{1}H NMR spectra.

The activation parameters for the epimerization of **27a** and **27a'** are given in Table 4-4. The epimerization in $CDCl_3/CH_3OH$ 9:1 starts with the cleavage of the Ru-Cl bond (Scheme 4-4) to form two strongly solvated ions. Therefore, the entropy of activation is negative, as discussed in the context of the Cl/I exchange reactions.

Compared to the rates k_1 and $k_{1'}$ of the Hal exchange reactions the rates $k_{\rightarrow}$ and $k_{\leftarrow}$ for the forward and backward reactions in the epimerization are about 10 times slower, because in the

epimerization reaction the intermediates (S_{Ru},R_C)- and (R_{Ru},R_C)-[CpRu(Prophos)]$^+$ have to cross another barrier of appreciable height in the basilica type energy profile of Scheme 4-4.

Epimerization of [CpRu(Prophos)Cl] in $CDCl_3/CD_3OD$ 1:1. The epimerization of (S_{Ru},R_C)/(R_{Ru},R_C)-[CpRu(Prophos)Cl] in $CDCl_3/CD_3OD$ 1:1 was about 10-20 times faster than in $CDCl_3/CH_3OH$ 9:1, the equilibrium compositions and activation parameters remaining about the same (Table 4-5). Thus, at 323 K the half-life of the epimerization was only a few min.

Table 4-5. Kinetics of the epimerization of (R_{Ru},R_C)/(S_{Ru},R_C)-[CpRu(Prophos)Cl] **27a'**/**27a** in $CDCl_3/CD_3OD$ (1:1, v/v) and activation parameters.

Starting ratio (S_{Ru},R_C):(R_{Ru},R_C) Act. param.	Temp. (K)	equilibrium ratio (S_{Ru},R_C):(R_{Ru},R_C)	K	k_{ep} (min^{-1})	$\tau_{1/2}$ (h)	$k_{\rightarrow}$ (min^{-1})	$k_{\leftarrow}$ (min^{-1})
63.2:36.8	293[a)]	85.3:14.7	5.8	5.6×10^{-3}	2.06	4.6×10^{-3}	9.7×10^{-4}
13.0:87.0	300[b)]	87.0:13.0	6.8	1.4×10^{-2}	0.85	1.2×10^{-2}	2.1×10^{-3}
19.7:80.3	308[b)]	83.9:16.1	5.2	4.5×10^{-2}	0.26	3.6×10^{-2}	8.6×10^{-3}
27.2:72.8	313[b)]	84.2:15.8	6.3	6.8×10^{-2}	0.17	5.7×10^{-2}	1.1×10^{-2}
51.3:48.7	323[b)]	86.8:13.2	6.6	1.7×10^{-1}	0.070	1.4×10^{-1}	2.6×10^{-2}

Activation energy $E_{a\rightarrow}$ = 89 kJ mol^{-1}	$E_{a\leftarrow}$ = 91 kJ mol^{-1}
Frequency factor $A_{\rightarrow}$ = 4.5×10^{13} min^{-1}	$A_{\leftarrow}$ = 1.8×10^{13} min^{-1}
Activation enthalpy $\Delta H^{\ddagger}_{\rightarrow}$ (300 K) = 87 kJ mol^{-1}	$\Delta H^{\ddagger}_{\leftarrow}$ (300 K) = 89 kJ mol^{-1}
Activation entropy $\Delta S^{\ddagger}_{\rightarrow}$ (300 K) = -26 J mol^{-1} K^{-1}	$\Delta S^{\ddagger}_{\leftarrow}$ (300 K) = -34 J mol^{-1} K^{-1}
Gibbs free energy $\Delta G^{\ddagger}_{\rightarrow}$ (300 K) = 95 kJ mol^{-1}	$\Delta G^{\ddagger}_{\leftarrow}$ (300 K) = 99 kJ mol^{-1}

a) Measurements were performed using the Cp signals of the ^{1}H NMR spectra. b) Measurements were performed using the methyl signals in the Prophos ligand of the ^{1}H NMR spectra.

Epimerization of [CpRu(Prophos)I]. The epimerization kinetics of [CpRu(Prophos)I] was measured in $CDCl_3/CD_3OD$ = 1:1 at 50 °C using the Cp signals in the NMR spectra for integration. With an equilibrium ratio of (R_{Ru},R_C)-/(S_{Ru},R_C)-[CpRu(Prophos)I] **27c**/**27c'**= 89.7:10.3 the first-order rate constants were $k_{\rightarrow} = 1.42 \times 10^{-4}$ and $k_{\leftarrow} = 1.63 \times 10^{-5}$ [s^{-1}]. The half-life of the approach to equilibrium was $\tau_{1/2}$ = 73 min ($k_{ep} = 1.58 \times 10^{-4}$ [s^{-1}]). Thus, the configurational stability of [CpRu(Prophos)I] is higher than that of [CpRu(Prophos)Cl] by a factor of about 17.

In $CDCl_3/CD_3OD$ = 9:1 the rate of epimerization of **27c**/**27c'** decreased by a factor of more than 10 compared to $CDCl_3/CD_3OD$ = 1:1 due to the reduced polarity of the solvent mixture.

Contrary to $CDCl_3/CD_3OD$ mixtures, **27c** and **27c'** did not epimerize in nonpolar solvents. Highly enriched samples of **27c**/**27c'** were heated to 80 °C in toluene-d_8 for 12 h and to 50 °C in $CDCl_3$ for 17 h without an observable change in the diastereomer ratio.

Epimerization of [CpRu(Norphos)I]. [CpRu(Norphos)I] was only sparingly soluble in methanol. Therefore, the epimerization kinetics was measured in $CDCl_3/CD_3OD$ = 1:1. Using a sample **28c**/**28c'** = 30:70 kinetics of the approach to the epimerization equilibrium (R_{Ru},R_C) = (S_{Ru},R_C) at 50 °C was monitored by integrating the olefinic signals of the Norphos ligands in the diastereomers. After 20 h at 50 °C the system was equilibrated, the equilibrium ratio being **28c**/**28c'** = 58.4:41.6 (K = 1.40). Analysis of the data according to first-order gave $k_{\rightarrow}$ = 4.97 x 10^{-5} [s^{-1}] and $k_{\leftarrow}$ = 3.54 x 10^{-5} [s^{-1}] equivalent to a half-life of $\tau_{1/2}$ = 136 min (k_{ep} = 8.51 x 10^{-5} [s^{-1}]) for the approach to equilibrium. This shows a higher configurational stability of the Norphos complexes compared to the Prophos complexes which had already been observed in the Hal exchange reactions.

4.5.4 X-ray Analyses

The molecular structures of different diastereomers of [CpRu(Prophos)Br], [CpRu(Prophos)I], [CpRu(Norphos)Br] and [CpRu(Norphos)I] have been determined.
The major diastereomers **27b** of [CpRu(Prophos)Br] and **27c** of [CpRu(Prophos)I] have (R_{Ru},R_C)-configuration and closely related structures. In both of them the methyl groups of the Prophos ligand are oriented away from the Ru-Hal bond. The bond lengths Ru-PCHMe and Ru-PCH_2 and the angles Centre-Ru-PCHMe and Centre-Ru-PCH_2 as well as PCHMe-Ru-Hal and PCH_2-Ru-Hal obey the same trends (Figs. 4-5 and 4-6).

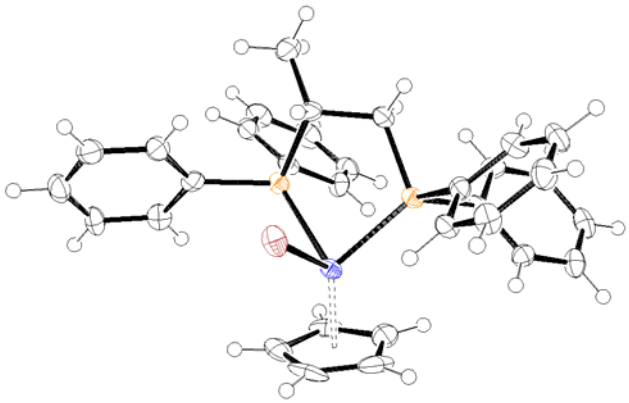

Figure 4-5. Molecular structure of (R_{Ru},R_C)-[CpRu(Prophos)Br] **27b**. Bond lengths (Å) and angles (°): Centre-Ru 1.8387(3), Ru-PCHMe 2.2755(11), Ru-PCH_2 2.2762(9), Ru-Br 2.5654(4); Centre-Ru-PCHMe 129.119(26), Centr-Ru-PCH_2 130.981(27), Centre-Ru-Br 121.981(12), PCHMe-Ru-PCH_2 83.080(35), PCHMe-Ru-Br 84.997(25), PCH_2-Ru-Br 93.007(25).

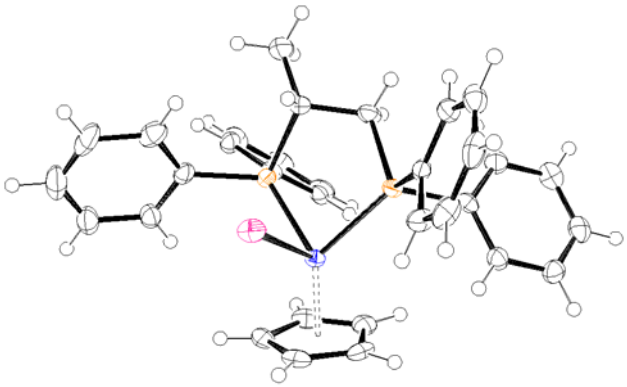

Figure 4-6. Molecular structure of (R_{Ru},R_C)-[CpRu(Prophos)I] **27c**. Bond lengths (Å) and angles (°): Centre-Ru 1.8518(2), Ru-PCHMe 2.2768(8), Ru-PCH_2 2.2859(8), Ru-I 2.7320(4); Centre-Ru-PCHMe 129.162(23), Centr-Ru-PCH_2 131.010(21), Centre-Ru-I 119.147(10), PCHMe-Ru-PCH_2 83.448(28), PCHMe-Ru-I 87.575(21), PCH_2-Ru-I 93.918(21).

The same tendencies in the bond lengths and angles are observed in the major (R_{Ru},R_C)-diastereomers **28b** of [CpRu(Norphos)Br] and **28c** of [CpRu(Norphos)I] (Figs. 4-7 and 4-8). The minor (S_{Ru},R_C)-diastereomers **28c'** of [CpRu(Norphos)I], on the other hand, is distinctly different (Fig. 4-9).

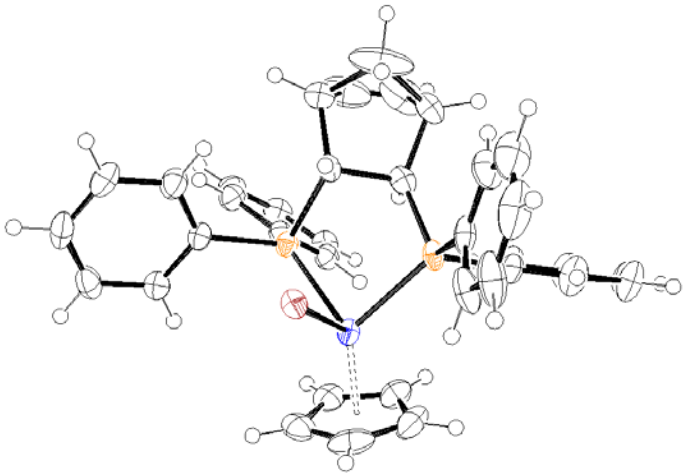

Figure 4-7. Molecular structure of (R_{Ru},R_C)-[CpRu(Norphos)Br] **28b**. Bond lengths (Å) and angles (°): Centre-Ru 1.8405(2), Ru-P_{endo} 2.2989(8), Ru-P_{exo} 2.2985(8), Ru-Br 2.5767(3); Centre-Ru-P_{endo} 130.647(21), Centre-Ru-P_{exo} 126.616(21), Centre-Ru-Br 123.957(10), P_{endo}-Ru-P_{exo} 86.105(28), P_{endo}-Ru-Br 84.629(21), P_{exo}-Ru-Br 91.579(21).

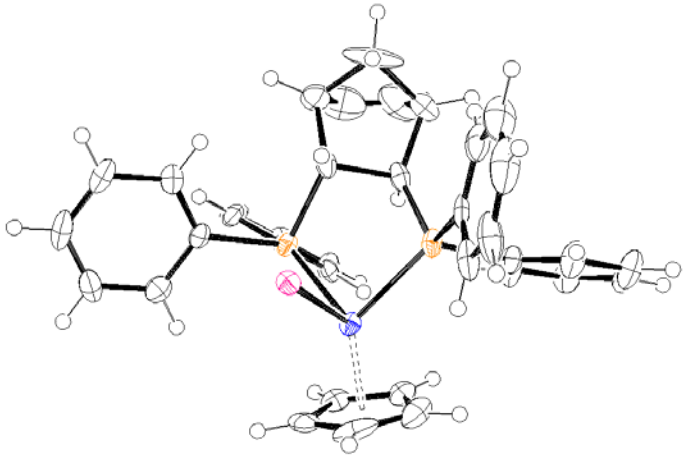

Figure 4-8. Molecular structure of (R_{Ru},R_C)-[CpRu(Norphos)I] **28c**. Bond lengths (Å) and angles (°): Centre-Ru 1.8387(3), Ru-P_{endo} 2.2957(13), Ru-P_{exo} 2.2974(14), Ru-I 2.7312(4); Centre-Ru-P_{endo} 130.957(36), Centre-Ru-P_{exo} 126.654(36), Centre-Ru-I 122.245(16), P_{endo}-Ru-P_{exo} 86.139(47), P_{endo}-Ru-I 85.690(33), P_{exo}-Ru-I 92.475(34).

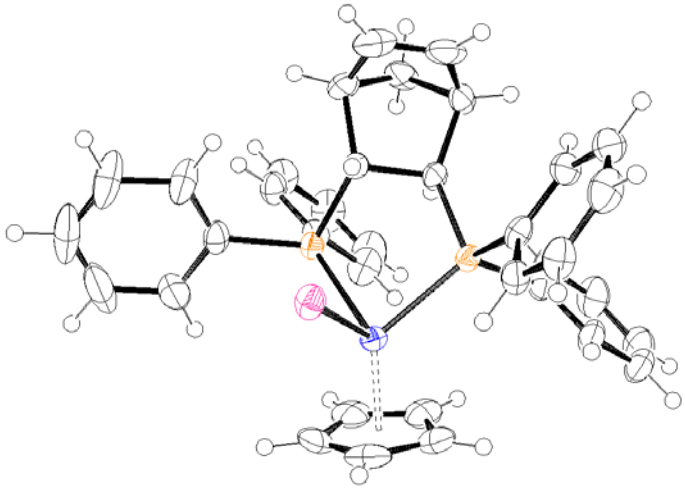

Figure 4-9. Molecular structure of (S_{Ru},R_C)-[CpRu(Norphos)I] **28c'**. Bond lengths (Å) and angles (°): Centre-Ru ,1.8427(4) Ru-P_{endo} 2.3022(12), Ru-P_{exo} 2.2963(10), Ru-I 2.7185(4); Centre-Ru-P_{endo} 126.867(33), Centre-Ru-P_{exo} 130.023(31), Centre-Ru-I 120.930(17), P_{endo}-Ru-P_{exo} 85.107(37), P_{endo}-Ru-I 94.719(29), P_{exo}-Ru-I 87.516(30).

4.6 Discussion

Mechanism, 16-electron intermediates [CpRu(P-P')]$^+$, and configurational stability. In polar media such as methanol the Ru-Hal bond in compounds of the type [CpRu(Prophos)Hal] and [CpRu(Norphos)Hal] tends to dissociate according to equation (4-1).

$$[CpRu(P\text{-}P')Hal] \rightarrow [CpRu(P\text{-}P')]^+ + Hal^- \qquad (4\text{-}1)$$

For [CpRu(Prophos)Cl] and [CpRu(Norphos)Cl] these dissociations occurred in methanol already at room temperature, obvious from a series of halogen exchange reactions presented in this paper which followed first-order kinetics. Thus, in $CDCl_3/CD_3OD$ 1:1 the Cl/Br and Cl/I exchange in the thermodynamically less stable diastereomer ($R_{Ru,}R_C$)-[CpRu(Prophos)Cl] **27a'** (left side of Scheme 4-4) had a half-life of 23 min at 20 °C to give ($S_{Ru,}R_C$)-[CpRu(Prophos)Br] **27b'** and ($S_{Ru,}R_C$)-[CpRu(Prophos)I] **27c'** (Table 4-2). In $CDCl_3/CD_3OD$ 9:1 these halide exchange reactions were about 10 slower due to reduced solvation of the ions [CpRu(P-P')]$^+$/Hal$^-$ formed in the rate determining step.

The halide exchange in the thermodynamically more stable diastereomer ($S_{Ru,}R_C$)-[CpRu(Prophos)Cl] **27a** (right side of Scheme 4-4), giving ($R_{Ru,}R_C$)-[CpRu(Prophos)Br] **27b** and ($R_{Ru,}R_C$)-[CpRu(Prophos)I] **27c**, was slower by a factor of about 10-15 compared to the thermodynamically less stable diastereomer **27a'**.

These halide exchange reactions occurred with predominant retention of configuration at the metal atom in agreement with the retention reactions described by Consiglio and Morandini.[2] However, Consiglio and Morandini did not take into account that the substitution reactions were accompanied by partial inversion of the metal configuration. This can be understood on the basis of a basilica-type energy profile such as Scheme 4-4. In the cleavage of the Ru-Cl bond in **27a'** and **27a** the 16-electron intermediates ($R_{Ru,}R_C$)- and ($S_{Ru,}R_C$)-[CpRu(Prophos)]$^+$ **29a'** and **29a** are formed which are pyramidal keeping their original configurations. As in the presence of excess Br^- and I^- the activation energies for the reaction with the halides are much smaller than the barrier for pyramidal inversion, the substitution products form with predominant retention of configuration. Quantitative measures for the competition between inversion and substitution with retention are the competition ratios k_3/k_2 and $k_{3'}/k_{2'}$. For **27a'** values around 0.1 in Tables 4-2 and 4-3 show that, given the conditions of the Hal exchange reactions, only about 10% of the intermediates cross the central barrier with inversion of configuration, whereas 90% stay on the left side of Scheme 4-4 with retention of configuration.

The 16-electron cyclopentadienyl species (R_{Ru},S_C)- and (S_{Ru},S_C)-[CpRu(P-P')]$^+$ in Schemes 4-4 and 4-5 are high-energy intermediates which cannot be observed spectroscopically. This seems to be different in the pentamethylcyclopentadienyl series. According to the literature the chloro ligand in [Cp*Ru(P-P')Hal] is so labile that a mobile equilibrium between [Cp*Ru(P-P')Hal] and [Cp*Ru(P-P')]$^+$/Hal$^-$ is established.[32)] If so, the substitution steps in the energy profile would be pre-equilibria. Furthermore, halide abstraction from compounds [Cp*Ru(P-P')Hal] with Ag^+ salts allows the isolation of solvent stabilized and solvent free salts [Cp*Ru(P-P')]$^+X^-$ and [Cp*Ru(P-P')]$^+X^-$, as these compounds are much more stable in the Cp* series than in the Cp series.

The lability of the chloride ligand in [CpRu(P,P)Hal] and [CpRu(P-P)Hal] as well as their Cp* analogs in solvents such as alcohols was discussed in several papers. In a 1976-paper it was claimed on the basis of conductometric measurements that [CpRu(PPh_3)$_2$Cl] appreciably

dissociates in methanol into $[CpRu(PPh_3)_2(CH_3OH)]^+$ and Cl^-.[33] However, there are no experimental data in the paper. $[CpRu(PP)]^+$ was discussed as an intermediate, but up to now such species have not been isolated.[32] This is different for their $[Cp^*Ru(PP)]^+$ counterparts which are much more stable. $[Cp^*Ru(PMe^iPr_2)_2]^+$ was isolated and characterized by X-ray analysis.[34] Centre, Ru and the two P atoms lie in a plane. The angle P-Ru-P is 101.43(5), close to the angle L-M-L =100 ^{o} used in the calculations.[22] As trialkylphosphanes such as PMe^iPr_2 are good donors, $[Cp^*Ru(PMe^iPr_2)_2]^+$ fits the planarity predicted in the calculation. Interestingly, the complex $[Cp^*Ru(\ ^iPr_2PCH_2CH_2P^iPr_2)]^+$ containing the chelate ligand $^iPr_2PCH_2CH_2P^iPr_2$, also a trialkylphosphane, is not planar but pyramidal, having an agostic C-H interaction in its sixth coordination position.[34] The reason for this is the small angle P-Ru-P of 83.13(4) which prevents planarization. In contrast to $[Cp^*Ru(P-P)]^+$ the planar skeletons in $[Cp^*Ru(N-N)]^+$ and even $[CpRu(N-N)]^+$ tolerate small angles N-Ru-N of 80-81 ^{o} for the hard donor *N,N'*-tetramethylethylenediamine.[35-37] Interestingly, a high barrier for the planar/pyramidal rearrangement was ascribed to these cations.[36,37] The planar complexes [Cp*Ru(N-N)], N-N = amidinate ligands, form a strange Ru-C(amidinate) contact.[38]

(R_{Ru},R_C)- and (S_{Ru},R_C)-[CpRu(Prophos)Cl] **27a'** and **27a** epimerized in methanol containing solvents following first-order kinetics. The half-lives of the approach to the equilibrium **27a'**/**27a** = 15:85 in $CDCl_3/CD_3OD$ 9:1 were 35 h at 20 ^{o}C and 1.5 h at 50 ^{o}C. In $CDCl_3/CD_3OD$ 1:1 these values were down to 2 h and 4 min. A comparison of the rate constants k_1 and $k_{\rightarrow}$ as well as k_2 and $k_{\leftarrow}$ in Tables 4-1, 4-2, 4-3, 4-4 and 4-5 shows that the epimerization is slower than the halide exchange by a factor of about 10, because for inversion the intermediates (R_{Ru},R_C)- and (S_{Ru},R_C)-[CpRu(Prophos)]$^+$ have to cross another appreciable barrier.

(R_{Ru},R_C)- and (S_{Ru},R_C)-[CpRu(Prophos)Cl] had been synthesized in a ratio close to 1:1 by reacting $[CpRu(PPh_3)_2Cl]$ and (*R*)-Prophos in boiling benzene under conditions of kinetic control.[6] On the basis of solubility differences it was possible to separate the diastereomers. It was shown that the diastereomers did not epimerize in toluene at 80 ^{o}C. However, epimerization took place in C_6D_5Cl at the same temperature resulting in an equilibrium mixture **27a'**/**27a** = 30:70.[6] Thus, **27a** is the thermodynamically more stable diastereomer. The configurational stability of **27a'** and **27a** in methanol solution had not been studied, although both diastereomers were extensively used as starting materials in the solvent methanol. To the synthesized organometallic products retention of configuration and,

implicitly, the same stereochemical purities as the starting materials were assigned as indicated by comparison of CD spectra etc. As our study showed that **27a'** and **27a** change the metal configuration in methanol solution, slowly at room temperature but fast at higher temperatures, loss of stereoselectivity must have occurred in these substitution reactions. In most of these reactions **27a'** and **27a** were dissolved at room temperature in methanol and the other reagents were added. In these cases some epimerization must have lowered the stereoselectivity depending on how long it took to form the configurationally stable organometallic compound. However, in the reactions carried out in boiling methanol significant epimerization must have taken place and consequently extensive loss of stereoselectivity is to be expected.

Calculations of pyramidal stability and angles Cp-Ru-P and P-Ru-P. With the extended Hückel methodology as well as with density functional theory the structure of coordinatively unsaturated, two-legged 16-electron piano stool complexes of the type [(η-C_nH_n)MLL'] was analyzed.[20,21] Whereas for fragments with strongly π-accepting ligands such as [$CpMn(CO)_2$] and [$CpFe(CO)_2]^+$ pyramidal structures with inversion barriers of about 10 kcal/mol were calculated, fragments with σ-donor ligands such as [$CpMn(PH_3)_2$] and [$CpFe(PH_3)_2]^+$ were predicted to adopt planar geometries. As Fe is the higher homologue of Ru, a comparison of the [CpRuPP'] species dealt with here with [CpFeLL'] species is particularly interesting. In the DFT geometry optimization of [$CpFe(CO)_2]^+$ the OC-Fe-CO angle in the pyramidal species was 94.14 °, whilst in the planar transition state it was 103.02 °. Consequently, the angle Cp_{Centre}-Fe-CO in the planar fragment was 128.49 °.

In [$CpRu(PPh_3)_2Cl$], the parent compound of the chelate complexes studied here, the P-Ru-P angle is 97.1 °. Usually, in five-membered chelate rings the P-M-P angles are smaller. Thus, the P-Ru-P angle in [CpRu(Prophos)Cl] is 82.9 ° and in [CpRu(Norphos)I] it is 86.1 °. The puckered Ru-Prophos chelate ring, the λ-conformation of which is dictated by the equatorial orientation of the methyl group, is relatively rigid and cannot increase the P-Ru-P angle appreciably. Imposed by the norbornene skeleton, the Ru-Norphos chelate ring, also having λ-conformation, is completely rigid. Both chelate rings will resist a widening of the P-Ru-P angle. This is a fact which strongly favors a pyramidal structure of the 16-electron fragments [CpRuPP']. Not only this, it also will increase the inversion barrier, because in the planar transition state even larger P-Ru-P angles are required. This should be analogous to the inversion of the amine nitrogen which is slowed down dramatically by introducing the

nitrogen atom into small rings. Thus, aziridines with their 60 ^{o} angles greatly resist planarization which needs expanded angles in the transition state. It is to be expected that increasing the P-Ru-P angle, e.g. with the ligand Chairphos Ph_2P-CHMe-CH_2-CH_2-PPh_2 having one CH_2 group more than Prophos, will decrease the barrier of the pyramidal inversion. On the contrary decreasing the size of the chelate ring, e.g. to a four-membered system, should increase the inversion barrier significantly.

4.7 References

1. Brunner, H. *Adv. Organomet. Chem.* **1980**, *18*, 223.
2. Consiglio, G.; Morandini, F. *Chem. Rev.* **1987**, *87*, 761.
3. Brunner, H. *Angew. Chem*. **1999**, *111*, 1248-1263; *Angew. Chem. Int. Ed.* **1999**, *38*, 1194.
4. Bruce, M. I.; Wong, F. S.; Skelton, B. W.; White, A. H. *J. Chem. Soc. Dalton Trans.* **1981**, 1398-1405.
5. Consiglio, G.; Morandini, F.; Bangerter, F. *Inorg. Chem.* **1982**, *21*, 455.
6. Morandini, F.; Consiglio, G.; Straub, B.; Ciani, G.; Sironi, A. *J. Chem. Soc., Dalton Trans.* **1983**, 2293.
7. Nishiyama, H.; Brunner, H. *J. Organomet. Chem.* **1991**, *405*, 247.
8. Cahn, R. S.; Ingold, C.; Prelog, V. *Angew. Chem.* **1966**, *78*, 413; *Angew. Chem., Int. Ed. Engl.* **1966**, *5*, 385.
9. Brunner, H. *Angew. Chem.* **1969**, *81*, 395-396; *Angew. Chem., Int. Ed. Engl.* **1969**, *8*, 382.
10. Brunner, H.; Schindler, H.-D. *Chem. Ber.* **1971**, *104,* 2467.
11. Brunner, H.; Schindler, H.-D. *J. Organomet. Chem.* **1971**, *24*, C7.
12. Brunner, H.; Schindler, H.-D. *Z. Naturforsch.* **1971**, *26 b*, 1220.
13. Brunner, H.; Aclasis, J. A.; Langer, M.; Steger, W. *Angew. Chem.* **1974**, *86*, 864; *Angew. Chem., Int. Ed. Engl.* **1974**, *13*, 810.
14. Brunner, H.; Langer, M. *J. Organomet. Chem.* **1975**, *87*, 223.
15. Brunner, H.; Aclasis, J. A. *J. Organomet. Chem.* **1976**, *104*, 347.
16. Brunner, H.; Steger, W. *J. Organomet. Chem.* **1976**, *120,* 239.
17. Brunner, H.; Steger, W. *Bull. Soc. Chim. Belg.* **1976**, *85*, 883.
18. Brunner, H.; *Angew. Chem.* **1971**, *83*, 274-285; *Angew. Chem. Int., Ed. Engl.* **1971**, *10*, 249.
19. Brunner, H. *J. Organomet. Chem.* **1974,** *94*, 189.

20. Brunner, H. *Top. Curr. Chem.* **1975**, *56*, 67.
21. Hofmann, P. *Angew. Chem.* **1977**, *39*, 551; *Angew. Chem. Int., Ed. Engl.* **1977**, *16*, 536.
22. Ward, T. R.; Schafer, O.; Claude, D.; Hofmann, P. *Organometallics* **1997**, *16*, 3207.
23. Campion, B. K.; Heyn, R. H.; Don Tilley, T. *J. Chem. Soc., Chem. Commun.* **1988**, 278.
24. Joslin, F. L.; Johnson, M. P.; Mague, J. T.; Roundhill, D. M. *Organometallics* **1991**, *10*, 2781.
25. Fryzuk, M. D.; Bosnich, B. *J. Am. Chem. Soc.* **1977**, *99*, 6262-6267.
26. Brunner, H.; Pieronczyk, W. *Angew. Chem.* **1979**, *91*, 655; *Angew. Chem. Int., Ed. Engl.* **1979**, *18*, 620.
27. Brunner, H.; Pieronczyk, W.; Schönhammer, B.; Streng, K.; Bernal, I.; Korp, J. *Chem. Ber.* **1981**, *114*, 1137.
28. Brunner, H.; Muschiol, M.; Zabel, M. *Synthesis*, submitted for publication.
29. Disley, S. P. M.; Grime, R. W.; McInnes, E. J. L.; Spencer, D. M.; Swainston, N.; Whiteley, M. W. *J. Organomet. Chem.* **1998**, *566*, 151.
30. Brunner, H.; Klankermayer, J.; Zabel, M. *Eur. J. Inorg. Chem.* **2002**, 2494.
31. Morandini, F.; Consiglio, G.; Lucchini, V. *Organometallics* **1985**, *4*, 1202.
32. de los Rios, I.; Tenorio, M. J.; Padilla, J.; Puerta, M. C.; Valerga, P. *J. Chem. Soc., Dalton Trans.* **1996**, 377-381.
33. Haines, R. J. ; du Preez, A. L. *J. Organomet. Chem.* **1975**, *84*, 357-367.
34. Tenorio, M. J.; Mereiter, K.; Puerta, M. C.; Valerga, P. *J. Am. Chem. Soc.* **2000**, *122*, 11230.
35. Gemel, C.; Mereiter, K.; Schmid, R.; Kirchner, K. *Organometallics* **1997**, *16*, 5601.
36. Gemel, C.; Sapunov, V. N.; Mereiter, K.; Ferencic, M.; Schmid, R.; Kirchner, K. *Inorg. Chim. Acta* **1999**, *286*, 114.
37. Gemel, C.; Huffman, J. C.; Caulton, K. G.; Mereiter, K.; Kirchner, K. *J. Organomet. Chem.* **2000**, *593-594*, 342.
38. Yamaguchi, Y.; Nagashima, H. *Organometallics* **2000**, *19*, 725.

Appendix

5.1 Crystallographic data for Dichloro[2-[(1R)-1-(diphenylphosphino-κP)-2-methylpropyl]-6-(1R,2S,5R)-menthoxylpyridine](η^5-1,2,3,4,5-pentamethylcyclopentadienyl)rhodium(III) ($L_{Menb}R_C$)-11

Empirical formura	$C_{41}H_{55}Cl_2NOPRh$
Formula weight	782.64
Crystal system	Orthorhombic
Space group	$P2_12_12_1$
a (Å)	14.5510(10)
b (Å)	15.6678(9)
c (Å)	16.8954(12)
α (°)	90
β(°)	90
γ (°)	90
V (Å^3)	3892.1(5)
Z	4
ρ_{calcd} (g cm^{-3})	1.336
Abs. coef. (mm^{-1})	0.649
Abs. correct.	Numerical
Transmiss min/max	0.9495/0.8926
F(0,0,0)	1640
Crystal size (mm)	0.260 x 0.180 x 0.140
θrange (°)	1.85-25.78
No. of rflns/unique	7349/33156
R_{int}	0.0576
No. of data/params.	7349/424
Goodness of fit. on F^2	0.938
R_1/wR_2 [$I > 2\sigma(I)$]	0.0277/0.0617
R_1/wR_2 (all data)	0.0362/0.0635
Largest diff. peak and hole (e Å^{-3})	0.567/-0.275
CCDC No.	233220

5.2 Crystallographic data for Dichloro[2-[(1S)-1-(diphenylphosphino-κP)-2-methylpropyl]-6-(1R,2S,5R)-menthoxylpyridine](η⁵-1,2,3,4,5-pentamethylcyclopentadienyl)rhodium(III) ($L_{Menth}S_C$)-11

Empirical formura	$C_{41}H_{55}Cl_2NOPRh$
Formula weight	782.64
Crystal system	Orthorhombic
Space group	$P2_12_12_1$
a (Å)	10.4475(8)
b (Å)	17.7055(16)
c (Å)	21.0407(15)
α (°)	90
β(°)	90
γ (°)	90
V (Å^3)	3851.8(4)
Z	4
ρ_{calcd} (g cm^{-3})	1.350
Abs. coef. (mm^{-1})	0.656
Abs. correct.	Numerical
Transmiss min/max	0.9620/0.9385
F(0,0,0)	1640
Crystal size (mm)	0.260 x 0.180 x 0.140
θrange (°)	1.94-25.21
No. of rflns/unique	6982/33162
R_{int}	0.17206
No. of data/params.	6982/424
Goodness of fit. on F^2	0.699
R_1/wR_2 [$I > 2\sigma(I)$]	0.0489/0.0766
R_1/wR_2 (all data)	0.1126/0.0910
Largest diff. peak and hole (e Å^{-3})	0.524/-0.359
CCDC No.	233222

5.3 Crystallographic data for (R_{Rh})/(S_{Rh})-Chloro[2-[(1R/1S)-1-(diphenylphosphino-κP)-2-methylpropyl]-6-(1R,2S,5R)-menthoxylpyridine-κN](η^5-1,2,3,4,5-pentamethylcyclopenta-dienyl)rhodium(III) hexafluorophosphate ($L_{Menth}R_C$)(R_{Rh})- and ($L_{Menth}S_C$)(S_{Rh})-15

Empirical formura	$2(C_{41}H_{55}ClNOPRh)$, $2(F_6P)$
Formula weight	1784.32
Crystal system	Triclinic
Space group	*P*1
a (Å)	8.8682(8)
b (Å)	15.1841(13)
c (Å)	16.5209(13)
α (°)	91.367(10)
β(°)	105.515(10)
γ (°)	100.659(10)
V (Å^3)	2100.3(3)
Z	1
ρ_{calcd} (g cm^{-3})	1.411
Abs. coef. (mm^{-1})	0.605
Abs. correct.	Numerical
Transmiss min/max	0.9765/0.9335
F(0,0,0)	924
Crystal size (mm)	0.16 x 0.08 x 0.04
θrange (°)	1.95-25.82
No. of rflns/unique	9496/10131
R_{int}	0.0739
No. of data/params.	9496/875
Goodness of fit. on F^2	0.735
R_1/wR_2 [$I > 2\sigma(I)$]	0.0454/0.0735
R_1/wR_2 (all data)	0.1078/0.0878
Largest diff. peak and hole (e Å^{-3})	0.646/-0.354
CCDC No.	233221

5.4 Crystallographic data for (S_{Rh})-Chloro[2-[(1S)-1-(diphenylphosphino-κP)-2-methylpropyl]-6-(1R,2S,5R)-menthoxylpyridine-κN](η^5-1,2,3,4,5-pentamethylcyclopentadienyl)rhodium(III) hexafluorophosphate ($L_{Menth}S_C$)(S_{Rh})-15

Empirical formura	$C_{41}H_{55}ClNOPRh$, $2(C_3H_6O)$, F_6P
Formula weight	1008.32
Crystal system	Monoclinic
Space group	$P2_1$
a (Å)	9.9515(7)
b (Å)	17.9193(12)
c (Å)	14.2159(11)
α (°)	90
β(°)	106.791(9)
γ (°)	90
V (Å^3)	2427.0(3)
Z	2
ρ_{calcd} (g cm^{-3})	1.380
Abs. coef. (mm^{-1})	0.535
Abs. correct.	Empirical
Transmiss min/max	0.879/0.596
F(0,0,0)	1052
Crystal size (mm)	0.580 x 0.100 x 0.040
θrange (°)	1.88-25.79
No. of rflns/unique	9250/17232
R_{int}	0.0346
No. of data/params.	9250/508
Goodness of fit. on F^2	0.968
R_1/wR_2 [$I > 2\sigma(I)$]	0.0391/0.0875
R_1/wR_2 (all data)	0.0487/0.0904
Largest diff. peak and hole (e Å^{-3})	0.788/-0.586
CCDC No.	233214

5.5 Crystallographic data for (R_{Ru})-Chloro[1-[(2S)-2-(diphenylphosphino-κP)-1,1-dimethyl-2-[6-[[(1R,2S,5R)-menthoxy-2-pyridinyl]ethyl]-η^5-cyclopentadienyl]-(triphenylphosphine)ruthenium(II) ($L_{Menth}S_C,R_{Ru}$)-17

Empirical formura	$C_{54}H_{58}ClNOP_2Ru$
Formula weight	935.47
Crystal system	Monoclinic
Space group	$P2_1$
a (Å)	14.0085(14)
b (Å)	13.2789(8)
c (Å)	14.4258(13)
α (°)	90
β(°)	101.792(11)
γ (°)	90
V (Å^3)	2626.8(4)
Z	2
ρ_{calcd} (g cm^{-3})	1.183
Abs. coef. (mm^{-1})	0.445
Abs. correct.	Numerical
Transmiss min/max	0.9541/0.8223
F(0,0,0)	976
Crystal size (mm)	0.580 x 0.126 x 0.100
θrange (°)	2.13-25.83
No. of rflns/unique	10042/10042
R_{int}	0.0
No. of data/params.	1042/553
Goodness of fit. on F^2	1.034
R_1/wR_2 [$I > 2\sigma(I)$]	0.0288/0.0740
R_1/wR_2 (all data)	0.0306/0.0747
Largest diff. peak and hole (e Å^{-3})	0.551/-1.005
CCDC No.	287095

5.6 Crystallographic data for (R_{Ru})-[1-[(2S)-2-(Diphenylphosphino-κP)-1,1-dimethyl-2-[6-[[(1R,2S,5R)-menthoxy-2-pyridinyl]ethyl]-η^5-cyclopentadienyl](phenylacetonitrile)-(triphenylphosphine)ruthenium(II) hexafluorophosphate (L_{Menth},S_C,R_{Ru})-25

Empirical formura	$C_{62}H_{65}F_6N_2OP_3Ru$
Formula weight	1162.19
Crystal system	Monoclinic
Space group	$P2_1$
a (Å)	14.427(1)
b (Å)	13.607(1)
c (Å)	14.624(1)
α (°)	90
β(°)	103.516(4)
γ (°)	90
V (Å^3)	2791.5(3)
Z	2
ρ_{calcd} (g cm^{-3})	1.283
Abs. coef. (mm^{-1})	3.569
Abs. correct.	None
Transmiss min/max	0.879/0.982
F(0,0,0)	12046
Crystal size (mm)	0.30 x 0.30 x 0.30
θrange (°)	3.1-68.3
No. of rflns/unique	5004/5314
No. of data/params.	4990/676
Goodness of fit. on F^2	2.250
R/*wR* [$I > 2\sigma(I)$]	0.536/0.635
Largest diff. peak and hole (e Å^{-3})	0.69/-0.64
CCDC No.	287095

5.7 Crystallographic data for (R_{Ru})-Bromo[η^5-cyclopentadienyl][[(1R)-1-methyl-1,2-ethanediyl]bis[diphenylphosphine-κP]]ruthenium(II) 27b

Empirical formura	$C_{32}H_{31}BrP_2Ru$
Formula weight	627.23
Crystal system	Monoclinic
Space group	$P2_1$
a (Å)	9.65602(10)
b (Å)	14.95694(10)
c (Å)	10.48788(10)
α (°)	90
β(°)	112.4786(12)
γ (°)	90
V (Å^3)	1399.62(2)
Z	2
ρ_{calcd} (g cm^{-3})	1.476
Abs. coef. (mm^{-1})	7.359
Abs. correct.	Multi-scan
Transmiss min/max	0.732/0.178
F(0,0,0)	602
Crystal size (mm)	0.128 x 0.106 x 0.088
θrange (°)	4.55-51.20
No. of rflns/unique	2909/2986
No. of data/params.	2986/626
Goodness of fit. on F^2	1.081
R/*wR* [$I > 2\sigma(I)$]	0.0173/0.0426

5.8 Crystallographic data for (R_{Ru})- [η^5-cyclopentadienyl]iodo[[(1R)-1-methyl-1,2-ethanediyl]bis[diphenylphosphine-κP]]ruthenium(II) 27c

Empirical formura	$C_{32}H_{31}IP_2Ru$
Formula weight	705.48
Crystal system	Monoclinic
Space group	$P2_1$
a (Å)	8.4821(15)
b (Å)	15.0654(8)
c (Å)	11.0948(8)
α (°)	90
β(°)	91.851(9)
γ (°)	90
V (Å^3)	1417.0(3)
Z	2
ρ_{calcd} (g cm^{-3})	1.653
Abs. coef. (mm^{-1})	1.775
Abs. correct.	Multi-scan
Transmiss min/max	0.933/1.07185
F(0,0,0)	700
Crystal size (mm)	0.260 x 0.249 x 0.229
θrange (°)	2.97 - 28.96
No. of rflns/unique	5544/ 6459
No. of data/params.	6459/326
Goodness of fit. on F^2	0.970
R/*wR* [$I > 2\sigma(I)$]	0.0303/0.0482

5.9 Crystallographic data for (R_{Ru})-[1R-(2-endo,3-exo)]-[Bicyclo[2.2.1]hept-5-ene-2,3-diylbis[diphenylphosphine]-P,P']bromo(η^5-cyclopentadienyl)ruthenium(II) 28b

Empirical formura	$C_{36}H_{33}BrP_2Ru$
Formula weight	708.53
Crystal system	Orthorhombic
Space group	$P2_12_12_1$
a (Å)	12.45942(10)
b (Å)	15.52669(14)
c (Å)	15.69572(14)
α (°)	90
β(°)	90
γ (°)	90
V (Å^3)	3462.57(14)
Z	4
ρ_{calcd} (g cm^{-3})	1.572
Abs. coef. (mm^{-1})	1.469
Transmiss min/max	0.918/1.078
F(0,0,0)	1648
Crystal size (mm)	0.229 x 0.213 x 0.147
θrange (°)	4.00 - 63.11
No. of rflns/unique	4736/4873
No. of data/params.	4873/361
Goodness of fit. on F^2	1.046
R/wR [$I > 2\sigma(I)$]	0.0208/0.0528

*5.10 Crystallographic data for (R_{Ru})-[1R-(2-endo,3-exo)]-[Bicyclo[2.2.1]hept-5-ene-2,3-diylbis[diphenylphosphine]-P,P'](η^5-cyclopentadienyl)iodoruthenium(II) 28*c

Empirical formura	$C_{36}H_{33}IP_2Ru$, $2(CH_4O)$
Formula weight	819.62
Crystal system	Monoclinic
Space group	*I*2
a (Å)	16.3029(3)
b (Å)	11.3714(3)
c (Å)	20.1949(4)
α (°)	90
β(°)	112.352(2)
γ (°)	90
V (Å^3)	3462.57(14)
Z	4
ρ_{calcd} (g cm^{-3})	1.653
Abs. coef. (mm^{-1})	6.892
Abs. correct.	Multi-scan
Transmiss min/max	0.634/1.146
F(0,0,0)	1432
Crystal size (mm)	0.170 x 0.130 x 0.040
θrange (°)	3.06 - 28.96
No. of rflns/unique	6864/8136
No. of data/params.	8136/385
Goodness of fit. on F^2	0.993
R/*wR* [$I > 2\sigma(I)$]	0.0459/0.0824

5.11 Crystallographic data for (S_{Ru})-[1R-(2-endo,3-exo)]-[Bicyclo[2.2.1]hept-5-ene-2,3-diylbis[diphenylphosphine]-P,P'](η^5-cyclopentadienyl)iodoruthenium(II) 28c'

Empirical formura	$C_{36}H_{33}IP_2Ru$
Formula weight	755.53
Crystal system	Orthorhombic
Space group	$P2_12_12_1$
a (Å)	12.5156(3)
b (Å)	15.5113(4)
c (Å)	15.8381(5)
α (°)	90
β(°)	90
γ (°)	90
V (Å^3)	3074.70(15)
Z	4
ρ_{calcd} (g cm^{-3})	1.632
Abs. coef. (mm^{-1})	1.642
Abs. correct.	Multi-scan
Transmiss min/max	0.634/1.146
F(0,0,0)	1504
Crystal size (mm)	0.180 x 0.060 x 0.030
θrange (°)	3.24 - 29.01
No. of rflns/unique	4846/6624
No. of data/params.	6624/361
Goodness of fit. on F^2	0.934
R/*wR* [$I > 2\sigma(I)$]	0.0692/0.0543

Acknowledgements

The author expresses thanks to the colleagues of Lehrstuhl für Anorganische Chemie, Prof. Dr. Henri Brunner.

The author thanks Mr. M. Muschiol for his helpful technical supports.

The author also thanks Dr. M. Zabel for his help with the X-ray structural studies.

The author's thanks are made to Dr. T. Burgemeister and Mr. F. Kastner for the measurements of the NMR spectra and Dr. K. K. Mayer for the measurements of the MS spectra.

The author expresses his thanks the colleagues in Department of Applied Molecular Chemistry, College of Industrial Technology, Nihon University. The author's thanks are also made many colleagues in his laboratory and other many friends have supported and encouraged him although they are not listed.

Finally, the author wishes to express his deep appreciation to his parents, his wife's parents, his wife Mrs. Rieko Tsuno, his son Sakuya Tsuno, and new comer in his family, baby 'Erika Tsuno' who was born in August "2007", for their continuous assistance and encouragement.